INVESTIGATION OF ADDED UTILITY OF NONLINEAR TECHNIQUES IN RESCALING SOIL MOISTURE DATASETS

A THESIS SUBMITTED TO
THE GRADUATE SCHOOL OF NATURAL AND APPLIED SCIENCES
OF
MIDDLE EAST TECHNICAL UNIVERSITY

BY

MAHDI HESAMI AFSHAR

IN PARTIAL FULFILLMENT OF THE REQUIREMENTS
FOR
THE DEGREE OF DOCTOR OF PHILOSOPHY
IN
CIVIL ENGINEERING

JANUARY 2019

Approval of the thesis:

INVESTIGATION OF ADDED UTILITY OF NONLINEAR TECHNIQUES IN RESCALING SOIL MOISTURE DATASETS

submitted by **MAHDI HESAMI AFSHAR** in partial fulfillment of the requirements for the degree of **Doctor of Philosophy in Civil Engineering Department, Middle East Technical University** by,

Prof. Dr. Halil Kalıpçılar
Dean, Graduate School of **Natural and Applied Sciences** ________________

Prof. Dr. Ahmet Türer
Head of Department, **Civil Engineering** ________________

Assoc. Prof. Dr. M. Tuğrul Yılmaz
Supervisor, **Civil Engineering, METU** ________________

Examining Committee Members:

Prof. Dr. İsmail Yücel
Civil Engineering Department, METU ________________

Assoc. Prof. Dr. M. Tuğrul Yılmaz
Civil Engineering, METU ________________

Assoc. Prof. Dr. Yakup Darama
Civil Engineering Department, Atılım University ________________

Assoc. Prof. Dr. Aynur Şensoy Şorman
Civil Engineering Department, Eskisehir Technical University ________________

Assoc. Prof. Dr. Koray K. Yılmaz
Geological Engineering Department, METU ________________

Date: 23.01.2019

I hereby declare that all information in this document has been obtained and presented in accordance with academic rules and ethical conduct. I also declare that, as required by these rules and conduct, I have fully cited and referenced all material and results that are not original to this work.

Name, Surname: Mahdi Hesami Afshar

Signature:

ABSTRACT

INVESTIGATION OF ADDED UTILITY OF NONLINEAR TECHNIQUES IN RESCALING SOIL MOISTURE DATASETS

Hesami Afshar, Mahdi
Doctor of Philosophy, Civil Engineering
Supervisor: Assoc. Prof. Dr. M. Tuğrul Yılmaz

January 2019, 156 pages

Soil moisture plays a key role in weather forecasting, hydrologic modeling, climate change studies and water resource management. There are multiple ways to estimate this essential variable (i.e., remote sensing, modeling, station-based observations) and clear benefits associated with merging independent estimates. However, the time series of these products generally contain systematic differences that must be removed through rescaling before the application of data merging approaches (e.g., data assimilation and data fusion). In this study, the added utility of nonlinear rescaling methods relative to linear methods in the framework of creating a homogenous soil moisture time series has been explored. The performances of 18 linear and nonlinear rescaling methods are evaluated in two different case studies of: 1) rescaling the AMSR-E LPRM soil moisture dataset to station-based watershed average soil moisture (WASM), and 2) fusing of four different soil moisture products (ASCAT, AMSR-E LPRM, API, and NOAH) via a naive data fusion scheme and multiple rescaling approaches. Accordingly, experiments are performed using various rescaling methods, where the rescaled and fused datastes are validated using observations obtained over four United States Department of Agriculture (USDA) Agricultural Research Service (ARS) watersheds, which are frequently used in the validation efforts of the soil moisture satellite missions. The results of a total of 18 different methods show that the nonlinear methods improve the correlation and error statistics of the rescaled product compared to the linear methods. In general, the method that yielded the best results using training data (ELMAN ANN) improved the validation correlations, on average, by 0.052, whereas JORDAN ANN and MARS, yielded correlation improvements of 0.038 and 0.01, respectively. On the other hand, results related to the validation of fusion of products obtained via a smooth-deviance decomposition rescaling technique, show, on average, a correlation improvement of 0.03, compared to the other widely implemented simple linear rescaling approaches. The overall results show that a large majority of the similarities between soil moisture datasets are due to linear relations; however, nonlinear relations clearly exist, and the use of nonlinear rescaling methods or implementation of linear methods with a proper rescaling approach clearly improves the accuracy of the rescaled product. Additionally, the selection of the reference dataset from higher quality datasets in the rescaling steps results in considerably increased fused product accuracy.

Keywords: Soil moisture, Rescaling, Data fusion, Remote sensing

ÖZ

LİNEAR OLMAYAN METODLARIN TOPRAK NEMİ VERİSETLERİNİN ÖLÇEKLENDİRMENE YAPTIPI KATKININ ARAŞTIRILMASI

Hesami Afshar, Mahdi
Doktora, İnşaat Mühendisliği
Tez Danışmanı: Doç. Dr. M. Tuğrul Yılmaz

Ocak 2019, 156 sayfa

Toprak nemi; hava tahmini, hidrolojik modellemede, iklim değişikliği çalışmalarında ve su kaynakları yönetiminde kilit bir rol oynar. Bu temel değişkeni elde etmenin birçok yolu vardır (örneğin, uzaktan algılama, modelleme, istasyon temelli gözlem yöntemleri). Bu ürünlerin zaman serileri genellikle veri birleştirme yaklaşımlarının (örneğin, veri özümseme ve veri birleştirme) uygulanmasından önce yeniden ölçeklendirme yoluyla çıkarılması gereken sistematik farklılıkları içerir. Bu çalışmada, homojen bir toprak nemi zaman serisi oluşturma işleminde doğrusal olmayan yeniden ölçeklendirme yöntemlerinin doğrusal yöntemlere göre ilave faydası araştırılmıştır. Doğrusal ve doğrusal olmayan toplam 18 adet yeniden ölçeklendirme yönteminin performansı, iki farklı durum çalışmasında değerlendirilmiştir: 1) AMSR-E LPRM toprak nemi veri setini istasyon bazlı su havzası ortalama toprak nemini (WASM) referans alarak yeniden ölçeklendirme ve 2) dört farklı toprak nemi ürününün eşit ağırlıklı ve çoklu yeniden ölçeklendirme yaklaşımlarıyla birleştirilmesi (ASCAT, AMSR-E LPRM, API ve NOAH). Deneyler çeşitli ölçeklendirme yöntemleri kullanılarak gerçekleştirilmiştir ve sonuçta elde edilen birleştirilmiş veri setleri birçok uydu toprak nemi miyonunun doğrulaması çalışmalarında yaygınlıkla kullanılan Amerika Birleşik Devletleri Tarım Bakanlığı (USDA) Tarımsal Araştırma Servisi'nin (ARS) dört havzasında elde edilen veri setleri kullanılarak doğrulanmıştır.

Toplam 18 farklı yöntem ile yeniden ölçeklendirilmiş ürünün korelasyon ve hata istatistikleri doğrusal olmayan yöntemlerin doğrusal yöntemlere kıyasla daha iyi sonuçlar verdiğini göstermektedir. Genel olarak, kalibrasyon verilerini kullanarak en iyi sonuçları veren yöntem (ELMAN ANN), doğrulama korelasyonlarını ortalama 0.052 artırırken, JORDAN ANN ve MARS, sırasıyla 0.038 ve 0.01 korelasyon artışı sağlamıştır. Öte yandan, pürüzsüz-sapma ayrıştırma yeniden ölçeklendirme tekniği ile elde edilen ürünlerin birleştirilmesi, yaygın olarak uygulanan diğer basit doğrusal yeniden ölçeklendirme yaklaşımlarına kıyasla, ortalama olarak 0.03 bir korelasyon gelişimi göstermektedir. Genel sonuçlar, toprak nemi veri setleri arasındaki benzerliklerin büyük çoğunluğunun doğrusal ilişkilerden kaynaklandığını ve bununla birlikte doğrusal olmayan ilişkilerin varlığı da açıkça görülmektedir. Doğrusal olmayan yeniden ölçeklendirme yöntemlerinin kullanılması veya doğrusal yöntemlerin uygun bir yeniden ölçeklendirme yaklaşımı ile kullanılması, yeniden ölçeklendirilen ürünün doğruluğunu açık bir şekilde arttırmaktadır. Öte yandan verilerin yeniden ölçeklendirilmesi esnasında seçilen referans veri setinin daha doğru veri setlerinin arasından seçimi birleştirilen ürünün doğruluğunu önemli bir şekilde arttırmaktadır.

Anahtar Kelimeler: Toprak nemi, Yeniden ölçeklendirme, Veri birleştirme, Uzaktan algilama

To My Beloved Parents

ACKNOWLEDGMENTS

This thesis is a product of a collaborative work supported by many people in their own ways. First of all I would like to thank my supervisor Assoc. Prof. Dr. M. Tuğrul Yılmaz who never gave up on me even when I was in another country and answered all my questions with patience. I am deeply grateful for his generous support.

I thank Michael Cosh of the U.S. Department of Agriculture for the USDA ARS watershed soil moisture datasets, Robert Parinussa of Vrije Universiteit Amsterdam for LPRM datasets, Wouter Dorigo of Technische Universitat Wien for ASCAT datasets, and NASA Goddard Earth Sciences (GES) Data and Information Services Center (DISC) for Noah datasets.

The committee members: Assoc. Prof. Dr. Yakup Darama, Assoc. Prof. Dr. Aynur Şensoy Şorman, Assoc. Prof. Dr. Koray K. Yılmaz, Prof. Dr. Ismail Yucel greatly assisted me through their insightful comments in shaping the final draft of this study. I am very thankful to them for spending their time and efforts.

I have greatly benefited from the feedbacks and comments of Assoc. Prof. Dr. Koray Yilmaz and Prof. Dr. Ismail Yucel during my PhD research. I would like to express my gratitude for sharing their knowledge and their constructive comments and suggestions on my study. I would also like to pay my deepest gratitude to Prof. Dr. Ali Unal Şorman. He helped me all along my PhD study. I will be appreciating this in my whole life.

I am very thankful to Dr. Wade T. Crow who collaborated in my research and helped to conduct my thesis research. His guidance was very important in the decision of my research topic.

I would like to thank my group members: Burak Bulut, Eren Duzenli, Erhan Ersoy, Alper Önen, Muhammed Amjad, Kaveh Yousefi, Nilay Dogulu, Rizwan Aziz, Faisal Baig, Ipek Karasu and Farhad Ghiaei for all their help and support.

Not only my friends from the academic circle but also my friends with whom I share the burden of our lives were always with me through their endless love, joy and support. For this, I would like to thank: Farid Feyzolahpour, Hamed and Hadi Mahmoudzadeh, and Mehdi Komarizadeh.

I would also like to thank my uncles and my aunts for supporting and encouraging me both within this study and throughout my life.

In every decision I make, my brother Mohammad H. Afshar and my sisters Laleh and Maryam H. Afshar have always been backing me. I would like to thank them. I know that I will always become stronger when I have them beside me.

I would like to express my deepest gratitude to my parents Haleh Manavi and Farrokh H. Afshar for their unconditional and endless love.

This research is supported by TÜBİTAK ARDEB ÇAYDAG Career Development Program (3501) (Project No: #114Y676).

TABLE OF CONTENTS

LIST OF TABLES

TABLES

LIST OF FIGURES

FIGURES

LIST OF ABBREVIATIONS

AMB	Absolute mean bias
ANN	Artificial neural network
API	Antecedent Precipitation Index
ASCAT	Advanced Scatter meter
CCI	Climate Change Initiative
CDF	Cumulative Distribution Function
CDFM	CDF Matching
Cor	Correlation
DOY	Day of year
GLDAS	Global Land Data Assimilation System
GP	Genetical programming
Id	Identity
ISMN	International Soil Moisture Network
LPRM	Land Parameter Retrieval Model
LR	Little River
LW	Little Washita
MAR	Multiple Adaptive Regression Splines
MERRA	Modern-Era Retrospective Analysis for Research and Applications
ND	No Decomposition
RC	Reynolds Creek
REF	Reference
REG	Linear regression
SA	Seasonality Anomaly
SMAP	Soil Moisture Active Passive
SMOS	Soil Moisture and Ocean Salinity
SD	Smooth Deviance
SNR	Signal to noise ratio
SVM	Support vector machine
std	Standard deviation
TCA	Triple collocation analysis
Tr_best	Train best
TV	Time varying
VAR	Variance matching
WASM	Watershed average soil moisture
WG	Walnut Gulch

LIST OF SYMBOLS

μ	Mean
σ	Standard deviation
ρ	Correlation
C	Copula function
θ	Copula parameter
P	Copula parameter
B	Basis function
φ	Nonlinear mapper
K	Kernel function
e	Error
a	Lagrange multiplier
ε	Error
U	Added utility
F	Fused product

CHAPTER 1

INTRODUCTION

1.1. Importance of Soil Moisture and Its Applications

Soil moisture (both surface- and root zone- soil moisture) is one of the key variables in the heat and mass exchanges between surface and atmosphere (Koster et al., 2004) as well as in plant growth (Lawrence & Hornberger, 2007).

Among different drought types (e.g., meteorological-, hydrological-, agricultural-, and socio-economic- droughts), the agricultural drought is almost under direct impact of the soil moisture (Mishra & Singh, 2010). The amount of soil moisture content during growing period of plants adversely affects the crop yield, and consequently, the agricultural production (Panu & Sharma, 2002). Recently, the agricultural drought has been considered as one of the important factors of social conflicts in developing countries (Kelley, Mohtadi, Cane, Seager, & Kushnir, 2015).

Moreover, soil moisture, due to its retention (Han, Crow, Holmes, & Bolten, 2014), impacts the rainfall-runoff process, erosion, forecast skill, and many other aspects of life (Figure 1.1). The spatiotemporal dynamics of the soil moisture are commonly used to qualify the vulnerability of the catchment in runoff generation (Bronstert et al., 2012). In fact, the spatial patterns of soil moisture is particularly valuable for calibration and validation of hydrological models (Parajka et al., 2006; Rinderer, Kollegger, Fischer, Stähli, & Seibert, 2012) and the assimilation of observed soil moisture data in rainfall-runoff models significantly improves the accuracy of flood forecasting (Aubert, Loumagne, & Oudin, 2003; Bronstert et al., 2012). Hence, describing the spatial distribution and temporal changes of soil moisture contributes significantly to the development of accurate climate, ecological and hydrological models at global, regional and local levels scales (W. Dorigo et al., 2012).

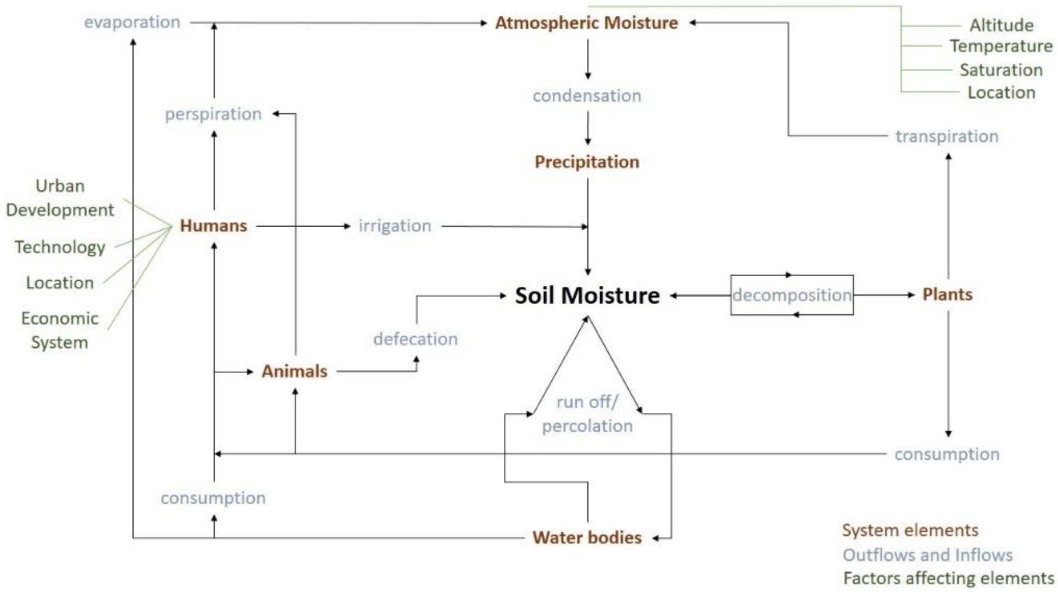

Figure 1.1. The water cycle surrounding soil water content (Explorations, 2011)

1.2. Soil Moisture Retrieval

Soil moisture can be retrieved through different methods (i.e., in-situ measurements, numerical modeling, and remote sensing). Direct monitoring methods, such as weighting method and electromagnetic methods, provide soil moisture information for specific fine spatial resolutions with high temporal resolution (e.g., 30 minutes or one hour; Figure 1.2). However, the use of these datasets are impractical for studies focusing on large areas. Instead, hydrological model- or satellite remote sensing-based soil moisture datasets are used for large scale applications related with drought monitoring (Afshar, Sorman, & Yilmaz, 2016), crop yield monitoring (Anderson et al., 2015, 2016), improvement of hydrological models via assimilation of observations (Wade T Crow & Wood, 2003; Houser et al., 1998; Lievens et al., 2015; Yilmaz, DelSole, & Houser, 2011).

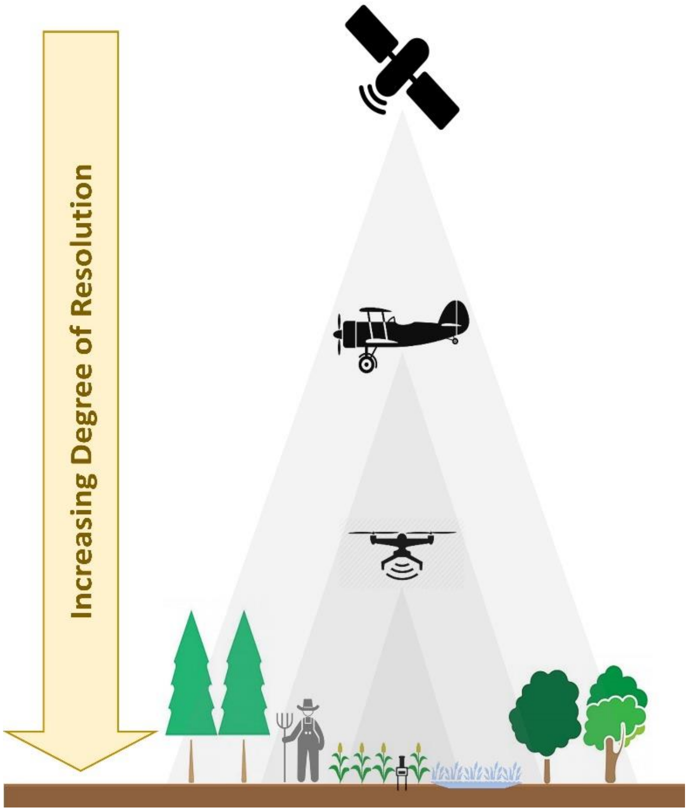

Figure 1.2. Differences among spatial resolution of different soil moisture sensors (from top to bottom: Satellite, Airborne, Drone, and Ground based sensors)

Owing to the high number of studies using these datasets in large scale applications, many soil moisture products have been produced using hydrological model- and remote sensing-based methods. Complex land surface models [e.g., Global Land Data Assimilation System (GLDAS), Modern-Era Retrospective Analysis for Research and Applications (MERRA), etc.] and much simpler hydrological models (e.g., Antecedent Precipitation Index, API) offer spatiotemporally continuous soil moisture datasets. However, these land surface models heavily rely on parameters that often have variability in time and space, while their actual measurements are often impractical (Figure 1.3).

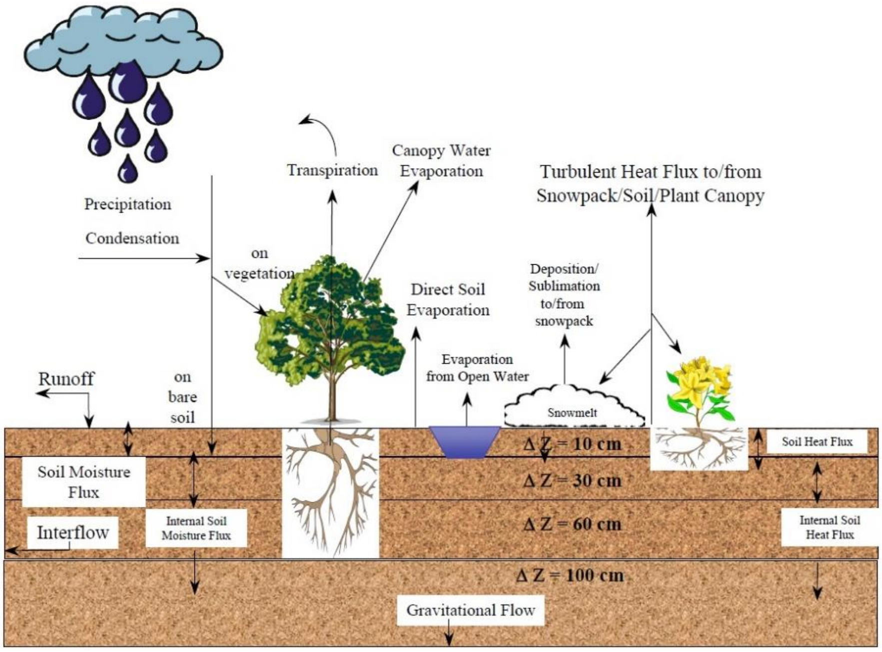

Figure 1.3. Schematic representation of NOAH LSM and forcing variables in it (Ek et al., 2003)

Remote sensing based approaches also provide spatially continuous soil moisture datasets (Figure 1.4) like Advanced Scatter meter [ASCAT; (Wolfgang Wagner, Lemoine, & Rott, 1999)], Soil Moisture and Ocean Salinity [SMOS; (Kerr et al., 2001)], and Soil Moisture Active Passive (SMAP; (Entekhabi, Njoku, et al., 2010)]. However, these datasets only reflect conditions related to the top of the soil surface (~ 3-5 cm), and their temporal and spatial resolutions are different from each other and mostly are lower than models, while the retrieval algorithms depend on many parameters (e.g., land cover, topography, and radiative activities).

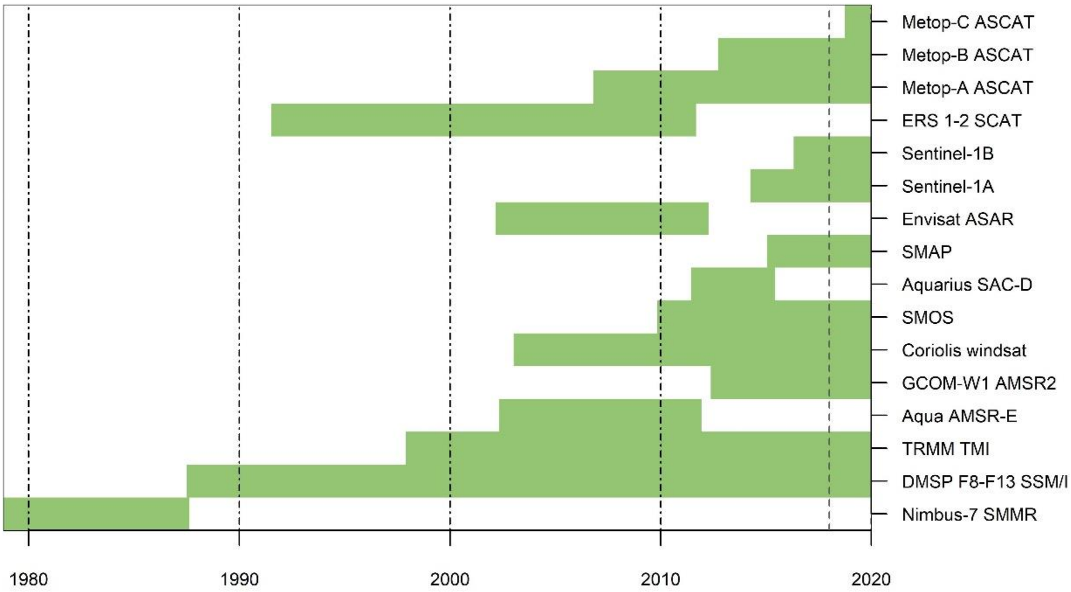

Figure 1.4. Availability of sensors used in soil moisture retrievals (both active and passive)

1.3. Literature Review

Given these approaches can provide different soil moisture datasets for the same location and same time period (they all contain random errors with different characteristics), it is often desirable to merge these different time series so that more accurate estimates could be obtained.

Liu, et al. (2011) merged the information derived from satellite based passive and active microwave sensors (AMSR-E and ASCAT). For this purpose, they initially rescaled parent product using CDF matching methodology (Reichle & Koster, 2004) to the space of land surface model data set and fused them in that space. Their results showed that, although the fusion framework increases the number of observations, it can minimally change the accuracy of soil moisture retrievals.

Yilmaz, et al. (2012) through merging of model-, thermal infrared remote sensing-, and microwave remote sensing-based soil moisture estimates, obtained a new product within a least squares framework. They validated their merged anomaly product against in-situ measurements and found their merged product to be more accurate than individual input products.

Schalie, et al. (2017) evaluated three different fusion approaches including neural networks, regressions, and the Land Parameter Retrieval Model (LPRM) and found out that the neural networks approach gives the highest correlation coefficient among different fusion approaches while the regression and LPRM approach can closely follow up the neural networks approach.

Beside of all above mentioned studies, the ESA Climate Change Initiative (CCI) team initiated a project with the goal of developing a complete and consistent global soil moisture dataset in year 2010 and released its first product in year 2012. The ESA-CCI soil moisture product (W. Dorigo et al., 2017; Gruber, Dorigo, Crow, & Wagner, 2017; Liu et al., 2012, 2011; W. Wagner et al., 2012) merges wide range of the active and passive soil moisture retrievals, with a methodology very similar to that of Liu, et al. (2011).

A review of the studies mentioned above indicates that fused soil moisture anomalies are more correlated with ground measurements and/or modeled soil moisture datasets rather than the individual products that have been merged. Moreover, all the mentioned studies confirm that the fundamental need of any data fusion study, is to have soil moisture products at the same temporal scale. However, before such merging methodologies can be implemented, the various systematic differences that exist between soil moisture estimates obtained from different platforms and/or sensors should be alleviated (Dirmeyer et al., 2004; Reichle, Crow, Koster, Sharif, & Mahanama, 2008; C.-H. Su & Ryu, 2015; Yilmaz & Crow, 2013; Yin et al., 2014). An example of such systematic differences (e.g., differences in their ranges, fluctuations, and availability over the same location (Little River watershed in Tifton, GA) at the same time period; September 19^{th} to November 18^{th} of year 2010) is presented in Figure 1.5, where three platforms of soil moisture retrieval (i.e., remote sensing, model based, and in-situ measurements) are arranged to three panels from top to bottom respectively.

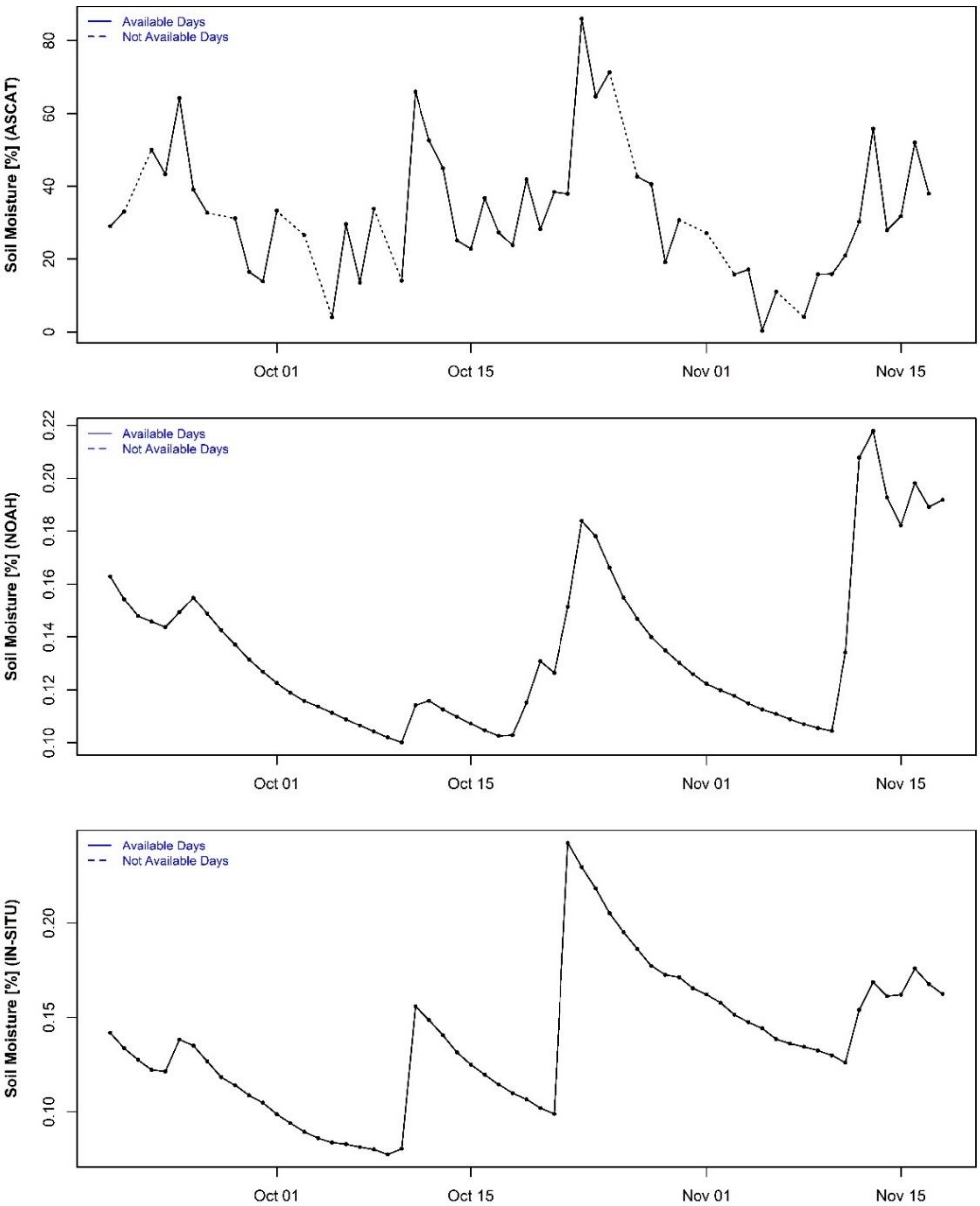

Figure 1.5. Systematic differences in remotely sensed- model based-, and in-situ based- soil moisture products over the same location (longitude:-98.10, latitude: 34.95) in time period of September 19th to November 18th of year 2010

Many different methods are proposed to handle these systematic differences between soil moisture products, where an unscaled original product Y is rescaled to the space of a reference product X. The goals of such methodologies include minimizing the variability of the difference between the rescaled product and the reference product, maximizing the correlation between them, or matching the total variability of an unscaled product to an arbitrary reference dataset (Hain, Crow, Mecikalski, Anderson, & Holmes, 2011; Miralles, De Jeu, Gash, Holmes, & Dolman, 2011; Parinussa et al., 2015; Scipal, Holmes, de Jeu, Naeimi, & Wagner, 2008; Stoffelen, 1998; Zwieback et al., 2016).

Based on above mentioned goals, the rescaling method can vary from linear ones [e.g., first order linear regression (REG), variance matching (VAR), Triple collocation analysis (TCA), etc.] to CDF matching (CDFM) and nonlinear techniques [e.g., multi adaptive regression splines (MAR), support vector machines (SVM), artificial neural networks (ANN), etc.].

Once a particular "rescaling method" (e.g., VAR, REG, CDFM, MAR, SVM, ANN, etc.) is selected for a specific application, this method can be implemented using different approaches that consider different time scales (Yilmaz et al., 2016). The rescaling approaches affect the accuracy statistics of the rescaled product, even though, by definition, a particular rescaling method is selected to be the optimum method (i.e., yield least errors) for a particular application. For example, a rescaling method can be tuned for the entire time series or for each month separately (rescaling coefficients or product dependencies are assumed to be constant or time-varying). If the reference product, that any given product is rescaled to, is more accurate than the rescaled product, then implementation of rescaling methods strongly using time-varying coefficients (e.g., using monthly rescaling coefficients rather than using a single coefficient for the entire time series, or rescaling seasonality and anomaly components separately rather than rescaling them using the same rescaling coefficients) yield higher accuracy rescaled product than weakly rescaled products. The reverse is also true that in the presence of relatively less accurate reference product, weakly rescaling products yield higher accuracy rescaling products (Yilmaz et al., 2016).

Both the rescaling method and its implementation approach can impact the optimality of the rescaled product's statistics (Yilmaz & Crow, 2013; Yilmaz et al., 2016). The optimality of a rescaling methods largely depend on the goal of the rescaling methodology (Yilmaz & Crow, 2013); yet performances of such rescaling methods are also affected by degree to which the underlying assumptions of the rescaling methods are met (Yilmaz & Crow, 2013) and by their implementation approach (Yilmaz et al., 2016).

Satellite-based soil moisture data are often validated with using in-situ measurements (Jackson et al., 2012, 2010), which exhibit significantly higher local non-linearity due to soil moisture dynamics (Wade T Crow & Wood, 2003). The spatial resolution difference between in-situ measurements and remotely sensed soil moisture products (i.e. point versus areal average) is another source that introduces nonlinearity into the system. Recently, Zwieback et al. (2016) introduced a non-parametric CDFM method to address the impact of non-linear relationships on the error statistics identified using TCA. The study of Zwieback et al. (2016) emphasizes the existing quadratic relationships between the actual signal components of different Soil moisture products, which can lead to non-linear relationships. Therefore, it is conventional that such nonlinear relationships existing between soil moisture data sets may not be captured by using linear methods and use of use of non-linear methods may be necessary.

1.4. Goal of the Study

Among commonly linear and nonlinear rescaling methods that are applied in studies focusing on removing systematic differences between soil moisture products, the CDFM (Reichle & Koster, 2004) is arguably the mostly commonly used. In addition, linear regression- (Wade T. Crow & Zhan, 2007), variance matching- (Draper, Walker, Steinle, de Jeu, & Holmes, 2009), triple collocation- (Yilmaz & Crow, 2013), copula- (Leroux et al., 2014), wavelet- (C.-H. Su & Ryu, 2015), quadratic polynomial- (Zwieback, et al., 2016) based methods have been also utilized for this purpose. However, the inter-comparison of the performance of abovementioned methods has not been explored in the soil moisture rescaling studies.

REG, VAR, TCA, and CDFM have unique results and are implemented widely in rescaling studies. Yilmaz and Crow (2014) have been investigated the optimality of linear methods in the context of data assimilation. However, because the limited usage of nonlinear methods in the soil moisture rescaling framework, the performance of them in comparison to the linear methods has been remained unexplored. Therefore there is still room to investigate and inter-compare the relative performance of linear and nonlinear methods in order to better understand the degree of nonlinearities existing in the soil moisture products.

Moreover, based on this fact that the rescaling methods are eventually used as the cornerstone of the soil moisture merging methodologies, the investigation of the impact of their selection over the performance of the final fused soil moisture estimates is also necessary. Earlier studies have investigated the performance of different rescaling methodologies (Yilmaz & Crow, 2013; Yilmaz et al., 2016), However, so far no study have specifically investigated the impact of the most of nonlinear methods (e.g., SVM, and MAR) in a data merging methodology.

This study is the first to use and compare different rescaling methods (including linear and nonlinear ones) in the context of rescaling soil moisture datasets. Meanwhile, beside of these inter-comparisons, this study is the first to investigate the impact of different linear and nonlinear rescaling methods and their way of implementation approach over the accuracy of the data fusion process. Hence the goal of this study in addition to the comparison of the rescaling methods in rescaling of soil moisture time series, is to investigate all of the aspects of data fusion (including the impact of the parent soil moisture product selection, the impact of rescaling methods, rescaling techniques, application style of rescaling methods, and the reference of data fusion frame work). The methodologies and the datasets used in this study are given in the Chapter 2; the results and their discussions are given in the Chapter 3, and concluding remarks are given in the last Chapter 4.

CHAPTER 2

MATERIALS AND METHODS

2.1. Rescaling Methods

2.1.1. Linear Regression

Linear rescaling methods have been widely used to rescale soil moisture time series to reduce their inconsistency (Brocca et al., 2011; W. T. Crow, Su, Ryu, & Yilmaz, 2015; Wade T. Crow & Zhan, 2007). Overall, linear rescaling methods are implemented by considering the most general linear relation between a reference dataset (X) and an original unscaled dataset (Y) in the form of:

$$Y^{*} = \mu_X + (Y - \mu_Y)c_Y \tag{1}$$

where Y^{*} is the rescaled version of Y; μ_X and μ_Y are time averages of X and Y, respectively; and c_Y is a scalar rescaling factor (Figure 2.1). Here, c_Y is found using REG, VAR, and TCA-based linear methods (Yilmaz & Crow, 2013):

$$c_Y^R = \rho_{XY}\,\sigma_X/\sigma_Y \tag{2}$$

$$c_Y^V = \sigma_X/\sigma_Y \tag{3}$$

$$c_Y^T = \Sigma_{xz}/\Sigma_{yz} \tag{4}$$

where Z is a third product that is similar to products X and Y; Σ_{xz} and Σ_{yz} are covariances between X-Z and Y-Z, respectively; c_Y^R, c_Y^V, and c_Y^T are the linear rescaling factors for the REG-, VAR-, and TCA-based methods, respectively; σ_X and σ_Y are the standard deviations of X and Y, respectively; and ρ_{XY} is the correlation coefficient between X and Y. Accordingly, the rescaled products are estimated as

$$Y_{REG}^{*} = \mu_X + (Y - \mu_Y)c_Y^R \tag{5}$$

$$Y_{VAR}^{*} = \mu_X + (Y - \mu_Y)c_Y^V \tag{6}$$

$$Y_{TCA}^{*} = \mu_X + (Y - \mu_Y)c_Y^T \tag{7}$$

where Y^*_{REG}, Y^*_{VAR}, and Y^*_{TCA} are the rescaled products using REG, VAR, and TCA methods, respectively. The schematic representation of linear regression lines for three linear methods of REG, VAR, and TCA and the differences in their slopes and intercept values is shown in Figure 2.1.

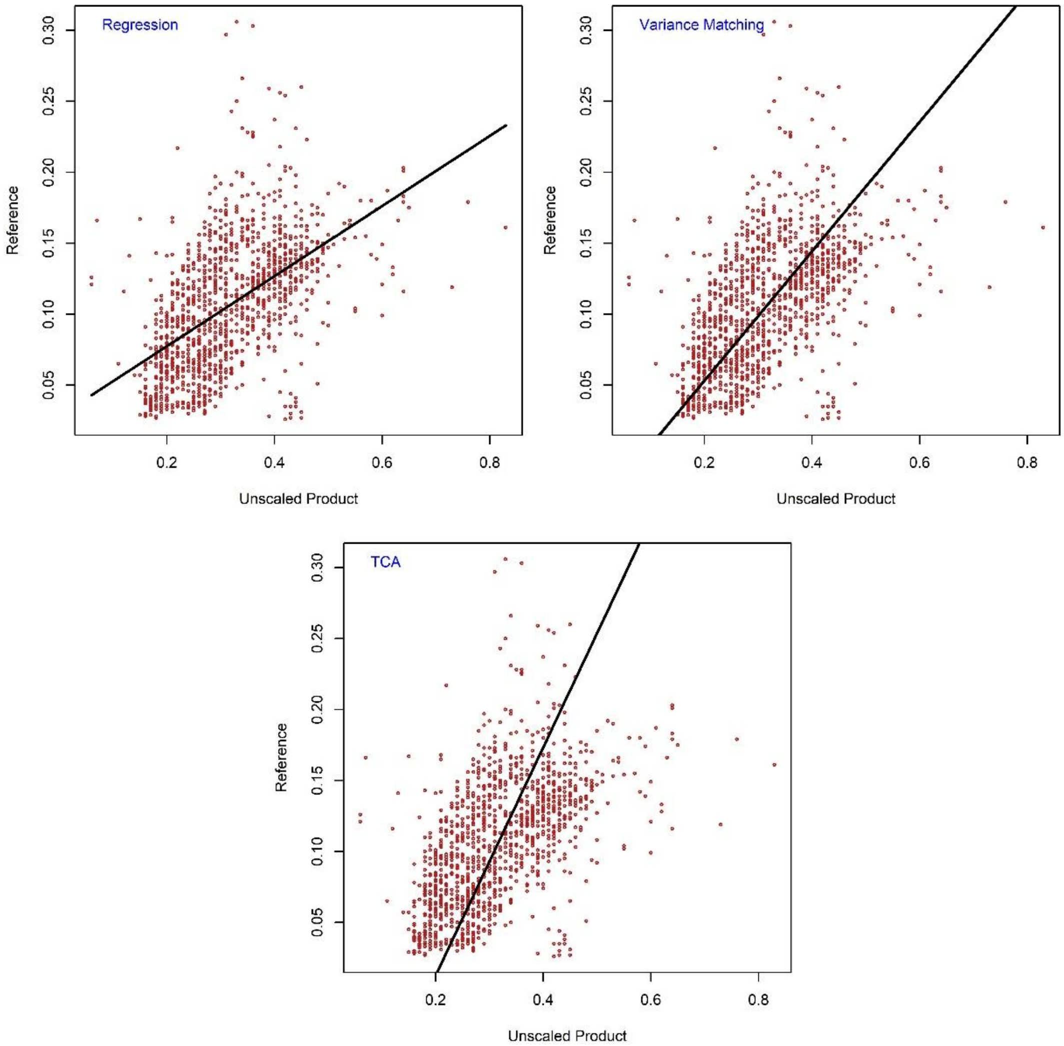

Figure 2.1. Comparison of REG, VAR, and TCA rescaling methods

2.1.2. CDF Matching

The CDFM (Reichle & Koster, 2004) is one of the earliest and arguably the most commonly used method in soil moisture rescaling studies. This method has been widely used in many applications, particularly in studies that focus on data assimilation (Drusch, 2007; Li et al., 2010). The aim of this method is to eliminate the differences between the statistical moments of two soil moisture datasets. The schematic representation of the CDFM used in this study is given in Figure 2.2 (i.e., the path shown with red color).

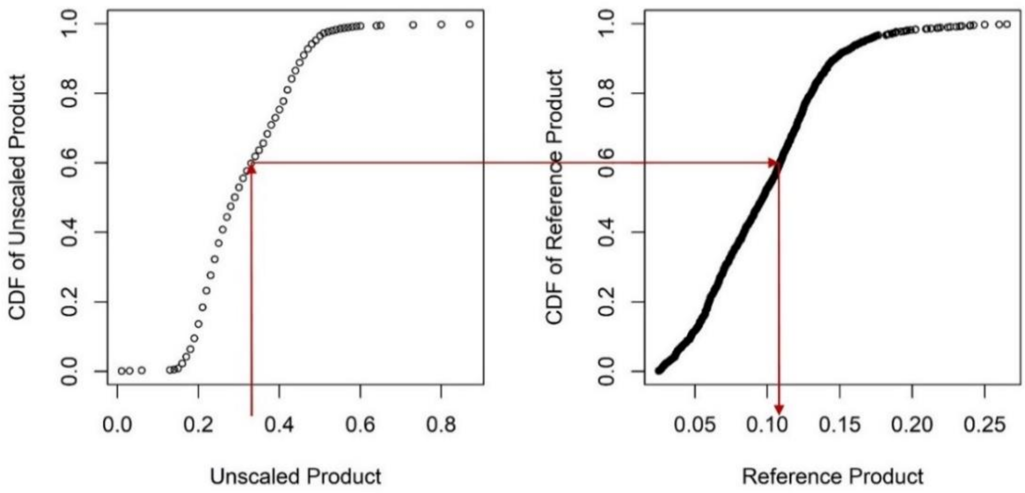

Figure 2.2. Schematic representations of the CDFM rescaling method

The CDFM rescaling method can be applied through two general approaches to the soil moisture products based on their cumulative distribution functions. The first approach tries to match the lower order moments of time series (e.g., the first and second) to the reference one (Variance matching). While the second approach (called here as CDFM) matches the empirical cumulative distribution functions of the unscaled product directly to the reference product ones. The difference between the two methods are represented in Figure 2.3. For more details, readers are referred to the study of Reichle and Koster (2004).

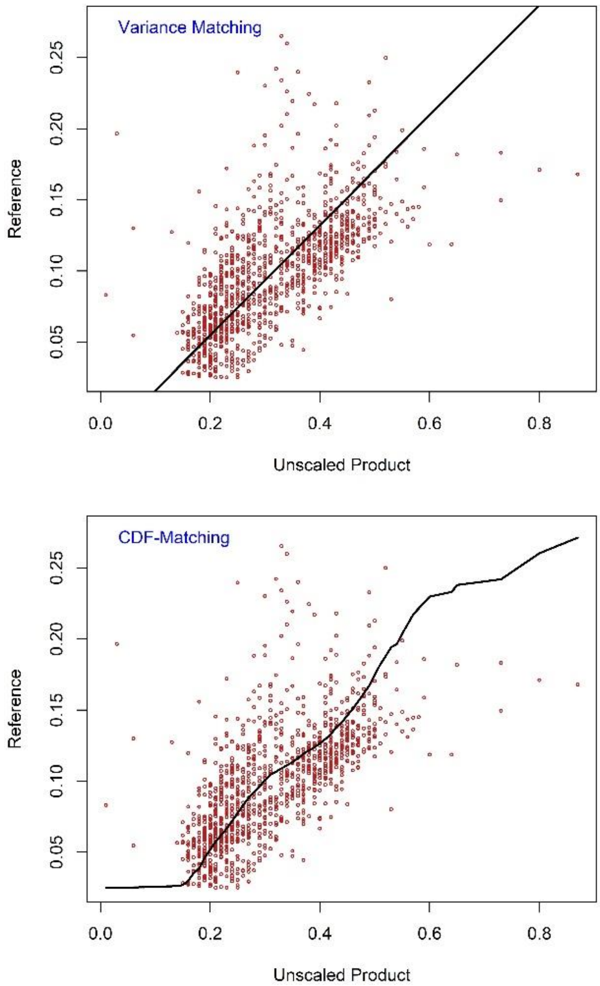

Figure 2.3. Comparison of VAR and CDFM rescaling methods

2.1.3. Copula

Copula functions are widely used to describe the multivariate dependence between random variables by using their univariate distributions. More specifically, this method enables the estimation of a multivariate CDF of random variables by using copula functions that utilize the univariate CDF of random variables, assuming the marginal probability distributions follow a uniform distribution. The general equation for the estimation of the multivariate distribution in the copula approach is described by Sklar (1959) as follows:

$$\mathrm{C}\left(\mathrm{CDF}_{\mathrm{u}_1}, \mathrm{CDF}_{\mathrm{u}_2}, \dots, \mathrm{CDF}_{\mathrm{u}_\mathrm{N}}\right) = \mathrm{Pr}(\mathrm{U}_1 \leq \mathrm{u}_1, \mathrm{U}_2 \leq \mathrm{u}_2, \dots, \mathrm{U}_\mathrm{N} \leq \mathrm{u}_\mathrm{N}) \qquad (8)$$

where C is a unique multivariate copula function that contains all of the dependence information among the datasets through a single parameter (e.g., P or θ). Here, Sklar's theorem implies that for any group of random variables $\mathrm{U_1, U_2, \dots, U_{N-1}}$, there exists a copula function $\mathrm{C\left(CDF_{u_1}, CDF_{u_2}, \dots, CDF_{u_N}\right)}$ that links these variables through an estimation of the multivariate probability distribution of these random variables.

The copula approach explicitly requires a conditional multivariate CDF to find the solution to a rescaling problem, which can be found via the partial derivative of the copula functions in the following form:

$$\mathrm{C_{U_N|U_1,U_2,\dots,U_{N-1}}} = \frac{\partial \mathrm{C(CDF_{u_1}, CDF_{u_2}, \dots, CDF_{u_N})}}{\partial \mathrm{C(CDF_{u_1}, CDF_{u_2}, \dots, CDF_{u_{N-1}})}} \tag{9}$$

Here, the goal is to first estimate $\mathrm{CDF_{u_N}}$ and to then retrieve the value of $\mathrm{U_N}$ by utilizing the CDF of the observed variables $(\mathrm{U_1, U_2, \dots, U_{N-1}})$. Here, these observed variables could be selected as observations from different platforms as well as lagged values of the same variable to be predicted. However, the solution of equation 14 requires knowledge of the conditional CDF of the observed variables $(\mathrm{CDF_{U_N|U_1,U_2,\dots,U_{N-1}}})$, which can be found through an iterative procedure (for details on this optimal solution, see the study of Leroux et al., 2014).

1- Estimation of $\mathrm{CDF_{u_1}, CDF_{u_2}, \dots, and\ CDF_{u_N}}$,
2- Fitting of copulas to $\mathrm{CDF_{u_1}, CDF_{u_2}, \dots, and\ CDF_{u_N}}$ (i.e., estimation of P and θ parameters),
3- Calculation of errors and correlations between true dataset and predicted $\mathrm{U_N}$ separately for $\mathrm{C_{U_N|U_1,U_2,\dots,U_{N-1}}} = 0.01$ to 0.99.
4- Selection of the best $\mathrm{C_{U_N|U_1,U_2,\dots,U_{N-1}}}$ value which minimizes the standard deviation of the difference between $\mathrm{U_N}$ and $\mathrm{U_N}^*$ and maximizes ρ between $\mathrm{U_N}$ and $\mathrm{U_N}^*$ simultaneously,
5- Estimation of $\mathrm{CDF_{u_N}}$ using $\mathrm{C\left(CDF_{u_1}, CDF_{u_2}, \dots, CDF_{u_N}\right)}$, $\mathrm{C(CDF_{u_1}, CDF_{u_2}, \dots, CDF_{u_{N-1}})}$, obtained P and θ parameters (step 2), and selected $\mathrm{C_{U_N|U_1,U_2,\dots,U_{N-1}}}$ (step 4),
6- Estimation of $\mathrm{U_N}$ using inverse relation of $\mathrm{U_N}$ and $\mathrm{CDF_{u_N}}$.

The summary of copula method procedures and differences between copula and CDFM methods is presented in the Figure 2.4 where copula projection plane (panel C in Figure 2.4) has curved shape compared to projection line of CDFM (i.e., straight line in panel A). The optimal shape and location of this projection line curvature in panel C can be found by altering the parameters P, θ, and/or $C_{U_N|U_1,U_2,\ldots,U_{N-1}}$ respectively, while the optimality depends on the goal of the application.

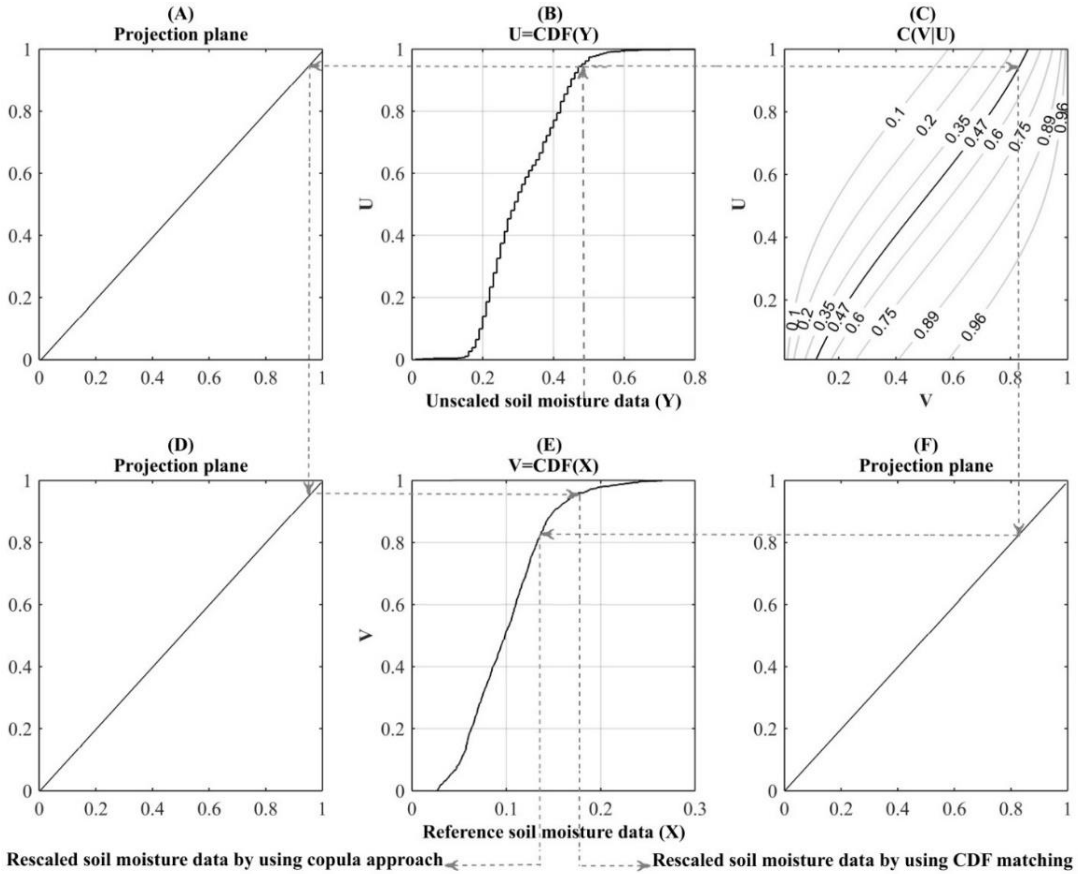

Figure 2.4. Schematic representations of the CDFM and Copula based rescaling methods. The paths in the BADE and BCFE panels represent the CDFM and Copula methods for rescaling of unscaled product Y to the space of reference product X, respectively. C(X|Y)=0.47 is plotted with darker color in panel C to represent the best performing projection line of the Copulated with darker color in panel C to represent the best performing projection line of the Copula

The list of copula functions used in this study [five total: NORMAL (Frahm, Junker, & Szimayer, 2003), CLAYTON (CLAYTON, 1978), GUMBEL (Gumbel, 1960), FRANK (Genest, 1987), and JOE (Joe, 1997)] and their properties are given in

Table 2.1. Moreover, the differences between the conditional CDF line of them (different copula flavors) and their impact over rescaling of soil moisture products is shown in in Figure 2.5. In this study, all of the steps, including the calculation of the CDFs and the fitting of different copulas, are performed using the R programming language package "Copula", which was written by Hofert et al. (2012). For more information about the mathematical properties of the copula function and families, fitting procedures, and simulation issues, see the studies by Genest and Favre (2007) and Nelsen (1999).

Table 2.1. *Copula functions (in two dimension space), parameters (P and θ), and characteristics used in this study.*

Copula	$C_{YX}(F_Y, F_X)$	*Family*
Normal	$\int_{-\infty}^{\emptyset^{-1}(F_Y)} \int_{-\infty}^{\emptyset^{-1}(F_X)} \frac{\exp\left[-\frac{{F_Y}^2 - 2PF_YF_X + {F_X}^2}{2(1-P^2)}\right]}{2\pi(1-P^2)^{1/2}} dF_Y dF_X$	Elliptical
Clayton	$({F_Y}^{-\theta} + {F_X}^{-\theta} - 1)^{-1/\theta}$	Archimedean
Gumbel	$\exp\{[(-\ln F_Y)^{\theta} + (-\ln F_X)^{\theta}]^{\frac{1}{\theta}}\}$	Archimedean
Frank	$\frac{-1}{\theta}\ln[1 + \frac{(e^{-\theta F_Y} - 1)(e^{-\theta F_X} - 1)}{e^{-\theta} - 1}]$	Archimedean
Joe	$1 - [(1-F_Y)^{\theta} + (1-F_X)^{\theta} - (1-F_Y)^{\theta}(1-F_X)^{\theta}]^{\frac{1}{\theta}}$	Archimedean

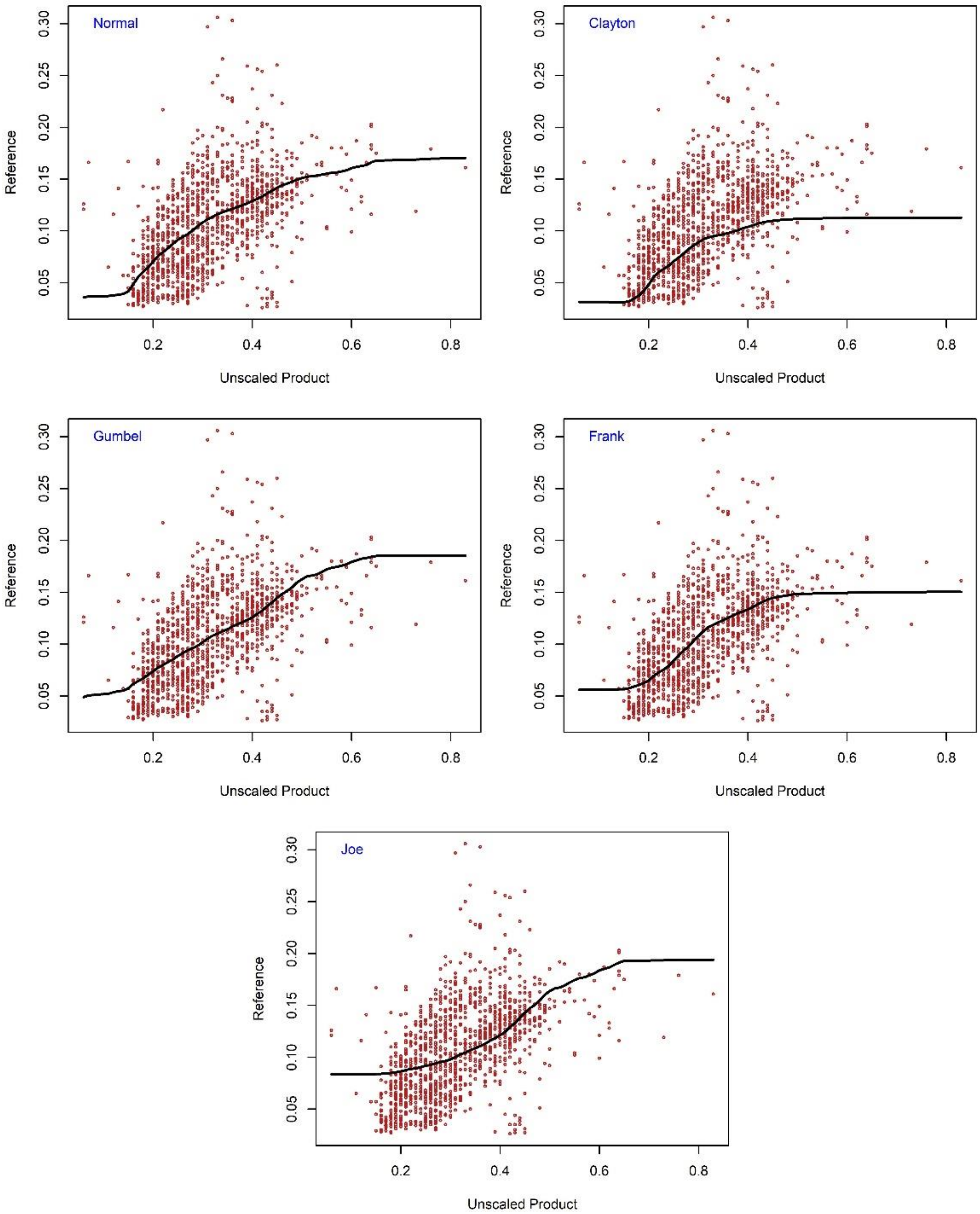

Figure 2.5. Differences among copula flavors used in this study for rescaling of soil moisture

2.1.4. Multi Adaptive Regression Splines

MAR (Friedman, 1991) is an advanced form of stepwise regression, that uses a series of local so-called basis functions to model the nonlinearities between independent and dependent variables (here unscaled and reference products). The principle of MAR is to split the unscaled product's space to distinct intervals and fit an individual spline (basis function) to each interval separately (Hastie et al., 2009). The final model is built up by connecting of these basis functions at the knot points (the end point of intervals). The general MARS model of reference (X) product with M basis functions can be written as:

$$Y^* = a_0 + \sum_{m=1}^{M} a_m B_m(Y) \tag{10}$$

where a_0 is a constant coefficient, a_m is the coefficient of the m^{th} basis function, $B_m(Y)$ is the m^{th} basis function in the form of $\max(0, Y - t)$ or $\max(0, t - Y)$ with a knot occurring at value t, and M is the number of basis functions built in the model. Figure 2.6 represents the differences between REG and MAR methods in rescaling of unscaled soil moisture product to the space of reference product.

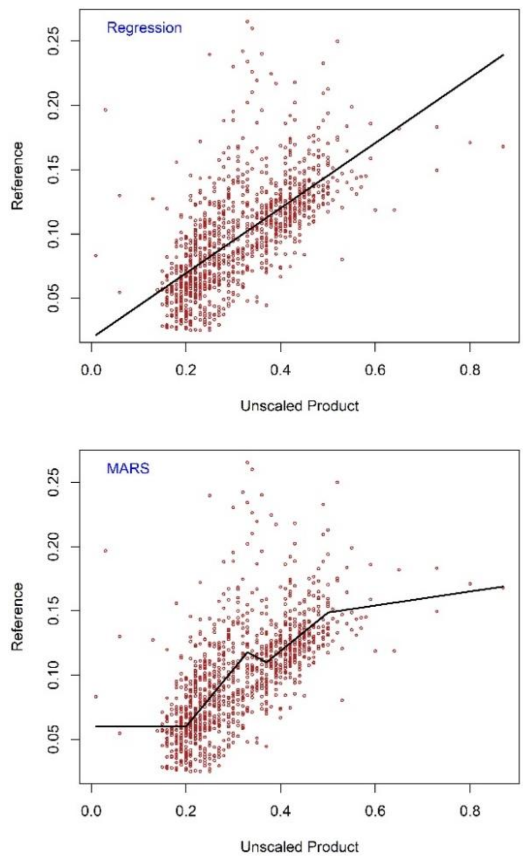

Figure 2.6. Comparison of REG and MAR rescaling methods.

The MAR consists of separate forward and backward stepwise procedures. In the forward phase, the model adds basis functions and tries to find potential knots to reduce errors between rescaled and reference products in terms of mean square error (MSE), resulting in a very complicated and over fitted model (Andrés Suárez, Lorca Fernández, Cos Juez, & Sánchez Lasheras, 2011). In the backward phase, the MAR model prunes the least effective terms among the previously added basis functions based on a generalized cross-validation (GCV) measure of MSE. The GCV procedure determines which basis function to keep in the model and which one to eliminate by introducing a penalty to the system based on the number of terms (including intercept) more than maximum number of terms allowed to be remained in pruned model (this threshold is semi automatically calculated based on the number of variables).

In this study, the fitting phase of MAR to the unscaled and reference products is conducted in R programming environment by using earth package (Milborrow, 2016). For more information about the MAR and technical details about it please see studies of Hastie, et al. (2009) and Sharda, et al. (2008).

2.1.5. Genetic Programming

GP (Koza, 1994; Vladislavleva, Smits, & den Hertog, 2009) is an automatic programming technique that is based on Darwin's theory of population evolution (abandoning poor members of society and creating modified children selectively). GP uses the Genetic Algorithm (GA) to create tree-structured computer programs as a solution for defined problems (e.g., rescaling unscaled variables to the reference space).

Given the availability of relevant datasets, GP discovers their relationship through randomly created computer programs that are composed of mathematical functions and arithmetic operators without having *a priori* information about the datasets or their structures. GP utilizes these functions and picks the best-fitted ones (i.e., refines these functions) in a statistical sense by exchanging information through so-called crossover and mutation operators. Here, the crossover operator combines randomly selected parts of two programs and creates a new program for the new population, while the mutation operator creates a new program by randomly selecting one part of a program and randomly mutating it. This refining process evolves over a series of generations until reaching the termination criteria (e.g., evolving time, maximum generations, error threshold, etc.). The schematic representation of GP method in the scatterplot of unscaled and reference soil moisture products and its difference with linear regression is available in Figure 2.7.

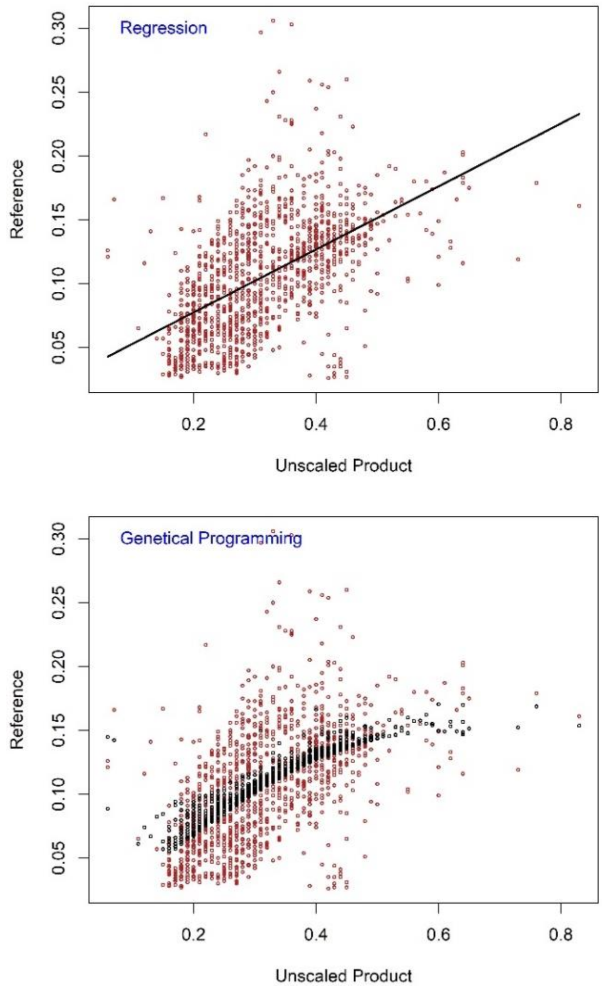

Figure 2.7. Comparison of REG and GP rescaling methods

All of the steps of GP in this study are performed by using the RGP package (Flasch, Mersmann, Bartz-Beielstein, Stork, & Zaefferer, 2015) in the R language programming environment. The preliminary required parameters of GP (e.g., the causality relationship between unscaled and reference soil moisture products, termination criteria, etc.) are presented in Table 2.2. The remaining required parameters (e.g., GA operator's probabilities and performing procedure of them) are defined as per their default values following the guidelines of the RGP package (Flasch et al., 2015).

Table 2.2. *Defined sets of GP*

Parameter	*Defined set*
Causality relationship	$X = f(Y)$
Function set	"Sine", "Cosine", "Tangent", "Square root", "Exponential", "Logarithm", "+", "-", "*", "/", "^"
Fitness function	$\frac{(Y^* - X)^2}{N}$
Population size	100
Stop condition	Time (40 minutes)

where X, Y, and Y^* are the reference, unscaled, and rescaled soil moisture products respectively and N is the number of observations.

2.1.6. Support Vector Machine

The SVM (V. N Vapnik & Chervonenkis, 1974; Vladimir Naumovich. Vapnik, 1998) is a novel technique based on statistical learning theory that uses the principle of structural risk minimization (Hernández, Kiralj, Ferreira, & Talavera, 2009) In the regression model of SVM, a function associated with the dependent variable (here X), which itself is a function of independent variable (here Y), is estimated (Olson & Delen, 2008). Similar to other rescaling methods, it is assumed that the relationship between X and Y is characterized by an algebraic function as following:

$$f(y) = W^T \varphi(y) + b \tag{11}$$

$$Y^* = f(y) + noise \tag{12}$$

where Y^* is the rescaled product, φ(y) is a nonlinear mapping of the unscaled soil moisture products, and W and b are respectively the weights and the bias values of regression function, which are determined by minimizing the objective function of:

$$min_{w,e,b} j(w,e) = \frac{1}{2} W^T w + \frac{\gamma}{2} \sum_{i=1}^{N} e_i{}^2 \tag{13}$$

subjected to:

$$e_i = X_i - Y_i{}^*, \qquad i = 1,2, \dots, N \tag{14}$$

where γ is the real positive number that is used for penalizing an occurred error during calibration, e_i is the amount of error at time step i, X_i is the reference product at time step i, and N is the number of observations. The SVM solves this minimization problem with using of Lagrange multipliers method and ultimately turns it to the form of:

$$f(y) = \sum_{i=1}^{N} a_i K(y, y_i) + b \tag{15}$$

where a_i is average of the Lagrange multipliers, and $K(y, y_i)$ is the kernel function that can be written as an inner product in a feature space by following Mercer's theorem. There are different types of kernel functions available (e.g., linear, polynomial, radial basis, and sigmoid) that the SVM method can be applied through them, while in this study the radial basis kernel function type has been chosen by following studies of (Afshar & Yilmaz, 2017; Pasolli, Notarnicola, & Bruzzone, 2011). The optimization of above mentioned problems are performed with e1071 package (Meyer et al., 2015) in the R programming environment and the parameters of the kernel functions are found based on cross validation (the optimized values are not shown). Figure 2.8 shows the differences between simple linear regression and SVM method in rescaling of arbitrary unscaled soil moisture product to the space of reference product. For more information about the SVM and its technical details, readers are referred to the studies of Vapnik (1998) and Smola & Schölkopf (2004).

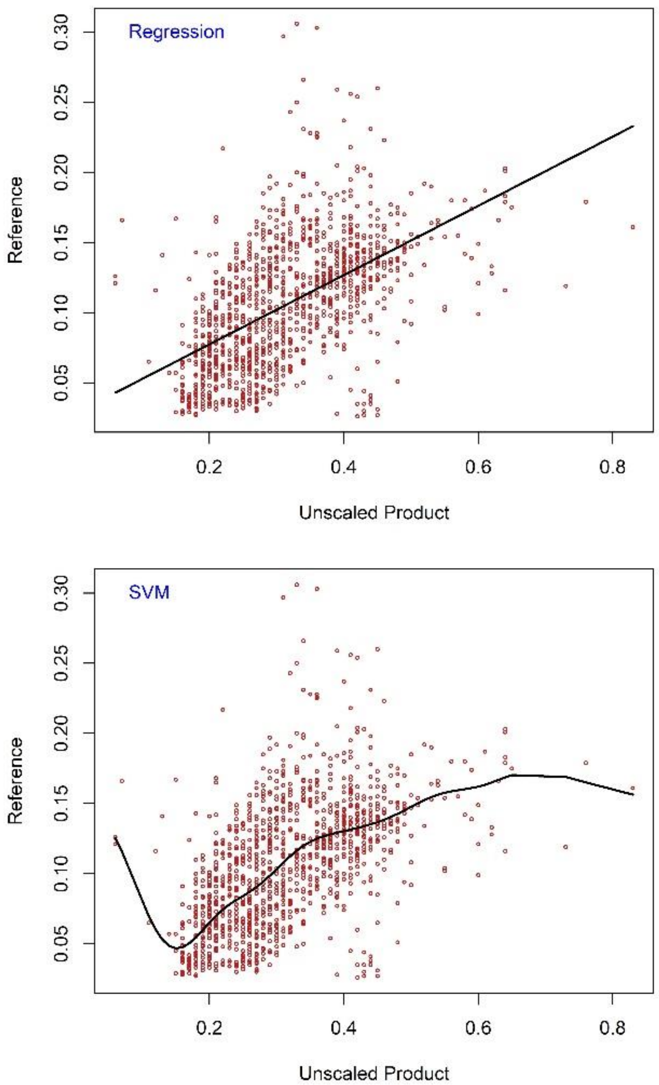

Figure 2.8. Comparison of REG and SVM rescaling methods

2.1.7. Artificial Neural Networks

ANNs, which are originally modeled from existing information processing paradigm of biological neural networks of human brain (S. Chen & Billings, 1992), provide methods for data set fitting, time series prediction, and dynamic system modeling (Principe, Rathie, & Kuo, 1992). ANNs are simply data processing systems that establish relations between input and output (i.e., Y and X) through networks of neurons (nodes) in the hidden layers. These neurons perform the information processing by weighting and exchanging them through activation functions to prepare the input value of the neurons in the next layer and consequently calculate the output values of the network. Every ANN can be determined with respect to its structure (the numbers of hidden layers and the way which the neurons are connected together), training method (the method which assigns the weights), and its activation function (the function which defines the input of the next layer from the outputs of pervious layer).

Strictly linear systems do not require any hidden layer at all, while a linear activation function suffices to relate the input dataset to output. On the other hand, the use of one or two hidden layers is sufficient to solve most (if not all) complex nonlinear problems, while the use of more hidden layers unnecessarily increase the complexity and the training time of the system (Karsoliya, 2012). On the other hand, the optimality of number of neurons has been an ongoing debate for almost two decades (Guang-Bin Huang & Babri, 1998; Murata, Yoshizawa, & Amari, 1994; Sheela, Deepa, Sheela, & Deepa, 2013; Xu & Chen, 2008), hence optimality of neuron number selection is not as clear as optimality of hidden layer number. In additional to the hidden layer and neuron number, ANN simulations often require selection of the maximum numbers of iterations allowed. Similar to selection of unnecessarily high numbers of hidden layers and neurons, selection of very high maximum iteration numbers also yields overtraining (Kentel, 2009) and results in loss of accuracy when validated using independent datasets.

In this study, four ANN functions: Multi-layer perceptron [MLP; (Rosenblatt, 1958)], Radial basis function [RBF; (Poggio & Girosi, 1990)], ELMAN (Elman, 1990), and JORDAN (Jordan, 1997) with different structures belonging to feed-forward, radial basis function, and recurrent networks are used to rescale Y to X. These four ANN functions have their own characteristics: for instance, the MLP network, probably the most common network in use (Mutlu, Chaubey, Hexmoor, & Bajwa, 2008), and RBF network have multiple layers (input, hidden, and output) that are fully connected in a feed-forward network shape (the information is carried forward: from input to nodes and to output, no cycles or loops in the network). However, the activation function of an RBF network is radially symmetric. Thus, data sets in the RBF networks are represented locally instead of globally (in MLP networks).

Another difference of RBF networks relative to MLP networks is that they are more robust against noise. Elman network, from recurrent networks, can also be considered as a basic modification of feed-forward networks with additional context units that take input (feedback) from the hidden units. These feedbacks allow Elman networks to identify and produce temporal patterns. Jordan network is also from recurrent typed networks. However, Jordan network have extra direct feedback through their context units, which actually get input from their output units. Thus, the number of context units in Jordan ANN is a function of the output unit’s dimension. This may be counted as a disadvantage of Jordan ANNs with respect to the Elman ANNs, as the number of hidden units in contrast to the number of output units is flexible in the Elman network and can be easily increased or decreased (Bergmeir & Benítez Sánchez, 2012).

In addition to the length of the datasets, user defined number of maximum iterations allowed, hidden layer, and neuron primarily govern the computational burden of ANN implementations. Selection of very high maximum iteration numbers yield over fitting of training datasets, hence in this study maximum iteration number is selected as 1000 following Kentel (2009). Different networks can evolve their topology automatically (e.g., evolutionary ANN), while the ANNs used in this study require explicit training (i.e., identification of the number of hidden layers and their neurons). In this study these number of hidden layers and neurons are optimized by a grid search within a domain of (1-2) and (1-40) for the number of hidden layers and their neurons, respectively. Given the range of neuron number is much higher than the range of hidden layer number, the most time consuming components of optimization efforts are the neuron number selections in ANN training. The properties of ANN functions used in this study are given in Table 2.3. Moreover, for better understanding of the difference among ANN flavors used in this study, the schematic representation of their procedure is showed in Figure 2.9.

Table 2.3. *Parameters of ANNs used in this study. (Id is identity)*

ANN	*Learning function*	*Update function*	*Output function*	*Activation function*		*Number of context layers*
MLP	Back-propagation	Topological order	Id.	Input	Id.	---
				Hidden	Id.	
				Context	---	
				Output	Id.	
RBF	Back-propagation	Topological order	Id.	Input	Id.	---
				Hidden	Gaussian	
				Context	---	
				Output	Id.+bias	
ELMAN	Back-propagation	JE Order	Id.	Input	Id.	≥ 1
				Hidden	Id.	
				Context	Id.	
				Output	Id.	
JORDAN	Back-propagation	JE Order	Id.	Input	Id.	1
				Hidden	Id.	
				Context	Id.	
				Output	Id.	

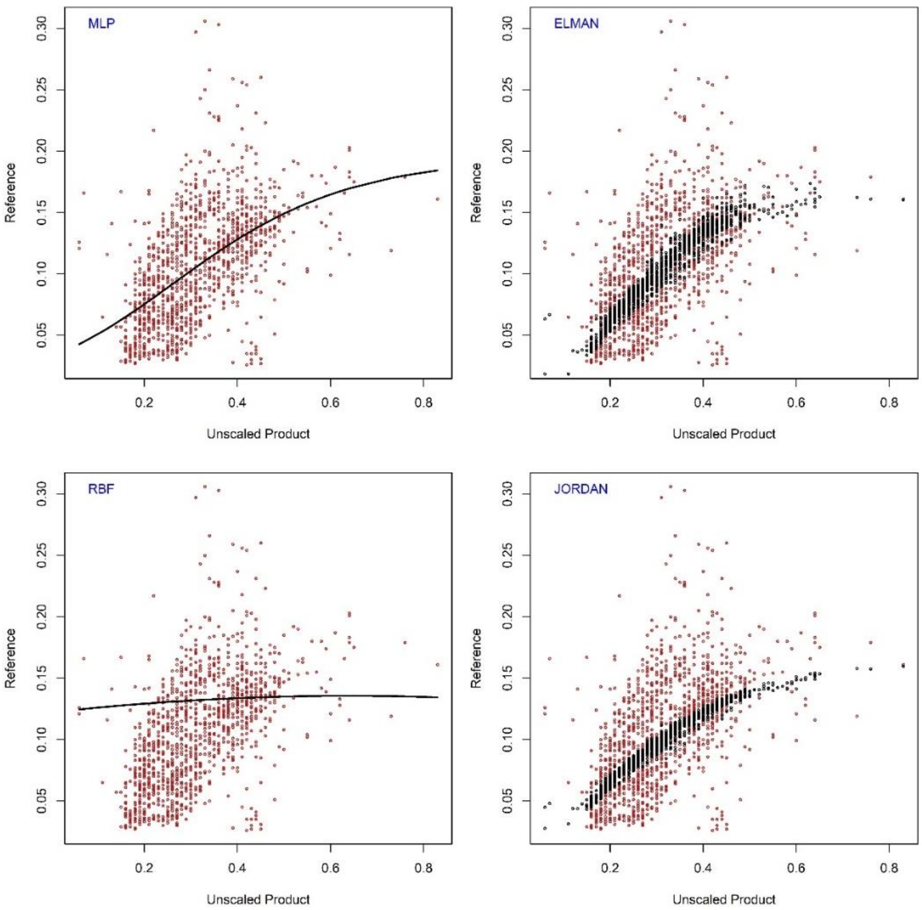

Figure 2.9. The differences among ANN flavors in rescaling of unscaled soil moisture product to the scale of the reference product

All ANN simulations presented in this study are implemented in R environment (R Core Team, 2015). Among various software packages (i.e., toolboxes) available for implementation of ANNs in R, the RSNNS package written by Bergmeir and Benitez (2012) is selected in this study. For more details about the networks and their parameters please see the user manual of RSNNS package (Bergmeir & Benítez Sánchez, 2012).

2.1.8. Comparison of Linear and Nonlinear Rescaling Methods

In this study, the rescaling methods are compared for their ability to minimize the error variance of rescaled product ($\sigma^2_{\epsilon_{Y^*}}$), minimize the error absolute mean bias (AMB), and maximize the correlation between reference and rescaled products. The details of these statistics are given below in case studies part. Here, the correlation between unscaled and reference product (ρ_{XY}), and rescaled and reference prudcts (ρ_{XY^*}), are the same for all linear rescaling methods. Among the linear methods, by definition, REG minimizes the $\sigma^2_{\epsilon_{Y^*}}$ of the training data; hence, REG is preferable over other linear methods (VAR, and TCA) if $\sigma^2_{\epsilon_{Y^*}}$ is the selection criterion when the training and validation datasets are the same. Accordingly, the comparison of linear methods may not be meaningful given that REG yields the minimum $\sigma^2_{\epsilon_{Y^*}}$, whereas all of the methods have an identical ρ_{XY^*} (if multiple linear regression method was used, it would have further reduced the training $\sigma^2_{\epsilon_{Y^*}}$). By contrast, the optimality of multiple linear regression is not guaranteed when the parameters obtained using the training datasets are applied to independent validation datasets. This implies that the inter-comparison of linear methods for the validation of Y^* is still necessary before confidently making conclusions about their performances.

Linear and nonlinear methods have particular advantages and disadvantages, which impact their optimality for different applications and goals. Among the linear methods, REG minimizes the mean square difference between X and Y^*, VAR matches the total variability components of X and Y, and TCA matches the signal variability components of Y and X so that the error variance of the analysis in data assimilation framework is minimized (Yilmaz & Crow, 2013). Accordingly, the applications that aim to linearly create a homogenous dataset for which Y^* is closest to X (i.e., those that seek to minimize mean square errors) may prefer REG (assuming that REG does not severely overfit the datasets). MAR is expected to yield better results than the other linear methods (due to their advantage of the use of splines at different knot points).

Given that merging-type studies (e.g., data assimilation) explicitly require the signal variability components of Y^* and X to be the same, TCA is a better candidate for such studies (Yilmaz & Crow, 2013). Among the nonlinear rescaling methods, copula links the $\mathrm{CDF_X}$ and $\mathrm{CDF_Y}$ multivariate functions instead of matching them, similar to CDF. By contrast, ANN, GP, and SVM machine-learning methods establish the relationships between datasets and act like a system in which the input-output relations may be too complex to be shown explicitly with equations or perhaps cannot be shown at all.

When ANN and GP are compared, GP has an advantage: first, the assembly of blocks (i.e., the input variables, target, and mathematical functions) is defined, and then, the optimized structure of the model and its coefficients are determined during the training process. By contrast, in ANNs, the structure of the network is specified first and the coefficients are then obtained during the training process. Conversely, the main drawback of GP is its high computational cost due to the infinite search space of symbolic expressions.

Overall, the relative performances of methods over independent datasets that are not used in their parameter estimation are analytically not predictable (it may not be possible to analytically prove that any particular rescaling method will result in a superior accuracy over independent validation data sets that are not used during parameter estimation of them). Accordingly, a comparison of the performances of linear and nonlinear methods is still needed to attain a greater understanding of their relative added utility.

Many of the methods discussed here (ANN, GP, SVM, and copula) have different structures and therefore different complexities. However, currently, these methods can be easily implemented in various applications using data analysis programming languages, such as R, Matlab, and Python. For example, training the networks of ANN rescaling method with available packages or toolboxes in these programming languages (e.g., optimize the weights of connections among the neurons of layers of the network) only require users to define certain parameters (e.g., the number of hidden layers and neurons and type of functions that ANNs have to implement, such as learning, update, activation, and output functions).

Despite the fact that these methods have greater computational complexity (i.e., much longer codes running in the background) than other simpler rescaling methods (e.g., linear methods and CDFM), these complex methods can be implemented using a couple of lines of codes that run for a very short time, similar to less-complex methods, once the optimized parameter sets are obtained (this optimization phase of these complex methods could require relatively longer computational times). Hence, there is relatively very little difference between the simpler methods (e.g., linear methods) and the more complex methods (e.g., machine learning methods), especially in terms of the computational ease of implementing these rescaling methods, except for the optimization of components.

2.2. Rescaling Approaches

Once the "rescaling method" (VAR, REG, CDFM, MAR, SVM, ANN, etc.) is selected for implementation in a specific application, this method can be implemented using different approaches (Yilmaz et al., 2016). The rescaling approaches affect the accuracy statistics of rescaled product, even though, by definition, a particular rescaling method is selected to be the optimum method (i.e., yield least errors) for a particular application. The approaches used in this study are grouped in to two different parts. The first part focuses on using constant and time-varying rescaling factors (Style) and second part focuses on decomposition of time series in to its components (Technique). Below the definitions and the differences among different approaches used in this study (totally six; Figure 2.10) are illustrated.

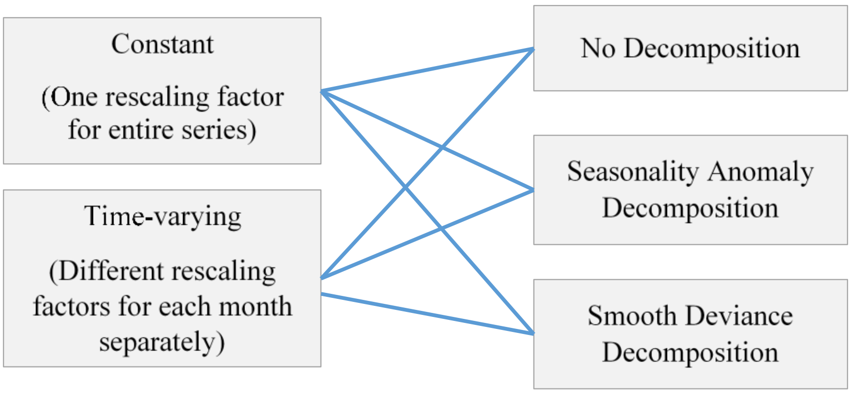

Figure 2.10. Rescaling approaches used for application of rescaling methods

2.2.1. Rescaling Style – Use of Time-varying Coefficients

The use of time-varying rescaling coefficients may also improve the accuracy of the rescaled time series (Yilmaz et al., 2016) owing to the time-varying relations that may exist between the products. Accordingly, rescaling of soil moisture time series can be implemented using constant or time-varying rescaling coefficients. Most studies use the constant coefficient selection (i.e., entire time series rescaled at once), which is considered a less-aggressive rescaling style than use of time-varying rescaling coefficients (Yilmaz et al., 2016). Such more-aggressive rescaling methodologies involve using varying rescaling coefficients in time (i.e., 12 different rescaling coefficients).

Accordingly, here in this study two different rescaling techniques are used for the stationarity assumption of the rescaling coefficients: single rescaling coefficient or monthly coefficients. Here, for the time-varying monthly rescaling case, all the soil moisture values obtained for a particular month is rescaled against the soil moisture values of the reference dataset for the same month; then this process is repeated for all months separately to form the continuous time series again. Here, the use of monthly rescaling coefficients is expected to create temporal discontinuities in the rescaled soil moisture time series, while the degree of these discontinuities are expected to increase with the increased rescaling coefficient differences between months. Figure 2.11 represents the overall procedure of time-varying application of REG method for rescaling of arbitrary unscaled product to the space of reference product.

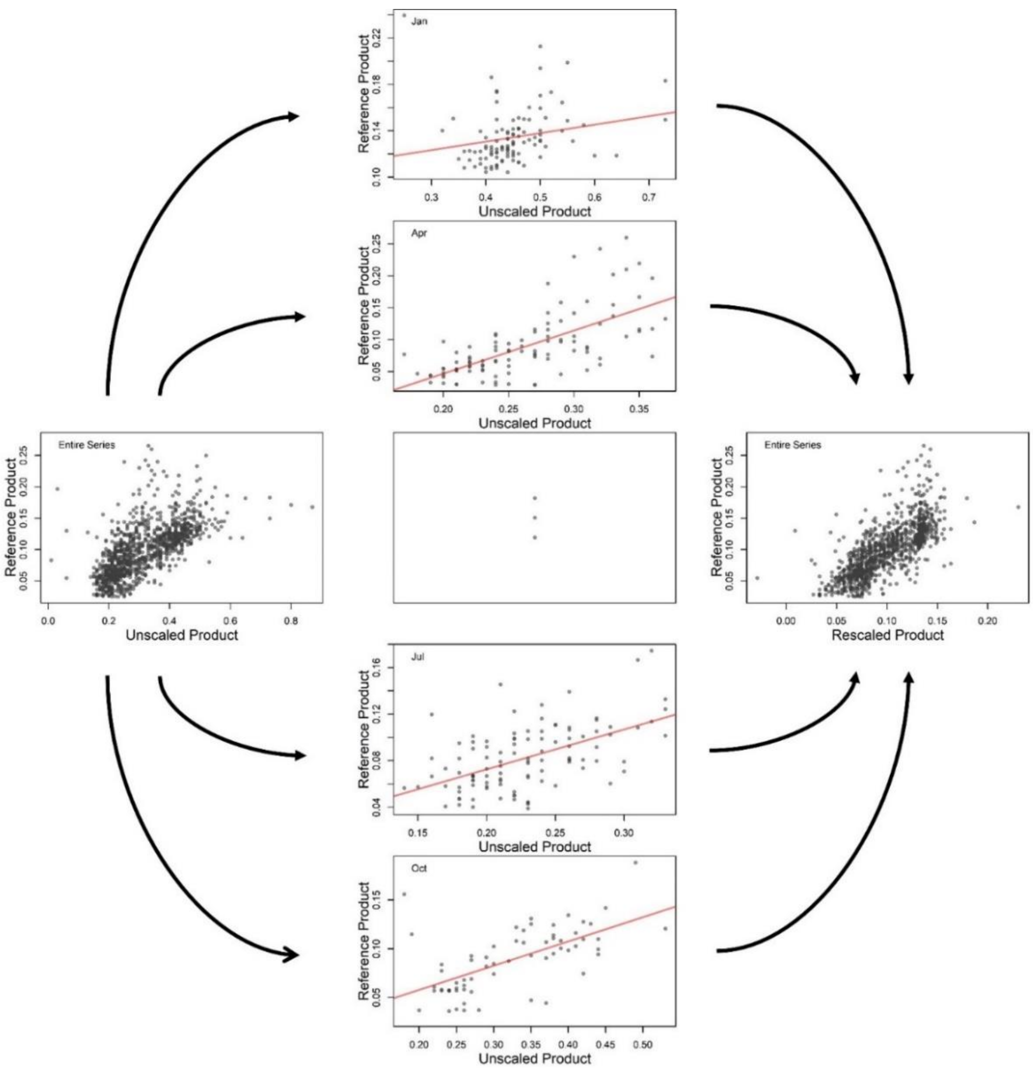

Figure 2.11. Time-varying application of REG method for rescaling of unscaled product to the reference space

2.2.2. Rescaling Techniques – Seasonality Anomaly vs. Smooth Deviance Decomposition

Rescaling methodologies are mostly implemented for the entire soil moisture time series (i.e., assumption that low and high frequency components of different products are related similarly). They are rarely implemented separately for the different decomposed components of the time series (e.g., low and high frequency components). Accordingly, once the rescaling methodology (VAR, REG, CDFM, MAR, SVM, ANN, etc.) is decided, then decisions should be given about the rescaling technique, which involve decisions about the decomposition of the time-series to its different components.

Given the low and high frequency signals of the time series may have different accuracies, they might as well be treated separately to further improve the rescaled product (Yilmaz et al., 2016). Such high and low frequency decomposition can be done in several different ways.

In many studies the low frequency component is assumed to be periodic and it does not vary from year to year (i.e., calculated as daily climatology using a moving-window average approach), or alternatively the low frequency component can be calculated as non-periodic (presented for the first time in this study). Once the low frequency component is acquired, the high frequency component is obtained using the remaining component from the native complete time series:

$$X_{i,j}^{Low-Periodic} = \frac{\sum_{i=1}^{n}\sum_{j-14}^{j+14} X_{i,j}}{29n} \quad (16)$$

$$X_{i,j}^{Low-NonPeriodic} = \sum_{j-14}^{j+14} X_{i,j} \times W_j \quad (17)$$

$$X_{i,j}^{High} = X_{i,j} - X_{i,j}^{Low} \quad (18)$$

where i refers to year (total n years), j refers to the day of the year (DOY), $X_{i,j}^{Low-Periodic}$ and $X_{i,j}^{Low-NonPeriodic}$ refer to the periodic and non-periodic low frequency components (hereinafter called “seasonality” and “smooth” for periodic and non-periodic cases, respectively), $X_{i,j}^{Low}$ refers to either “seasonality” or “smooth” of soil moisture product X, $X_{i,j}^{High}$ refers to the high frequency component (hereinafter called “anomaly” and “deviance” for periodic and non-periodic cases, respectively), and W_j refers to the weights to be used for window-averaging for the DOY j. Equation (16) indicates the seasonality of the dataset (X) for any DOY is found as the average of a 29-day moving average window centered on a specific DOY utilizing the available data using all available years of the dataset (Yilmaz et al., 2016). Equation (17) also passes a smooth filter over the time series using a weighted moving average window centered on a particular DOY, however, this filter yields a non-periodic low frequency product while equation (16) yields a periodic low frequency product (i.e., seasonality component has only 365 unique entries while smooth component has unique values for all different time steps).

Weights of the days for the calculation of the average value for any particular window differs for equations (16) and (17). Unlike the seasonality/anomaly decomposition assumes equal weighting for the available days in any given window for any given DOY, the smooth/deviance decomposition assumes varying weights for any given DOY. Days closer to the center of the 29-day window are assigned heavier weights than the weights assigned for the days further away from the center:

$$\begin{cases} C_j = \left|\frac{1}{j}\right| & -14 < j < 0 \\ C_j = 1 & j = 0 \\ C_j = \frac{1}{j} & 0 < j < 14 \end{cases} \tag{19}$$

$$W_j = \frac{C_j}{\sum_{j-14}^{j+14} C_j} \tag{20}$$

where j refers to the day in the 29-day window, C_j is a coefficient which relates the day j to its weight (W_j), and the domain is between [-14 to +14] days. Here an inverse relation is assumed for the weights of the days based on their distances from the center point of the window.

As a result, three rescaling techniques (represented in Figure 2.12 and Figure 2.13) are used about the temporal decomposition selections in this study (i.e., no decomposition, seasonality-anomaly decomposition, or smooth-deviance decomposition).

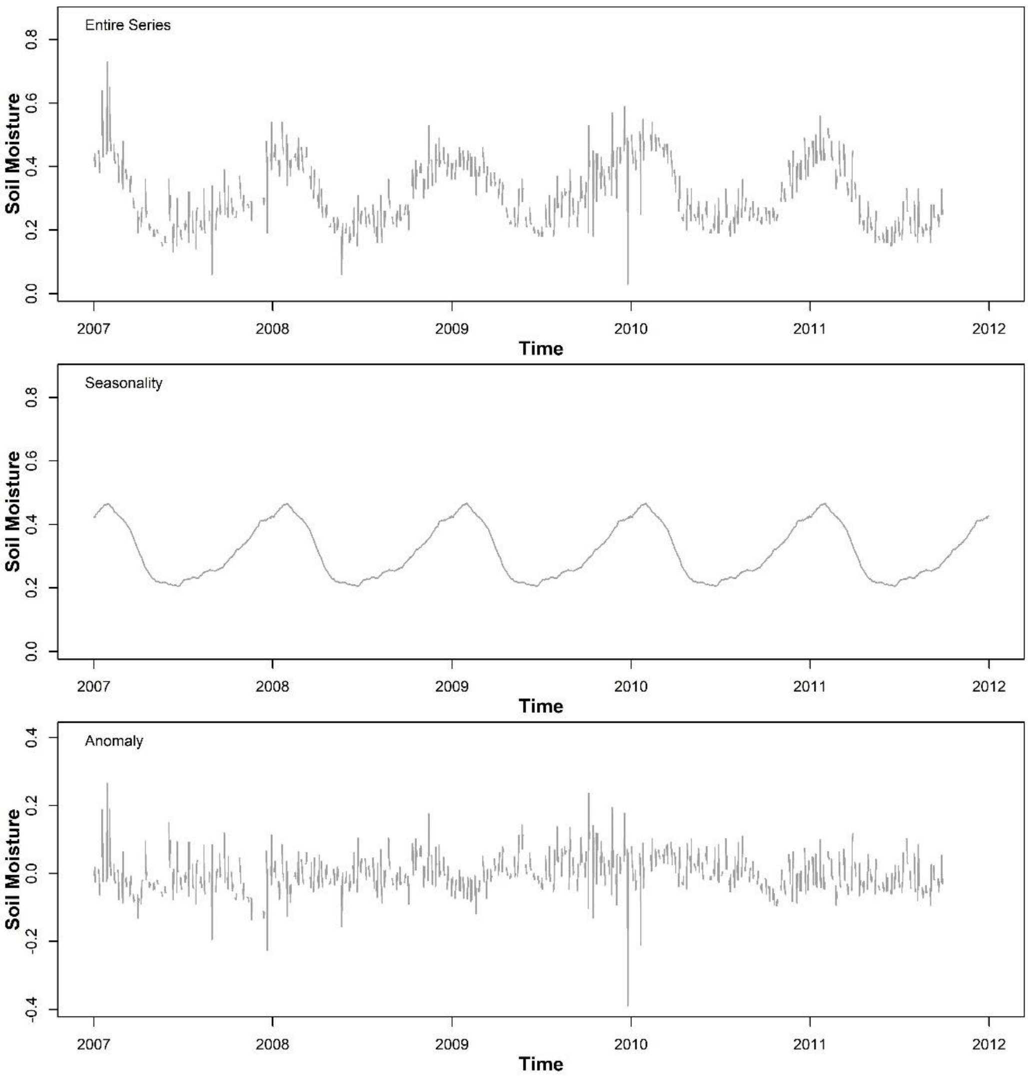

Figure 2.12. Decomposition of time series in to its seasonality and anomaly components

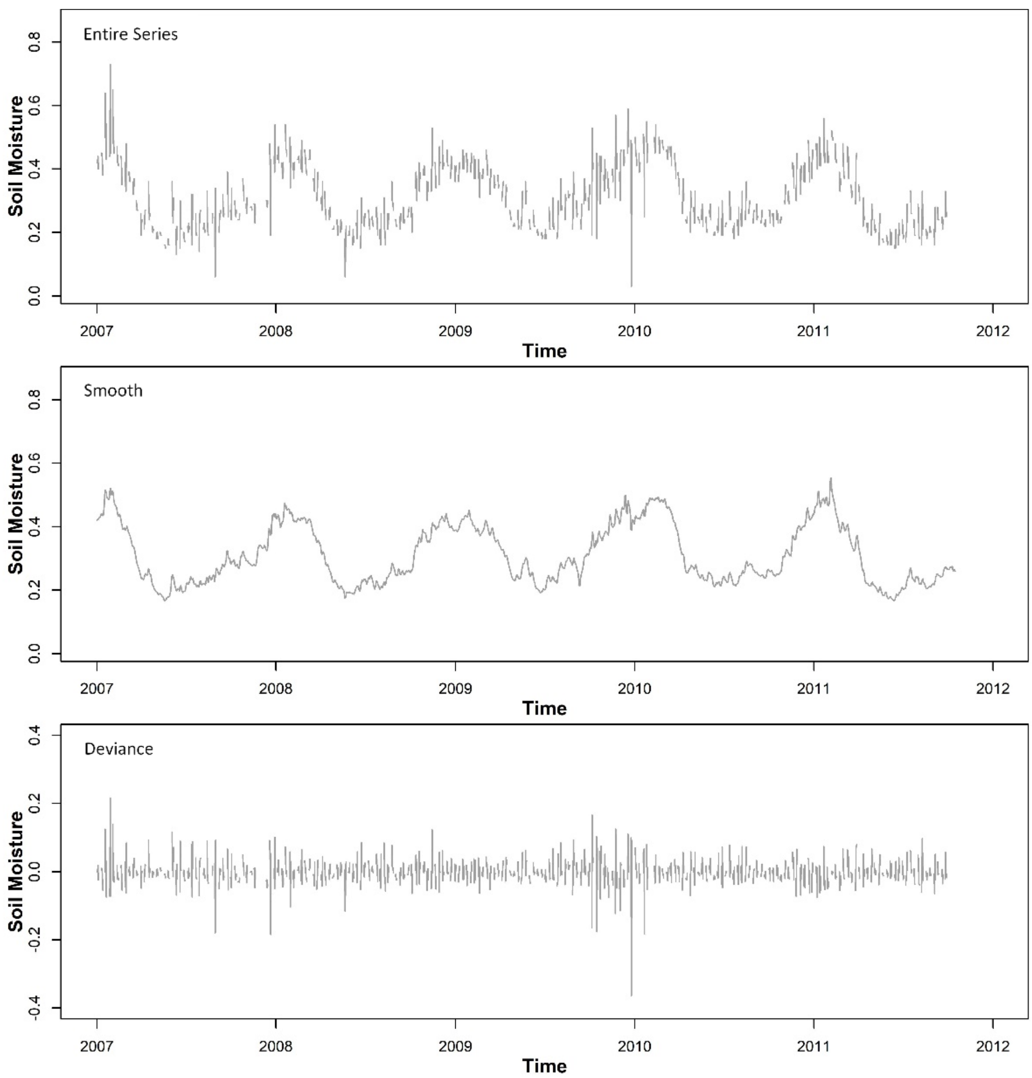

Figure 2.13. Decomposition of time series in to its smooth and deviance components

2.3. Data Sets

In this study, various remote sensing- and hydrological model-based soil moisture datasets are utilized to develop different experiments for evaluation of different rescaling methods/approaches. Moreover, for the validation of any experiment, the in-situ measurements are used over four different watersheds. Below the description of soil moisture products used in this study beside of the characteristics of the validation sites are provided.

2.3.1. ASCAT

The soil moisture product derived from the Advanced Scatterometer sensor onboard of the Metop satellite (C. Albergel et al., 2009; Bartalis et al., 2007; Wolfgang Wagner et al., 2007) retrieves soil moisture estimates from C-band backscatter observations. This real-aperture radar sensor scans the globe by six antennas under different azimuth and viewing angles (three antennas at both sides of the platform with 45°, 90°, and 135°) and retrieves observations with approximately 550 km swath width and 14 orbit revolutions per day resulting in ~ 1.5-day revisit time globally and twice a day over Western Europe. The basic sampling distance of this radar is 12.5 km; however, the operational and the research soil moisture products derived from these radar observations retrievals are available at 0.5° and 0.25° resolutions, respectively.

The ASCAT soil moisture dataset used in this study (i.e., the research product) are acquired for time period of January 2007 and May 2012 from the Technical University of Vienna using the algorithm described in (Wolfgang Wagner et al., 1999) and (Naeimi, Scipal, Bartalis, Hasenauer, & Wagner, 2009) which is based on the normalization of backscattering observations with respect to the incidence angle, dry and wet surface soil conditions, and vegetation conditions. Figure 2.14 and Figure 2.15 show some general information about spatio-temporal variability of ASCAT soil moisture product. For more information about the soil moisture retrieval algorithm and technical details see the studies of Wagner et al., (1999 and 2007).

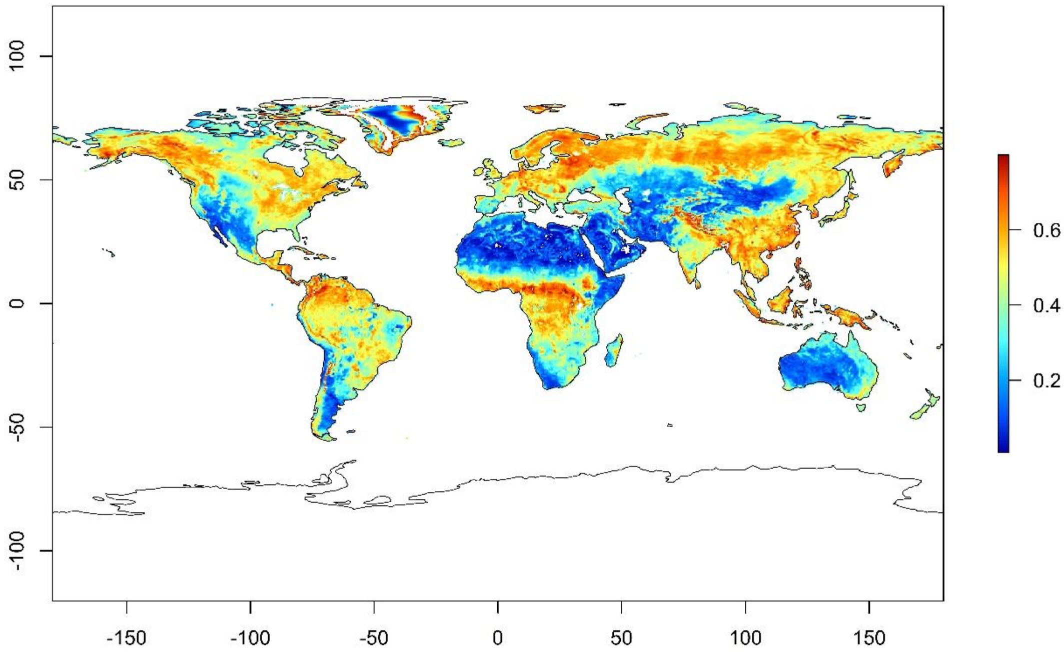

Figure 2.14. Average soil moisture between 2007 and 2011 measured with ASCAT

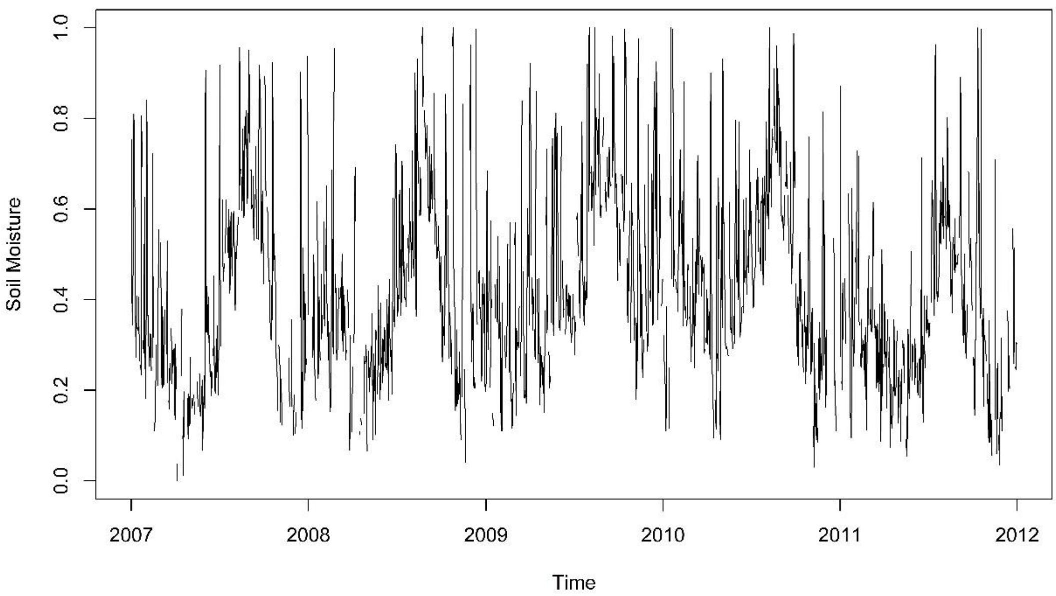

Figure 2.15. ASCAT soil moisture product's time series over little river watershed with longitude of -83.61, and latitude of 31.65 between 2007 and 2011

2.3.2. AMSR-E LPRM

The Advanced Microwave Scanning Radiometer for EOS (AMSR-E) on-board of Aqua satellite is a passive microwave radiometer that has provided near-daily observations at six different frequencies (between 6.9 and 89.0 GHz) in both horizontal and vertical polarizations. The AMSR-E measured brightness temperature with daily ascending and descending overpasses, with a swath width of 1445 km. These measurements are converted to soil moisture contents through different algorithms [e.g., REG (Al-Yaari et al., 2016), ANN (Rodríguez-Fernández et al., 2016), and etc.] resulting in different soil moisture datasets (Mladenova et al., 2014).

Among different soil moisture datasets derived from AMSR-E observations, The Land Parameter Retrieval Method [LPRM; (M. Owe, de Jeu, & Walker, 2001; Manfred Owe, de Jeu, & Holmes, 2008)]- based AMSR-E dataset is used in this study. LPRM utilizes three parameters (soil moisture, vegetation water content, and soil or canopy temperature) as well as passive microwave based X-band and C-band observations from AMSR-E for the retrieval of the surface soil moisture content. The LPRM-based soil moisture datasets used in this study are acquired from Vrije Universiteit Amsterdam (personal communication with Robert Parinussa, 2013) and are available online in a gridded format and spatial resolution of 0.25° between June 2002 and October 2011 in the url of "https://disc.gsfc.nasa.gov".

Figure 2.16 and Figure 2.17 show some general information about spatio-temporal variability of AMSR-E soil moisture product. For more details on the LPRM retrieval method, please see the studies by Owe, et al., (2001, 2008).

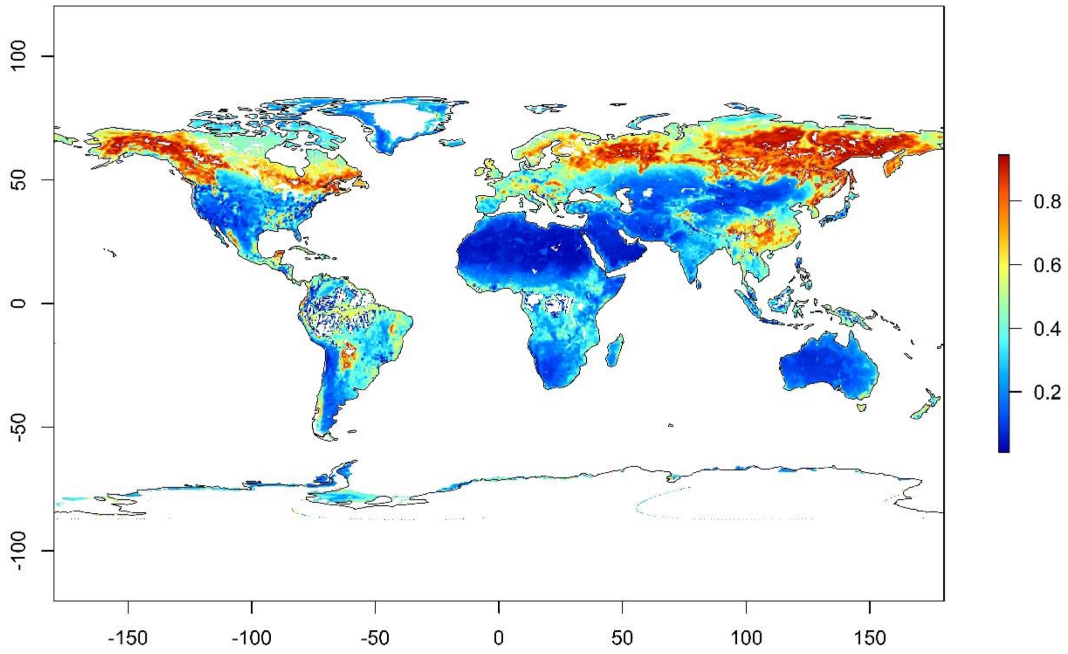

Figure 2.16. Average soil moisture between 2007 and 2011 measured with AMSR-E

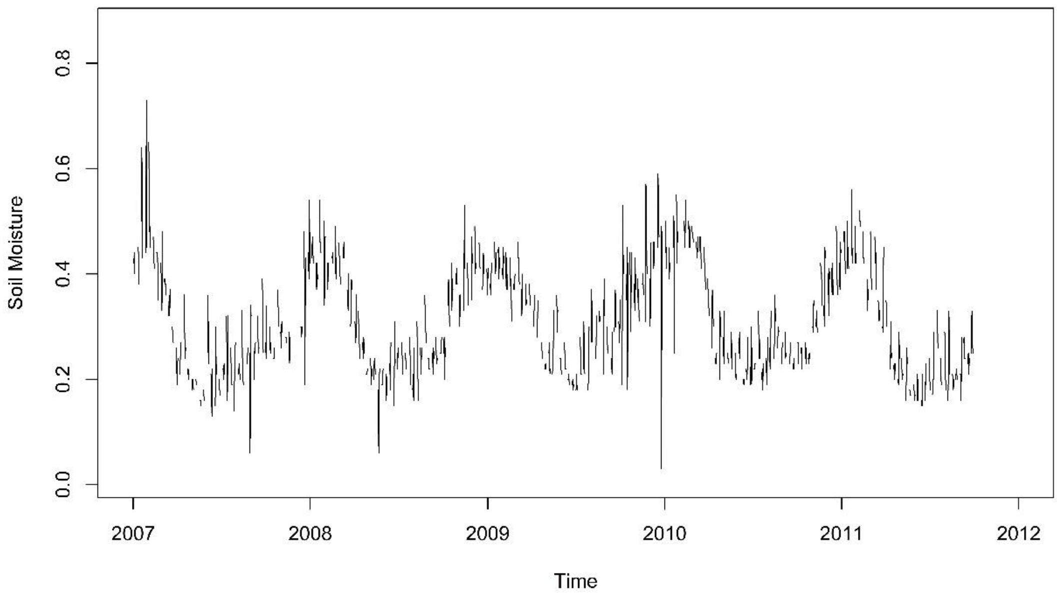

Figure 2.17. AMSR-E soil moisture product's time series over little river watershed with longitude of -83.61, and latitude of 31.65 between 2007 and 2011

2.3.3. NOAH GLDAS

NOAH land surface model [NOAH; (F. Chen et al., 1996; Ek et al., 2003; Koren et al., 1999)] is a 1-D column model, which can be executed in both offline and coupled modes. NOAH uses atmospheric data (longwave and shortwave radiations, precipitation, temperature, pressure, wind, and humidity) as well as soil and vegetation related parameters to solve for the energy and the water balance equations for different layers of soil profile. Even though different configurations can be implemented, the four soil profile layers having 10cm, 30cm, 60cm, 100cm depths respectively are frequently used in NOAH simulations. For more additional information about NOAH LSM and its interior equations, readers are referred to (Ek et al., 2003; Zheng et al., 2015).

NOAH soil moisture datasets used in this study are simulated by Global Land Data Assimilation System [GLDAS Version 2; Rodell et al., (2004)] using NOAH v2.7 at spatial resolution of 0.25°. The GLDAS NOAH soil moisture datasets representing the top 10cm soil layer used in this study are provided at three-hourly time steps. These soil moisture values are later averaged to daily values. The GLDAS NOAH soil moisture datasets used in this study are publicity available from January 2000 till present within the URL of "http://disc.sci.gsfc.nasa.gov".

Figure 2.18 and Figure 2.19 show some general information about spatio-temporal variability of NOAH soil moisture product. For more details about NOAH and GLDAS simulations please see study of Rodell, et al. (2004).

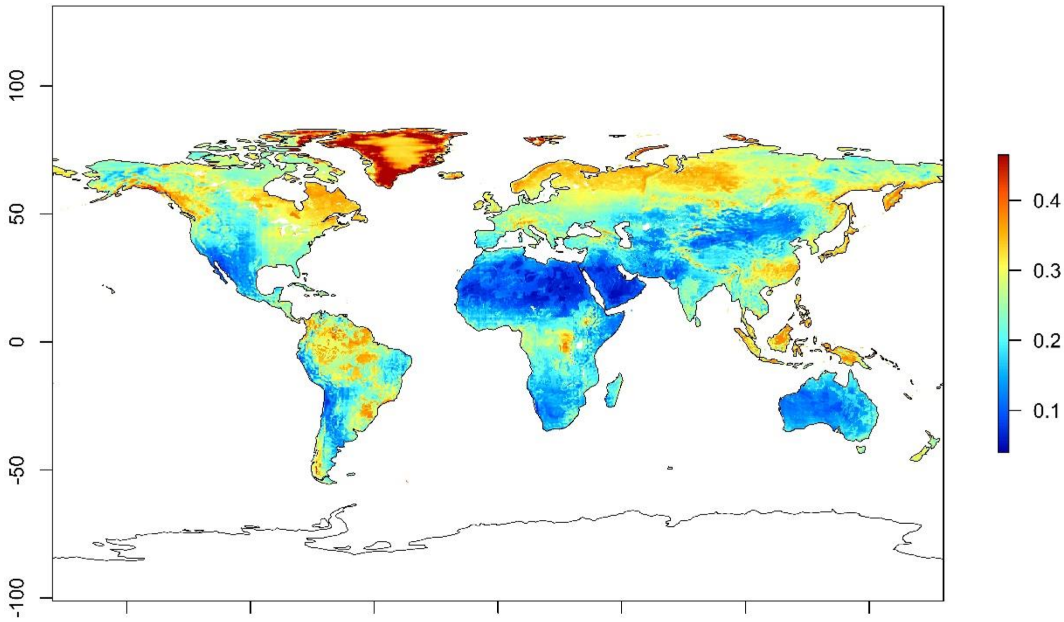

Figure 2.18. Average soil moisture between 2007 and 2011 measured with NOAH

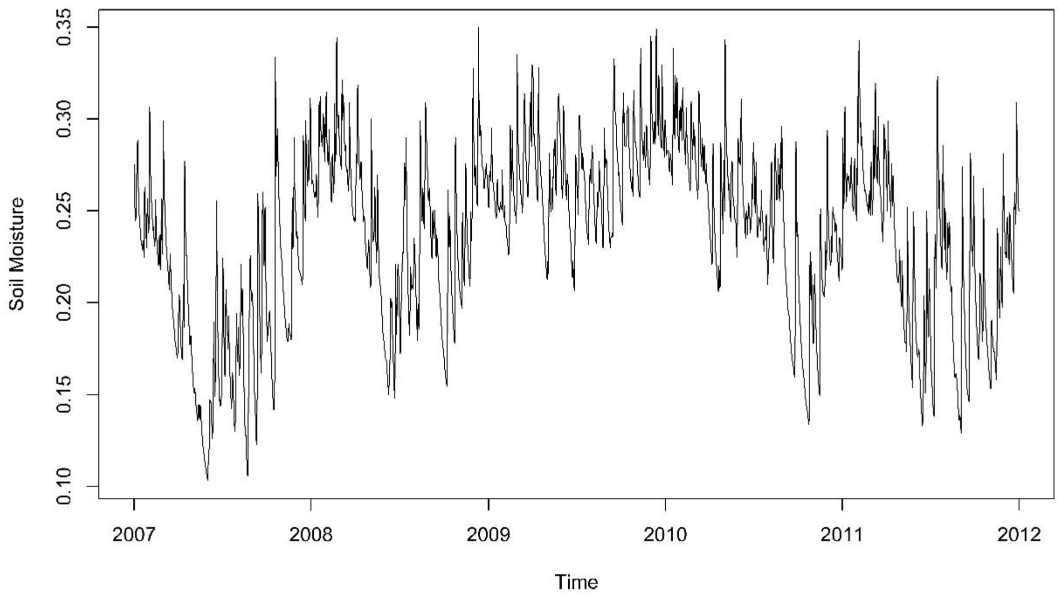

Figure 2.19. NOAH soil moisture product's time series over little river watershed with longitude of -83.61, and latitude of 31.65 between 2007 and 2011

2.3.4. API

The antecedent precipitation index [API; (Blanchard, McFarland, Schmugge, & Rhoades, 1981; McFarland & Blanchard, 1977)] is a proxy that estimates surface soil moisture based on either rainfall or rainfall and runoff (Blanchard et al., 1981). The simple and practical form of the API enables the users to track the internal processes more efficiently, which has turned API to a very common model among data assimilation processes (W. T. Crow & Ryu, 2009). The API soil moisture retrieval method basically relies on the fact that soil moisture depletion can be stated with an exponential function of the input moisture to the soil profile (Chow, 1964; Lindsey, Kohler, Jr., & Paulhus, 1949). This exponential relation can also be presented in a linear form of :

$$API_i = \gamma_i \times API_{i-1} + P_i \tag{21}$$

where API is the antecedent precipitation which will be considered as soil moisture; P is the daily precipitation or infiltration amount; γ is the depletion rate, and i is day of estimate. Based on the study of Yilmaz and Crow (2013), the value of γ in this study is taken as 0.85. As precipitation input, daily Tropical Rainfall Measuring Mission (TRMM) 3B42 version 7 product has been used (Huffman et al., 2007). This product has spatial resolution of 0.25° and are available online from January 1998 until present within URL of “https://disc.gsfc.nasa.gov”.

Figure 2.20 and Figure 2.21 show some general information about spatio-temporal variability of API soil moisture product. For more details about API model and its alternative types, please see the study by Blanchard et al., (1981).

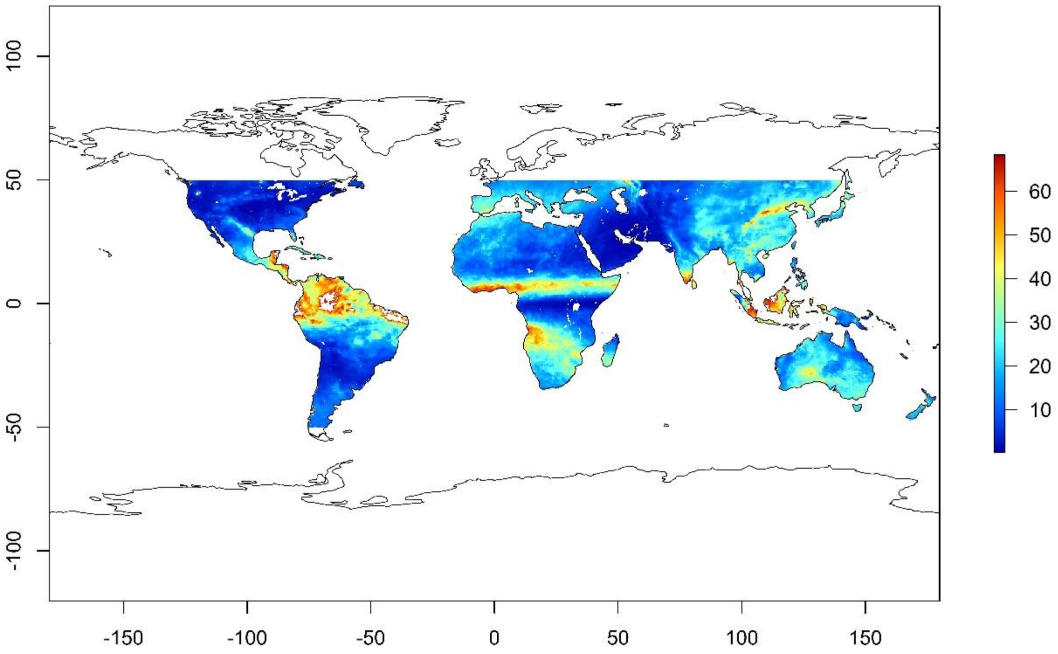

Figure 2.20. Average soil moisture between 2007 and 2011 measured with API

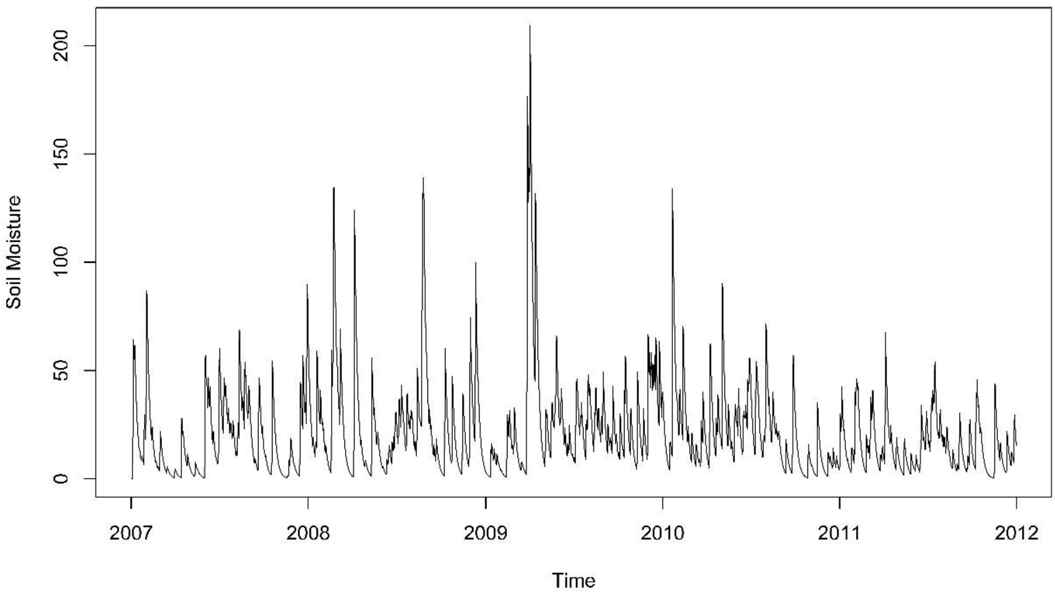

Figure 2.21. API soil moisture product's time series over little river watershed with longitude of -83.61, and latitude of 31.65 between 2007 and 2011

2.3.5. USDA-ARS Watershed Average Soil Moisture

Watershed average soil moisture (WASM) measurements used in this study are located at the experimental sites of U.S. Department of Agriculture (USDA) Agricultural Research Service (ARS). These experimental watersheds, Little River [LR; (Bosch, Sheridan, & Marshall, 2007)], Little Washita [LW; (Cosh, Jackson, Starks, & Heathman, 2006)], Walnut Gulch [WG; (Renard, Nichols, Woolhiser, & Osborn, 2008)], and Reynolds Creek [RC; (Slaughter, Marks, Flerchinger, Van Vactor, & Burgess, 2001)], contain dense soil moisture sensors that measure soil moisture since the year 2002 on hourly basis at a depth of 5 cm over different topographies and climatic regions. These sites have been verified via comparisons against gravimetric soil moisture observations (Cosh et al., 2006) and have been widely used in the validation of existing remotely sensed soil moisture products (Colliander et al., 2017; Jackson et al., 2010; Leroux et al., 2014). Table 2.4 summarizes the characteristics and dominant features of each watershed. For further details about USDA ARS watersheds and the sensor networks available in them please see the study of Jackson et al. (2010). The general view of these four watersheds are presented in Figure 2.22 to Figure 2.26.

Table 2.4. *Description of USDA ARS Experimental Watershed Soil Moisture Networks*

Watershed	*Little River*	*Little Washita*	*Walnut Gulch*	*Reynolds Creek*
Area (km^2)	334	610	148	238
Number of Sensor	29	16	21	19
Climate	Humid	Sub humid	Semiarid	Semiarid
Annual Rainfall (mm)	1200	750	320	500
Topography	Flat	Rolling	Rolling	Mountainous
Land Use	Forest	Wheat	Rangeland	Rangeland & forest
Watershed Centroid longitude	-83.61	-98.1	-110.0184	-116.775
Watershed Centroid latitude	31.65	34.9502	31.7216	43.1501

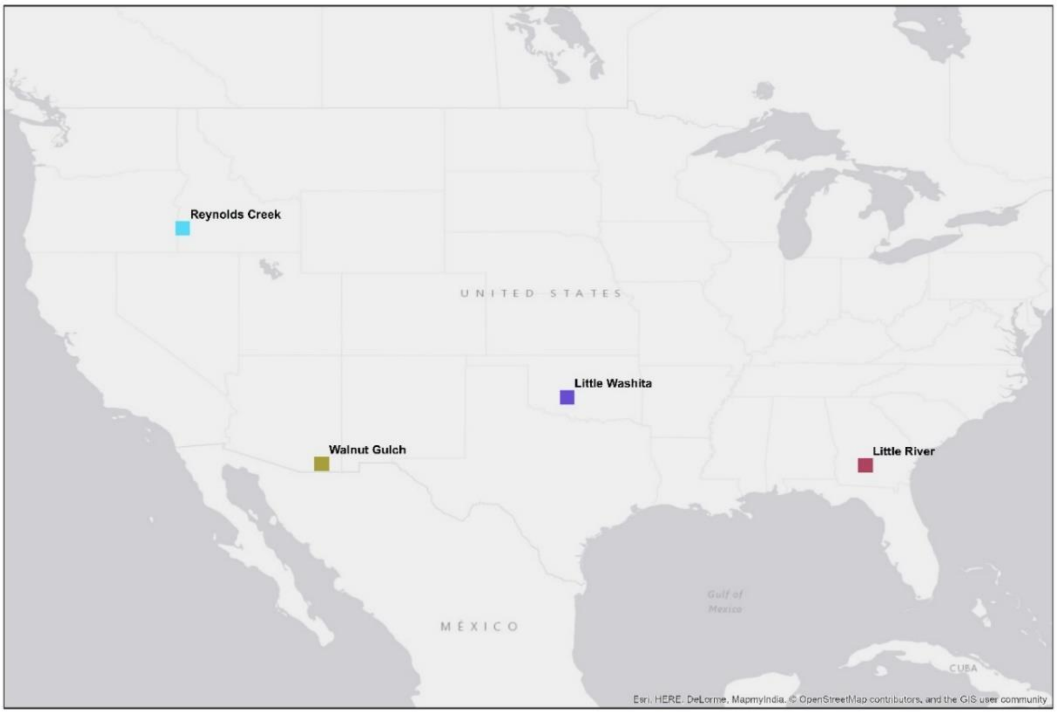

Figure 2.22. Location of the studied watersheds with their in-situ soil moisture networks

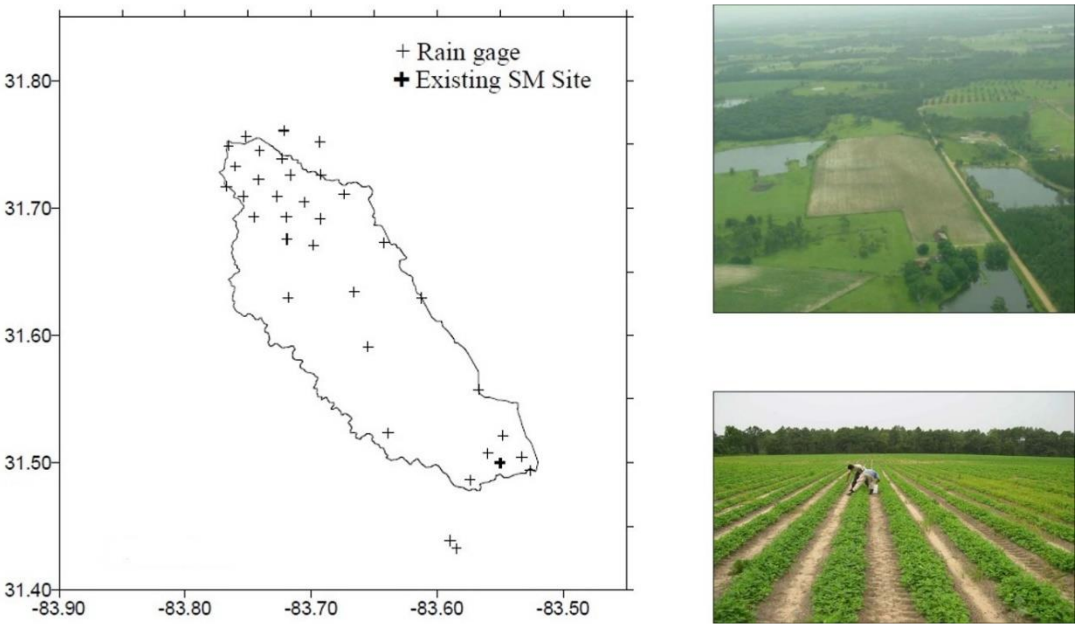

Figure 2.23. General view of Little River watershed

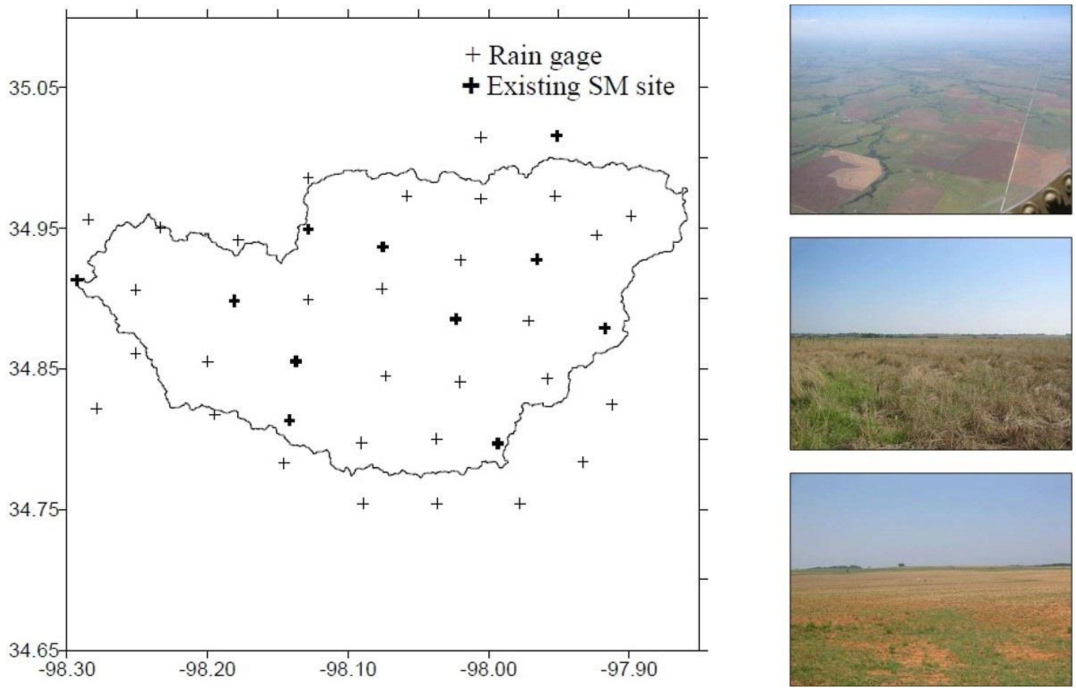

Figure 2.24. General view of Little Washita watershed

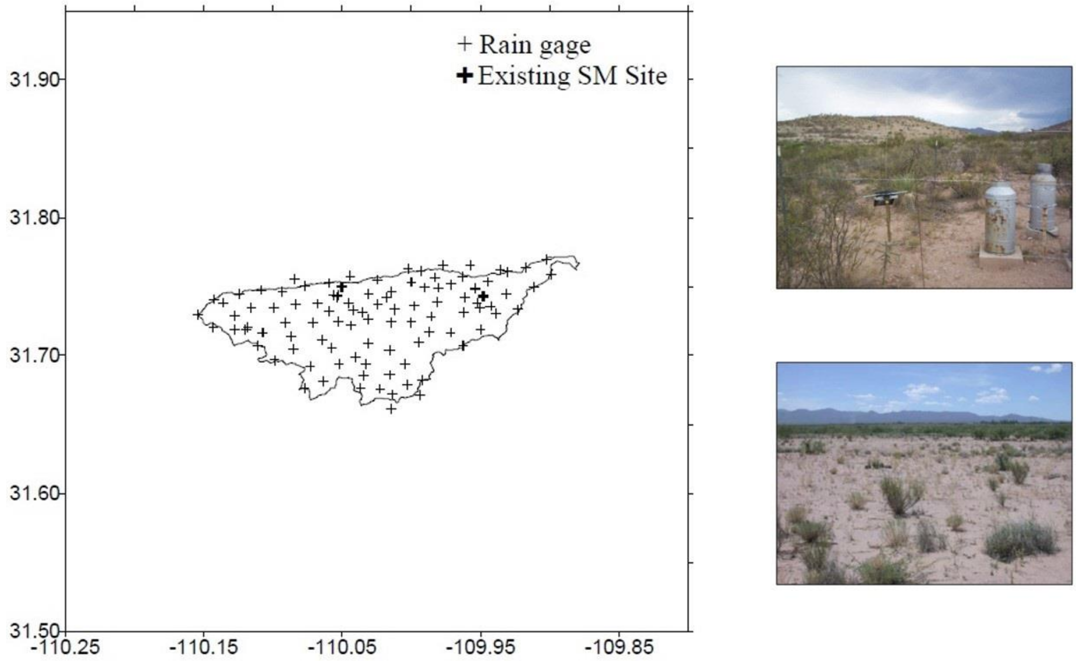

Figure 2.25. General view of Walnut Gulch watershed

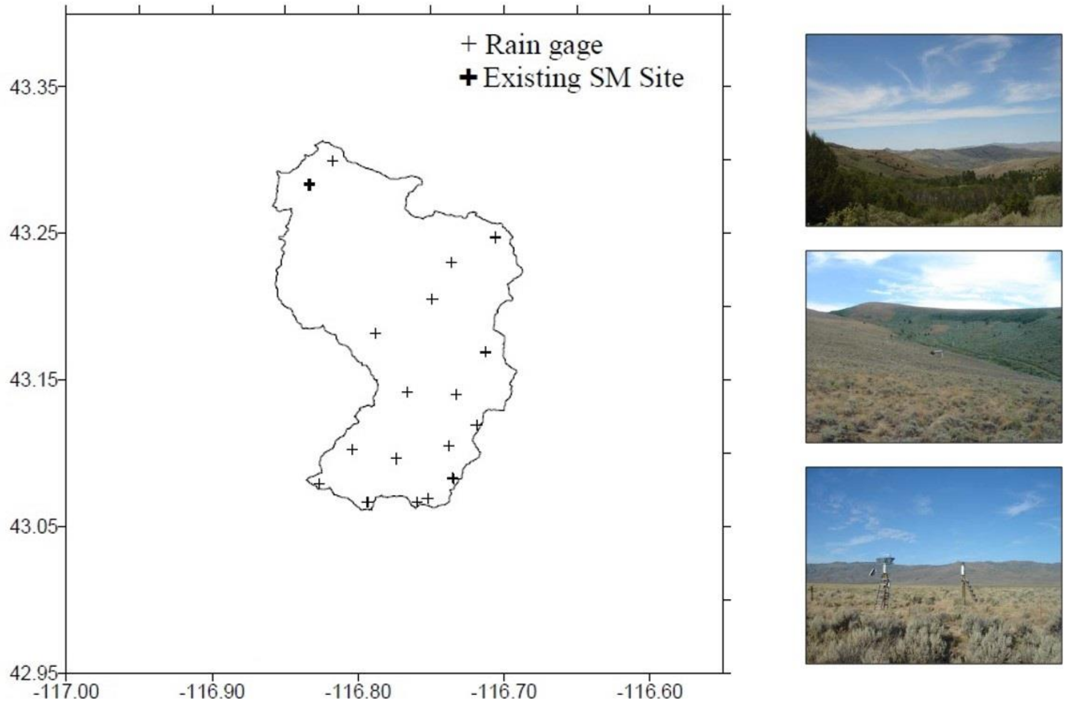

Figure 2.26. General view of Reynolds Creek watershed

2.4. Case Studies

In this study, for investigation of rescaling methods, two different case studies are considered to evaluate firstly, the added utility of rescaling methods in removing systematic difference between unscaled and reference products, and secondly, evaluate them in the data fusion framework. Below the description of these case studies and the evaluation processes are provided.

2.4.1. Case Study 1 (Added Utility of Rescaling Methods)

In this case study, the AMSR-E LPRM (called LPRM in first case study) soil moisture values are rescaled to WASM using REG, VAR, TCA, CDFM, COPULA, MAR, GP, SVM, and ANN methods. Where ANN has four (MLP, RBF, ELMAN, and JORDAN) and copula has five types (NORMAL, CLAYTON, GUMBEL, FRANK, and JOE). Overall, 18 different methods are considered in this case study (3 linear, and 15 nonlinear methods).

The calibration of rescaling methods in this case study are done by using training part of datasets. Later using calibrated rescaling methods, the validation part of datasets are rescaled to the reference products and the accuracy of rescaled datasets (LPRM^*) are assessed using independent WASM validation datasets using statistics below:

$$\varepsilon_i = \mathrm{Sta}_i - \mathrm{LPRM}_i^* \quad (22)$$

$$\mathrm{AMB}_i = |\mu_{\varepsilon_i}| \quad (23)$$

$$\sigma_{\varepsilon_i} = \sqrt{\sum \left(\varepsilon_i - \mu_{\varepsilon_i}\right)^2 / (n-1)} \quad (24)$$

$$\rho_i = \frac{\Sigma_{\mathrm{Sta}_i \mathrm{LPRM}_i^*}}{\sigma_{\mathrm{Sta}_i} \sigma_{\mathrm{LPRM}_i^*}} \quad (25)$$

where subscript i indicate each watershed (total four), Sta is station-based WASM dataset, ε is error of LPRM^*, μ_ε and σ_ε indicate temporal mean and standard deviation of the errors respectively, AMB indicate the absolute mean bias which is calculated based on the absolute value of the mean value of the errors of LPRM^*, n is number of available observations, and $\sum(\,)$ is summation operator. Statistics ρ, σ_ε, and AMB are calculated over four watersheds separately.

Given that WASM datasets are available only between June 2002 and July 2009 from the International Soil Moisture Network [ISMN (W. A. Dorigo et al., 2011)] database, this case study is limited between these dates, even though the LPRM dataset is available beyond 2009. Among the available data between these dates, soil moisture values for 131, 2, and 52 days, for LW, WG, and RC, are zero (0) respectively; these values are assumed to be missing and are not used in the analyses. Only mutually available LPRM and WASM datasets are used to calculate all statistics mentioned above in this study. The datasets are divided into training and validation periods. Given some rescaling methods explicitly use the autocorrelation information to rescale datasets, training and validation datasets cannot be selected via random sampling; accordingly temporally continuous data are selected for training and validation. To reduce the impact of sampling errors on the results two separate experiments are implemented: first experiment use the first (time-wise) 25% of the data for validation and the remaining 75% as training, while the second experiment use the first 75% as training and the remaining 25% as validation. Later, statistics for these two experiments are averaged while these averages are presented in this study.

The added utility (U) of rescaling methods is calculated with respect to the performance of REG method as

$$U_{m,s,l} = M_{m,s,l} - REG_{s,l} \tag{26}$$

where m represents 8 methods (listed below), s represents 4 locations (LR, LW, WG, and RC), and l represents 3 statistics (ρ, σ_ε, and AMB obtained as the average of above defined two experiments); M represents the method of interest, and U is the added utility with respect to REG. To ensure U is always positive for improvements and negative for degraded results, the bias and the standard deviation statistics are multiplied by -1 as their improvement is linked with their reduction. U is calculated only for selected methods: i) MAR, ii) CDFM, iii) GP, iv) SVM, v) ELMAN ANN, vi) best performing type of copula, vii) the method (among 18 methods) that gives the best statistic training part ("Tr_best"), viii) the method gives the best statistics when validation data is used ("Best"). For example, if MAR gives the best ρ over LR using training data, then MAR is selected as "Tr_best" method for ρ over LR while another method may perform better using the validation data ("Best"). Comparisons of U are performed separately over four watersheds. Similarly these comparisons are repeated for each performance statistic (ρ, σ_ε, and AMB; total 3).

2.4.2. Case Study 2 (Impact of Rescaling Approaches on Accuracy of Fused Products)

The second case study that has been conducted in this research focuses on the performance of different rescaling methods and their implementation approaches (rescaling techniques and style) over data fusion framework.

The fusion process can be implemented in different ways depending on the assumptions about the error characteristics of the datasets to be fused. Data assimilation techniques assume the error characteristics of the products are not stationary, while these techniques require more effort for their implementation. On the other hand, simple merging methodologies may yield similar accuracies for the fused product with much less effort (Yilmaz et al., 2012). The data fusion framework used in this study can be expressed in its form as:

$$F = W_{Y^*_1} Y^*_1 + W_{Y^*_2} Y^*_2 \tag{27}$$

where $W_{Y^*_1}$ and $W_{Y^*_2}$ are the weights for two rescaled product of Y^*_1 and Y^*_2. Here, different weights (e.g., time dependent, constant, etc.) can be used for W_{Y_1} and W_{Y_2}. In this study, for simplicity, these weights are simply selected as 0.5 (i.e., naive merging) following Yilmaz et al., (2012).

Fusion experiments merge a satellite- and a model-based estimate using an equal weighting (i.e., naïve merging). In this study, by using simple merging technique and fusion of six pairs for the four soil moisture products (ASCAT, AMSR-E, API, NOAH): ASCAT - AMSR-E; ASCAT - API; ASCAT - NOAH; AMSR-E - API; AMSR-E - NOAH; and API - NOAH] is investigated. While the fused product is obtained for these six pairs for all reference dataset selections.

The evaluation part of this case study uses correlation coefficient to validate the analysis and assess fused products:

$$\rho_i = \frac{cov(Sta_i, Fused_i)}{\sigma_{Sta_i} \sigma_{Fused_i}} \tag{27}$$

where the ρ_i is the amount of correlation between fused product ($Fused$) and WASM (Sta) over the i_{th} watershed (totally four). The various remote sensing- and hydrological model-based soil moisture datasets utilized in this study, are obtained and inserted to the analysis for the common observation period of them (between January 2007 and October 2011) while the validation efforts are performed using WASM for the same period (Figure 1.4). The summary of fusion process and the evaluation of fused products is represented in Figure 2.27.

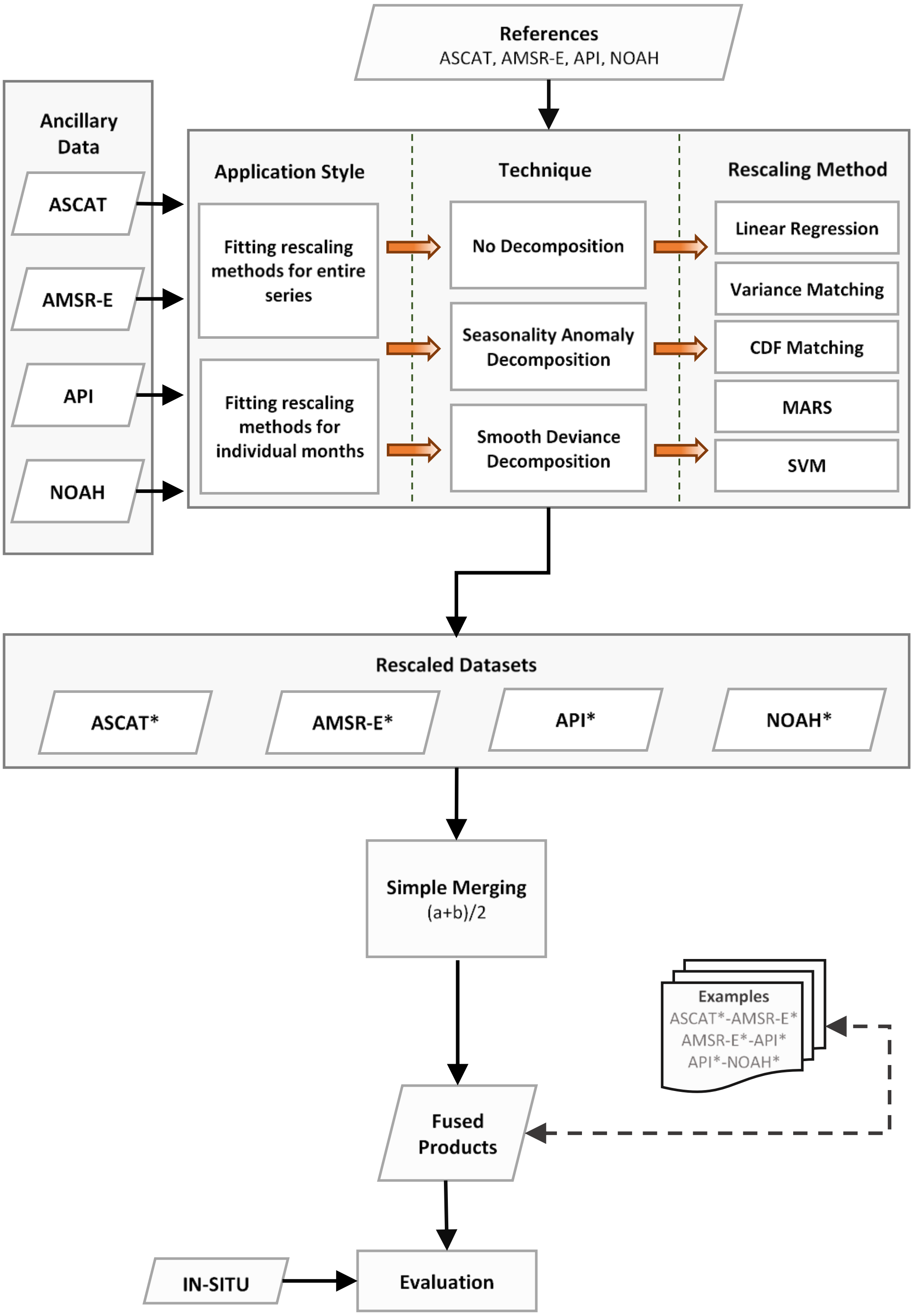

Figure 2.27. The rescaling and fusion procedure

CHAPTER 3

RESULTS AND DISCUSSION

3.1. Added Utility of Rescaling Methods

The statistics of the LPRM and WASM datasets are analyzed (Table 3.1) prior to evaluating the results of the two different rescaling experiment. On average, there are 1600 days where the LPRM and WASM data are mutually available between June 2002 and July 2009.

Table 3.1. *Statistics of the training and validation datasets used in two experiments prior to rescaling*

Experiments		*Location*	*Mean*		*Standard Deviation*		*Lag1 Autocorrelation*	
			LPRM	*WASM*	*LPRM*	*WASM*	*LPRM*	*WASM*
1	Training dataset (last 75%)	LR	0.311	0.105	0.099	0.046	0.784	0.819
		LW	0.282	0.125	0.104	0.057	0.728	0.863
		WG	0.18	0.046	0.074	0.022	0.801	0.889
		RC	0.227	0.118	0.121	0.075	0.831	0.969
	Validation dataset (first 25%)	LR	0.331	0.109	0.098	0.044	0.757	0.805
		LW	0.286	0.118	0.099	0.052	0.686	0.751
		WG	0.176	0.045	0.083	0.021	0.785	0.849
		RC	0.232	0.107	0.104	0.072	0.778	0.974
2	Training dataset (first 75%)	LR	0.316	0.106	0.1	0.046	0.757	0.826
		LW	0.285	0.122	0.109	0.058	0.733	0.841
		WG	0.18	0.044	0.077	0.022	0.789	0.879
		RC	0.234	0.117	0.113	0.077	0.796	0.972
	Validation dataset (last 25%)	LR	0.314	0.105	0.095	0.043	0.855	0.784
		LW	0.276	0.127	0.077	0.049	0.628	0.828
		WG	0.175	0.048	0.076	0.02	0.814	0.881
		RC	0.21	0.109	0.129	0.067	0.866	0.963

On average, 1200 of the available data points are used for training, for both experiments, whereas the remaining (~400) unused data points are left for independent validation. Overall, the statistics (μ, σ) of the datasets are very similar for the training and validation periods for both experiments (statistical significance tests are not performed). Unscaled original LPRM time series have 2-4 times larger μ and σ than the WASM. This clearly shows that these datasets should be reconciled in some statistical sense before they can be meaningfully compared or used to create a homogenous and consistent time series.

The WASM time series has 3.4%, 4.5%, 0.1%, and 5.5% missing data (results not shown) for the LR, LW, WG, and RC watersheds, respectively. The time series obtained over LR and RC have more missing data than those obtained over LW and WG, yet the autocorrelation values over RC are statistically significantly higher than the values over LW, WG, and WG (for both the LPRM and WASM datasets). Higher autocorrelation values, despite more missing data, over RC imply calculations over this site may not be considerably impacted by the missing data, even though the LPRM autocorrelations are, on average, 0.10 lower than the WASM values.

The correlation statistics related to the performance of different rescaling methods for both training and validation periods are presented in Table 3.2. Overall, the relative performances of these 18 methods are very consistent for the training and validation datasets (i.e., better performing methods using training datasets also performed better when using validation datasets). Among nonlinear methods, the SVM has performed better than other methods over LR and LW watersheds during training period while the ELM. method performed the best over WG and RC over training and almost over all watersheds during validation period. Here in the Table 3.2, the terms Tr_best and BEST refer to the best methodology (performing the best) over training and over the selected periods (either training or validation) respectively. Comparing the correlation values of Tr_best and linear methods unravel the impact of nonlinear methods in increasing the consistency of rescaled product with WASM.

Table 3.2. *Detailed performance (correlation) of rescaling methods during training and validation periods. The best performing method for training (Tr_best) and overall (BEST) are shown. The ones listed below are obtained by averaging over two different experiments*

Method	*Training*				*Validation*			
	LR	*LW*	*WG*	*RC*	*LR*	*LW*	*WG*	*RC*
ORG	0.567	0.514	0.696	0.698	0.53	0.495	0.684	0.666
REG	0.567	0.514	0.696	0.698	0.53	0.495	0.684	0.666
VAR	0.567	0.514	0.696	0.698	0.53	0.495	0.684	0.666
TCA	0.567	0.514	0.696	0.698	0.53	0.495	0.684	0.666
MAR	0.6	0.602	0.734	0.727	**0.547**	0.509	0.686	0.674
CDFM	0.577	0.566	0.721	0.687	0.54	0.504	0.667	0.653
GP	0.595	0.57	0.73	0.727	0.527	0.501	0.68	0.67
SVM	**0.602**	**0.604**	0.73	0.727	0.539	0.503	0.67	0.672
MLP	0.579	0.552	0.709	0.721	0.534	0.502	0.682	0.676
RBF	0.58	0.536	0.708	0.709	0.536	0.492	0.683	0.669
ELM.	0.595	0.583	**0.747**	**0.85**	0.535	**0.535**	**0.713**	**0.801**
JOR.	0.591	0.556	0.726	0.829	0.535	0.514	0.7	0.779
NOR.	0.585	0.561	0.722	0.708	0.536	0.502	0.678	0.666
CLA.	0.581	0.56	0.631	0.725	0.532	0.493	0.638	0.673
GUM.	0.566	0.55	0.721	0.697	0.524	0.499	0.671	0.659
FRA.	0.594	0.581	0.725	0.709	0.536	0.511	0.684	0.661
JOE	0.517	0.52	0.72	0.673	0.484	0.475	0.662	0.641
Tr_best	**0.602**	**0.604**	**0.747**	**0.85**	**0.539**	**0.503**	**0.713**	**0.801**
BEST	**0.602**	**0.604**	**0.747**	**0.85**	**0.547**	**0.535**	**0.713**	**0.801**

Table *3.3* on the other hand represents the error standard deviation of unscaled and rescaled LPRM soil moisture products when they are compared to WASM. In general the performance of linear and nonlinear methods in decreasing the error standard deviation of rescaled products are close to each other while the nonlinear methods slightly perform better than linear ones during training period. Among nonlinear methods the MAR, SVM, and ELM. methods performed better than other nonlinear methods in removing error standard deviation while among linear methods the simple linear regression performed better than others (as expected).

Table 3.3. *Detailed performance (error std) of rescaling methods during training and validation periods. The best performing method for training (Tr_best) and overall (best) are shown. The ones listed below are obtained by averaging over two different experiments*

Method	*Training*				*Validation*			
	LR	*LW*	*WG*	*RC*	*LR*	*LW*	*WG*	*RC*
ORG	0.083	0.091	0.062	0.084	0.082	0.077	0.067	0.088
REG	0.038	0.049	0.016	0.054	**0.037**	**0.043**	**0.015**	0.053
VAR	0.042	0.056	0.017	0.059	0.043	0.049	0.018	0.061
TCA	0.061	0.071	0.019	0.079	0.061	0.06	0.02	0.084
MAR	**0.036**	**0.046**	**0.015**	0.052	**0.037**	0.044	**0.015**	0.052
CDFM	0.042	0.053	0.017	0.06	0.043	0.054	0.017	0.061
GP	0.037	0.047	**0.015**	0.052	0.038	0.044	**0.015**	0.053
SVM	**0.036**	**0.046**	**0.015**	0.052	**0.037**	0.045	0.016	0.053
MLP	0.037	0.048	0.016	0.053	**0.037**	**0.043**	**0.015**	0.052
RBF	0.041	0.055	0.019	0.059	0.041	0.048	0.018	0.054
ELM.	0.037	**0.046**	**0.015**	**0.04**	0.038	**0.043**	**0.015**	**0.043**
JOR.	0.037	0.048	0.016	0.043	**0.037**	**0.043**	**0.015**	0.044
NOR.	0.037	0.047	**0.015**	0.054	**0.037**	0.044	**0.015**	0.054
CLA.	0.037	0.047	0.017	0.052	**0.037**	0.044	0.016	0.053
GUM.	0.038	0.048	0.016	0.055	0.038	0.044	0.016	0.055
FRA.	0.037	0.047	**0.015**	0.055	**0.037**	0.045	**0.015**	0.056
JOE	0.039	0.049	0.016	0.056	0.039	0.044	0.016	0.054
Tr_best	**0.036**	**0.046**	**0.015**	**0.04**	**0.037**	**0.043**	**0.015**	**0.043**
BEST	**0.036**	**0.046**	**0.015**	**0.04**	**0.037**	**0.043**	**0.015**	**0.043**

The linear regression method based on its formulation has always a smaller standard deviation and consequently lower error standard deviation with respect to the variance matching and other linear rescaling methods. The superiority of linear methods can also be seen in AMB statistic, where they perform the best among all rescaling methods with zero AMB (Table 3.4) in training part. Among nonlinear methods, conversely, a high variation can be seen in different sites. However it should be noticed as well that the superiority of a method to another in validation part is not that significant and in general all of rescaling methods perform well in removing the bias from unscaled soil moisture product.

Table 3.4. *Detailed performance (AMB) of rescaling methods during training and validation periods. The best performing method for training (Tr_best) and overall (BEST) are shown. The ones listed below are obtained by averaging over two different experiment*

Method	*Training*				*Validation*			
	LR	*LW*	*WG*	*RC*	*LR*	*LW*	*WG*	*RC*
ORG	0.208	0.16	0.135	0.113	0.216	0.159	0.129	0.113
REG	**0**	**0**	**0**	**0**	0.003	0.007	0.003	0.01
VAR	**0**	**0**	**0**	**0**	0.003	0.007	0.003	0.01
TCA	**0**	**0**	**0**	**0**	0.003	0.007	0.003	0.01
MAR	**0**	**0**	**0**	**0**	0.002	0.007	0.003	0.007
CDFM	**0**	**0**	**0**	**0**	0.003	**0.006**	0.003	0.009
GP	**0**	0.001	**0**	0.001	0.002	0.008	0.003	0.009
SVM	0.003	0.006	0.002	0.003	0.002	0.007	0.003	0.007
MLP	0.001	0.001	**0**	**0**	0.002	0.007	0.003	0.01
RBF	0.031	0.018	0.006	0.018	0.032	0.019	0.008	0.024
ELM.	0.003	0.008	0.002	0.004	0.004	0.016	0.004	**0.005**
JOR.	0.006	0.006	0.004	0.003	0.004	0.007	0.004	0.007
NOR.	**0**	**0**	**0**	0.001	0.002	0.008	0.003	0.008
CLA.	0.017	0.025	**0**	**0**	0.016	0.022	**0.002**	0.009
GUM.	0.001	**0**	**0**	0.007	**0.001**	0.009	0.003	0.012
FRA.	0.001	**0**	**0**	0.001	0.002	0.007	**0.002**	0.007
JOE	**0**	0.001	**0**	0.017	**0.001**	0.01	0.003	0.022
Tr_best	**0**	**0**	**0**	**0**	**0.003**	**0.007**	**0.003**	**0.01**
BEST	***0***	***0***	***0***	***0***	***0.001***	***0.006***	***0.002***	***0.005***

The added utility of nonlinear rescaling methods with respect to WASM are listed in Table 3.5 (only the best performing ones are presented) whereas the U values are calculated with respect to the REG values using equation (26). In general, a higher ρ is almost always associated with a lower σ_{ε} for both validation and training datasets (Table 3.3 and Table 3.4), implying that these statistics are consistent when representing the accuracy of the analyzed dataset. On average, using of nonlinear methods lead in gaining 0.08, and 0.05 correlation improvement in training and validation periods respectively. The improvement of rescaled products against WASM relative to the unscaled products are presented over the scatterplots of the datasets (Figure 3.1 through Figure 3.4) which impressively show the utility of nonlinear methods in rescaling of unscaled soil moisture products. On the other hand, when the AMB is considered as the tool of comparison of the added utility of nonlinear methods, it can be seen that the nonlinear methods perform better than linear methods over three sites (e.g., 0.005 improvement over Reynolds Creek watershed by using ELMAN ANN method for rescaling) and perform almost the same over other sites, implying that using nonlinear methods increase the accuracy of rescaled products beside of keeping it precise against WASM.

Table 3.5. *Added utility of the selected methods compared to the REG validation statistics (Table 3.2, Table 3.3, and Table 3.4) over four watersheds. Positive values indicate improvements, and negative values indicate degradation.*

Statistic	*Location*	*ADDED UTILITY OF METHODS AGAINST REG STATISTICS*							
		MAR	*CDFM*	*GP*	*SVM*	*ELMAN*	*NOMRAL*	*Tr_Best*	*Best*
ρ	LR	0.017	0.01	-0.003	0.009	0.005	0.006	0.035	0.017
	LW	0.014	0.009	0.006	0.008	0.04	0.007	0.09	0.04
	WG	0.002	-0.017	-0.004	-0.014	0.029	-0.006	0.051	0.029
	RC	0.008	-0.013	0.004	0.006	0.135	0	0.152	0.135
σ_ε	LR	0	-0.006	-0.001	0	-0.001	0	0.002	0
	LW	-0.001	-0.011	-0.001	-0.002	0	-0.001	0.003	0
	WG	0	-0.002	0	-0.001	0	0	0.001	0
	RC	0.001	-0.008	0	0	0.01	-0.001	0.014	0.01
AMB	LR	0.001	0	0.001	0.001	-0.001	0.001	0	0.001
	LW	0	0.001	-0.001	0	-0.009	-0.001	0	0.001
	WG	0	0	0	0	-0.001	0	0	0
	RC	0.003	0.001	0.001	0.003	0.005	0.002	0	0.005

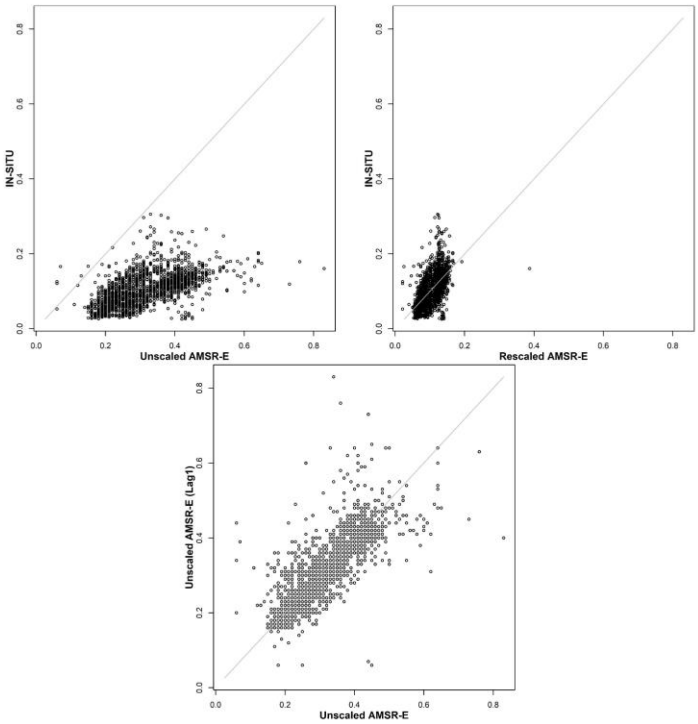

Figure 3.1. Scatter plot of the WASM and LPRM soil moisture data over Little River watershed

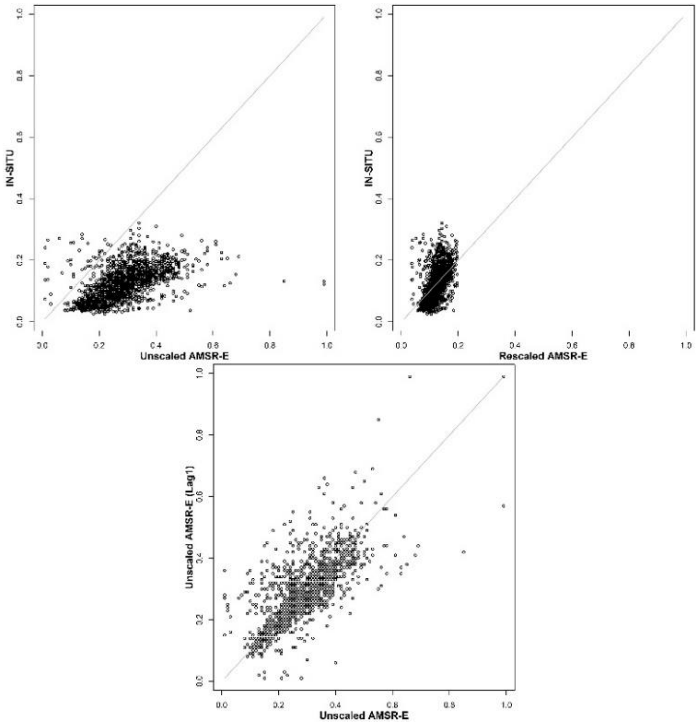

Figure 3.2. Scatter plot of the WASM and LPRM soil moisture data over Little Washita watershed

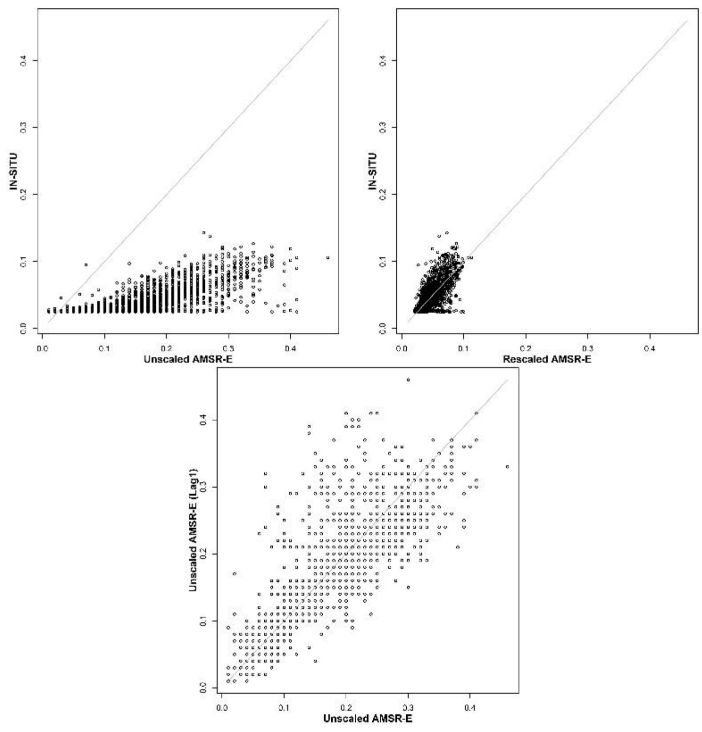

Figure 3.3. Scatter plot of the WASM and LPRM soil moisture data over Walnut Gulch watershed

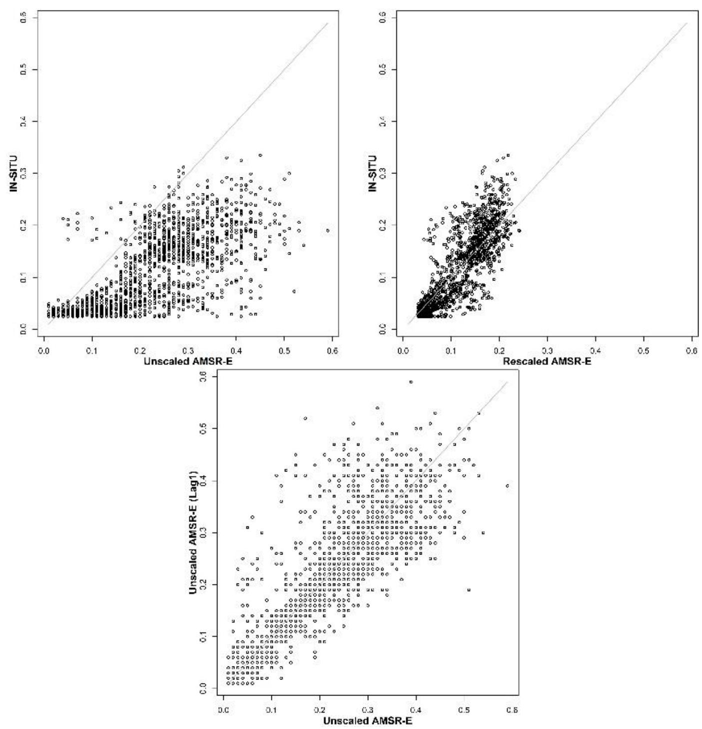

Figure 3.4. Scatter plot of the WASM and LPRM soil moisture data over Reynolds Creek watershed

Figure 3.5 and Figure 3.6 show the average values obtained by averaging the results of two experiments by using different training and validation periods and by averaging the results for four watersheds using the data presented in Table 3.3 and Table 3.4. When the results are averaged over all of the watersheds, all of the nonlinear methods (except for JOE copula) demonstrated improved correlations compared to the REG correlations using the training datasets (Figure 3.5). When validation datasets are used, MAR, GP, SVM, all four ANNs, and NORMAL copula still have superior correlations compared to REG (Table 3.2 and Figure 3.6). In particular, the improvements over LW, WG, and RC using ELMAN ANN (0.04, 0.03, and 0.135), respectively, are much higher than the improvements over other locations via various methods (Table 3.5).

Compared to the best performing linear method using the validation data (MAR), on average, the GP, SVM, ELMAN ANN, JORDAN ANN, and FRANK copula nonlinear methods yielded better results (Figure 3.6). These outcomes stressed the results of the first-order linear regression, which can be improved via higher order or more complex linear methods, and there is still added utility that can be gained via nonlinear methods compared to linear methods. Thus, nonlinear methods have a higher potential to give more accurate results compared to linear methods, and as a result, the existing nonlinear relations cannot be captured through linear methods.

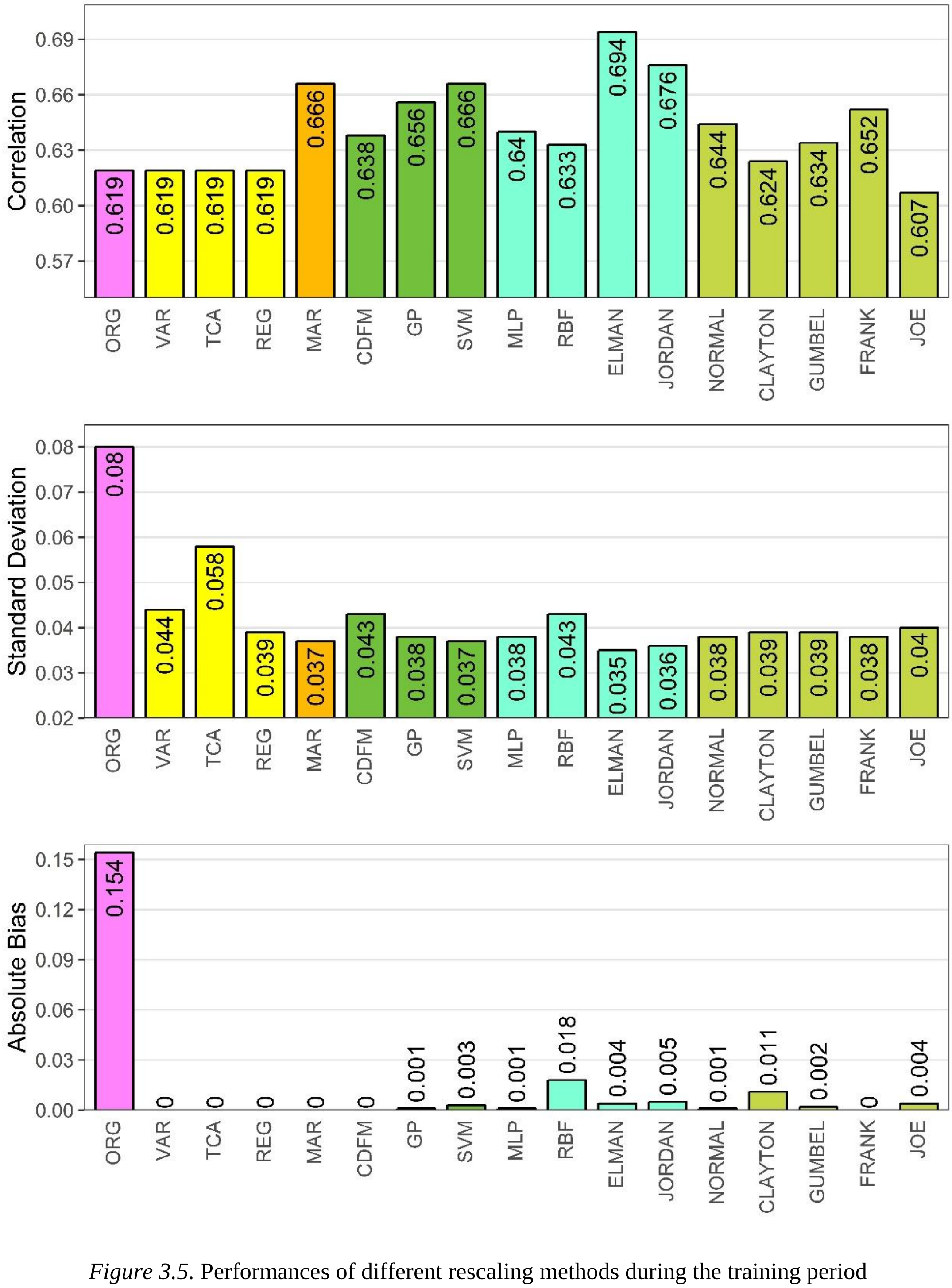

Figure 3.5. Performances of different rescaling methods during the training period

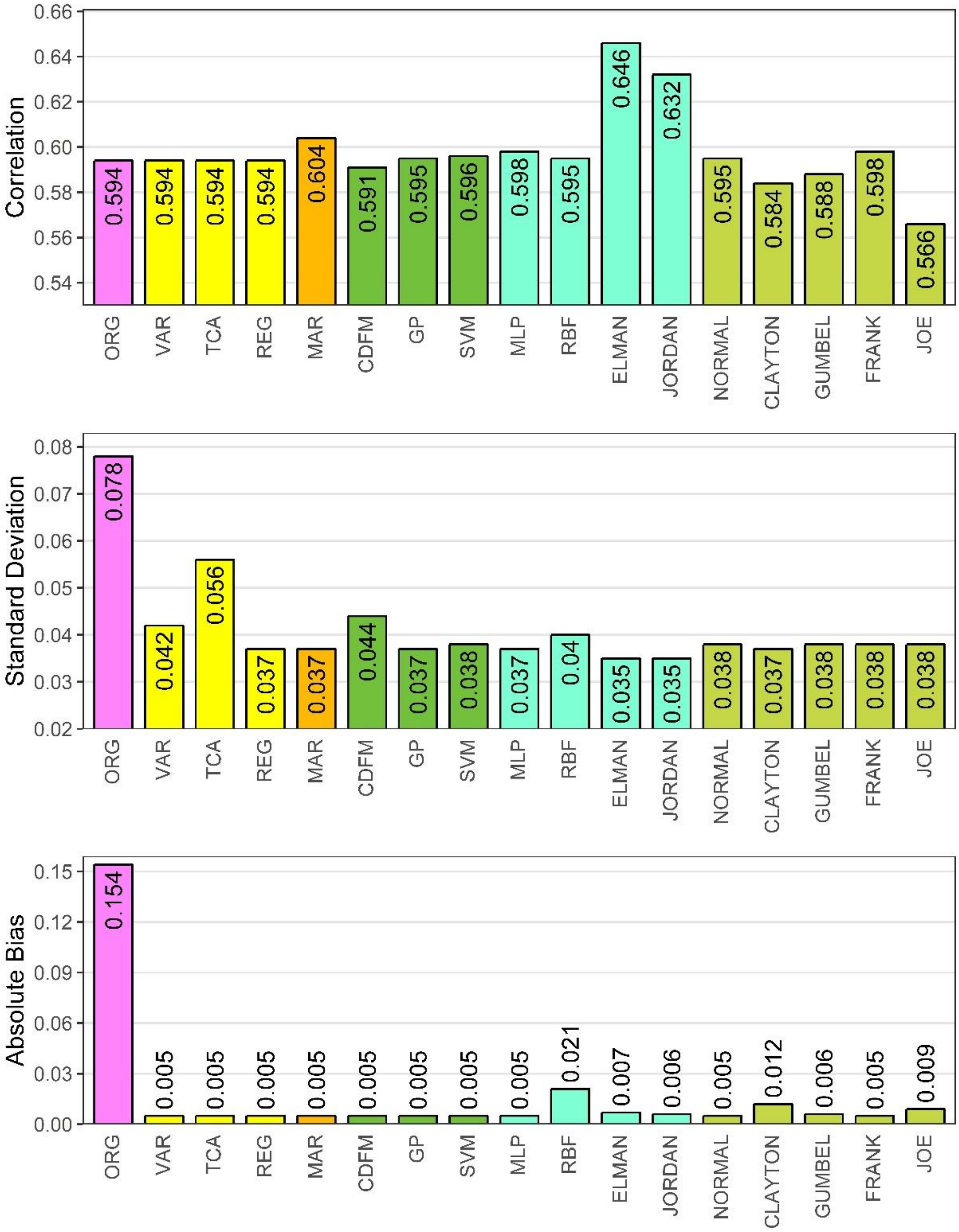

Figure 3.6. Performances of different rescaling methods during the validation period

Figure 3.7 represents the average values obtained for the four watersheds presented in Table 3.5. Overall, the relative performances of these 18 methods are very consistent for the training and validation datasets (i.e., better performing methods using training datasets also performed better when using validation datasets). This consistency can also be seen in the U values (Table 3.5 and Figure 3.7). This provides inferences about the relative performances of these rescaling methods when using training datasets, which could provide very meaningful information about independent data scenarios. The consistency between the training and validation results also supports the selection of training and validation periods; these two periods may not have a considerable difference in terms of the relation between the LPRM and WASM data, as well as in terms of the relative performances of the rescaling methods.

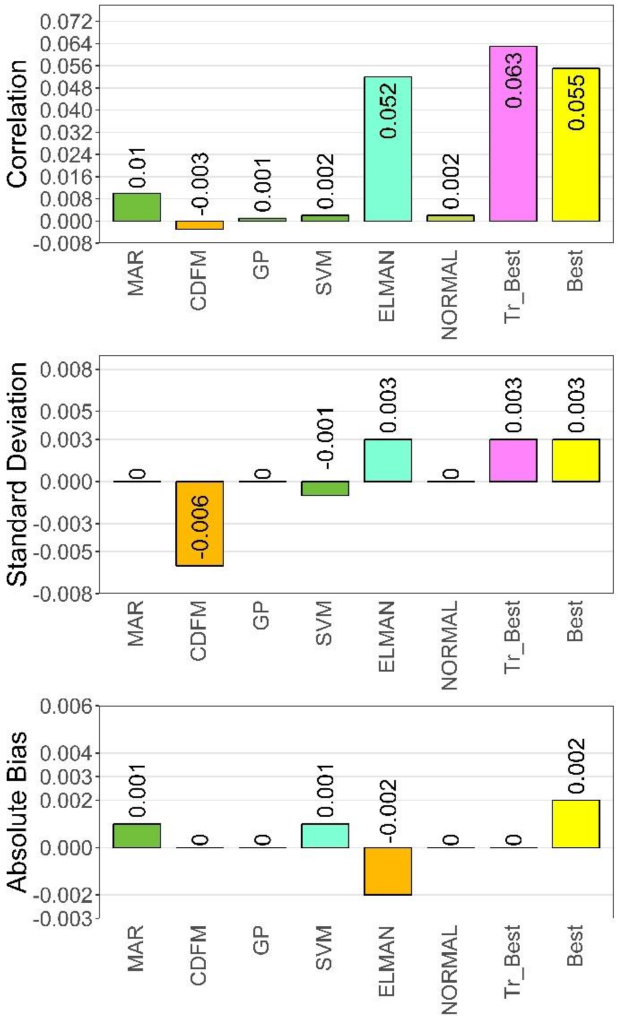

Figure 3.7. Added utility of the rescaling methods

On average, the ELMAN ANN methods yield a ρ improvement of ~0.05 using independent validation datasets. This improvement is lower (0.02 - 0.04 ρ improvement) for the GP, SVM, MAR, and NORMAL copula methods (Table 3.5 and Figure 3.7). In contrast to its wide use, the CDFM method has no added skill (Figure 3.7); in fact, on average, it yields degraded correlations compared to REG when validated using independent data (Table 3.5). When the method selection is consistent with the training results, these Tr_best methods yield better U values than any method alone, with U values that are similar to the best validation results ("Best") approximately 75% of the time (Figure 3.7). These results further support the above discussion that it is better to make a rescaling method selection that is consistent with the training data statistics, when this selection can yield better validation results than the selection of any other method alone.

When the parameters obtained using the training datasets are implemented over the validation datasets, some skill loss (i.e., artificial skill) is often observed because all of the methods overfit their datasets to some extent. Loosely speaking, an increase of 0.06 or 0.10 in ρ constitutes a statistically significant increase, especially when 1200 or 400 samples are used for training or validation experiments, respectively (e.g., an increase from 0.60 to 0.66 or from 0.60 to 0.70). Accordingly, MAR, SVM, and ELMAN ANN yield significant ρ improvements (with respect to REG ρ) over half of the training cases, whereas GP, FRANK copula, and JORDAN ANN also yield significant improvements over some locations (Table 3.2; most of the training improvements are over LW and RC, and only a few are over WG). By contrast, for validation experiments, only ELMAN and JORDAN ANNs resulted in significant ρ improvements (both over RC), showing that most of these improvements are artificial skills. Here, the degree to which the methods overfit the datasets is evaluated through the comparisons of ρ for the validation datasets (Figure 3.6) versus the training datasets (Figure 3.5), where higher differences indicate a higher degree of artificial skill. These results stress the use of independent validation data to avoid artificial skill.

The skills of nonlinear methods are heavily impacted by the number of iterations performed to optimally obtain certain parameters. By contrast, increasing the degree of these iterations eventually results in overtraining and hence overfitting. For example, in this study, the maximum number of iterations for ANN simulations is set at 1000. When this number is increased to 100,000, training correlations can be obtained between the reference and rescaled products (as high as 0.90 for certain cases). However, this gained training skill is quickly lost when the obtained ANN configurations and parameters are utilized on independent validation data. Such dramatic differences are more common for ANN than other methods (GP, SVM, and copula), whereas the degree of overfitting using other methods does not depend as much on user specifications as ANN (results not shown).

Among the copula methods, CLAYTON, GUMBEL, and JOE have asymmetric tail dependence properties (strong in one tail and weak in the other) and do not perform as well as NORMAL or FRANK, which have symmetric tail dependence for both training and validation experiments (Table 3.2 to Table 3.4). Both the copula and CDFM methods use $\mathrm{CDF_X}$ and $\mathrm{CDF_Y}$ to rescale observations. However, it is stressed that the performances of copula methods are very sensitive to the $\mathrm{C}_{\mathrm{U_N|U_1,U_2,\ldots,U_{N-1}}}$ values (equation (9), which are selected during training. The optimality of these $\mathrm{C}_{\mathrm{U_N|U_1,U_2,\ldots,U_{N-1}}}$ values depends on the objective of the training process (e.g., the minimization of AMB only, the maximization of ρ only, the minimization AMB and σ_ϵ simultaneously, or the minimization of AMB and σ_ϵ, and the maximization of ρ simultaneously). In this study, the penalty function is formed and $\mathrm{C}_{\mathrm{U_N|U_1,U_2,\ldots,U_{N-1}}}$ values are obtained in a way that training is penalized for increased AMB and σ_ϵ and decreased ρ. Investigations for the added utility of lagged observations show only Normal Copula (Elliptical family) utilizing this information, whereas the remaining copula types (Archimedean family) result in degraded rescaled products (Figure 3.6). This result is consistent with the study of Hesami Afshar et al., (2016), who found the Elliptical family to be better at capturing the dependency among variables than the copula functions of the Archimedean family.

3.2. Impact of Rescaling Approaches on Accuracy of Fused Products

In second case study different soil moisture products are rescaled using different methods, styles, and techniques for the purpose of the systematic differences between them to be alleviated. Later these rescaled products are fused for the accuracy assessment using correlation statistic over different locations. Overall experiments are performed using six different parent couples, five different rescaling methods, three different rescaling techniques, two different rescaling styles, and four different reference datasets selection over four different locations (total 6*5*3*2*4*4=2880 experiments; the detail results of all 2880 experiments are available in appendix 1 and 2).

Before rescaling methods, styles, and techniques are implemented, the variability and the accuracy differences between products are investigated. Here higher accuracy for any product is defined as higher correlation against similar component of WASM. The accuracy and the variability assessments performed over each of the four watersheds (Figure 3.8 to Figure 3.11) and then averaged (Table 3.6 and Figure 3.12). Overall, NOAH and AMSR-E soil moisture time series have higher accuracy than ASCAT and API owing to the accuracy of their low frequency (i.e., seasonality and smooth) components; while ASCAT and API accuracies stem from their high frequency (i.e., anomaly and deviance) components. On the other hand, even though overall accuracy of API is relatively lower than the accuracies of AMSR-E and NOAH products, API high frequency component has the highest accuracy (Figure 3.12). The different temporal decomposition techniques (i.e., seasonality/anomaly vs smooth/deviance) result in varying low/high frequency variability contributions to overall variability. Results show smooth component carry higher percentage of the low frequency variability than climatology component; in fact, climatology low frequency variability is lower than the anomaly high frequency variability while for the smooth/deviance decomposition smooth low frequency variability has higher variability weight when compared to the total variability (Table 3.6).

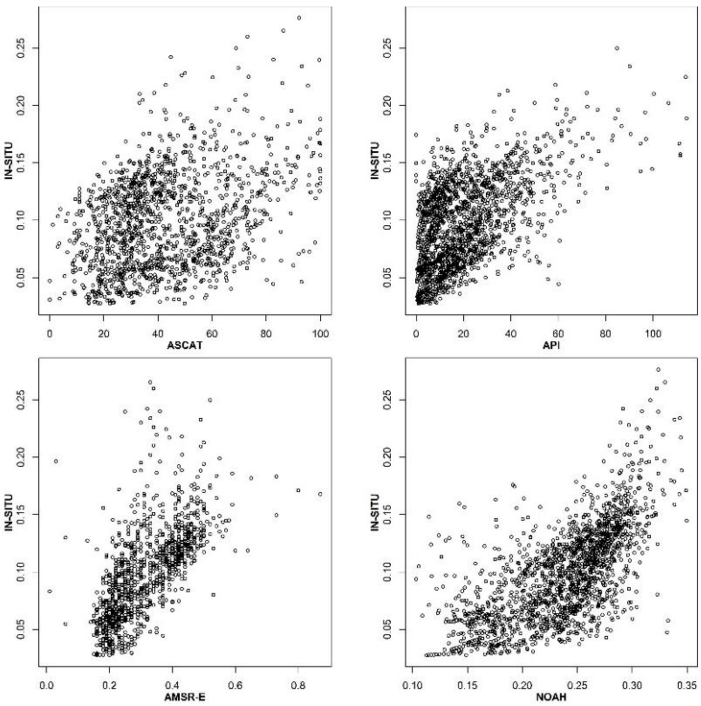

Figure 3.8. Scatterplot of different soil moisture products against WASM over Little River watershed

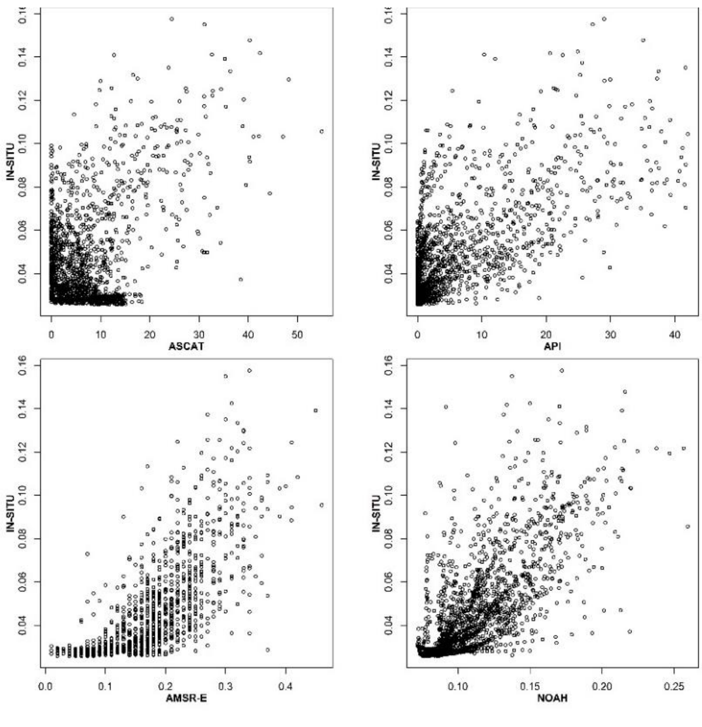

Figure 3.9. Scatterplot of different soil moisture products against WASM over Little Washita watershed

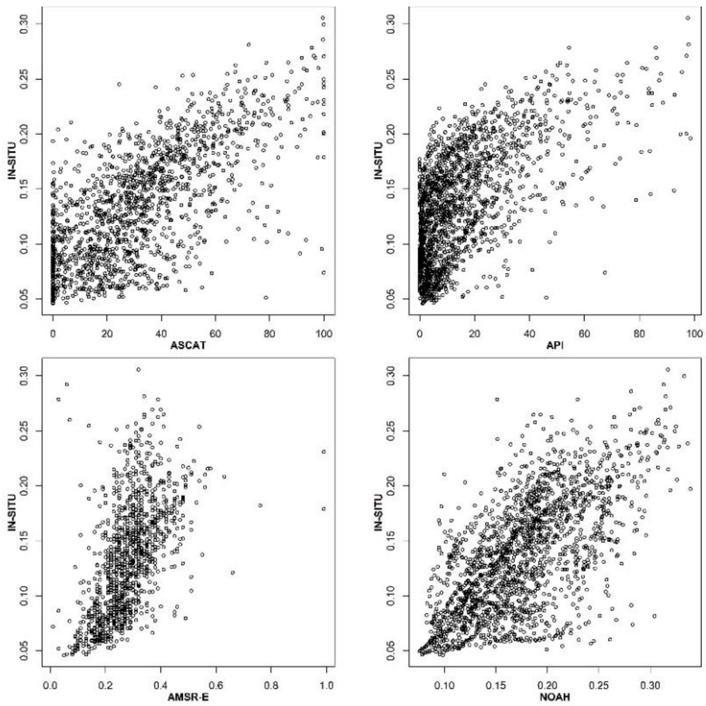

Figure 3.10. Scatterplot of different soil moisture products against WASM over Walnut Gulch watershed

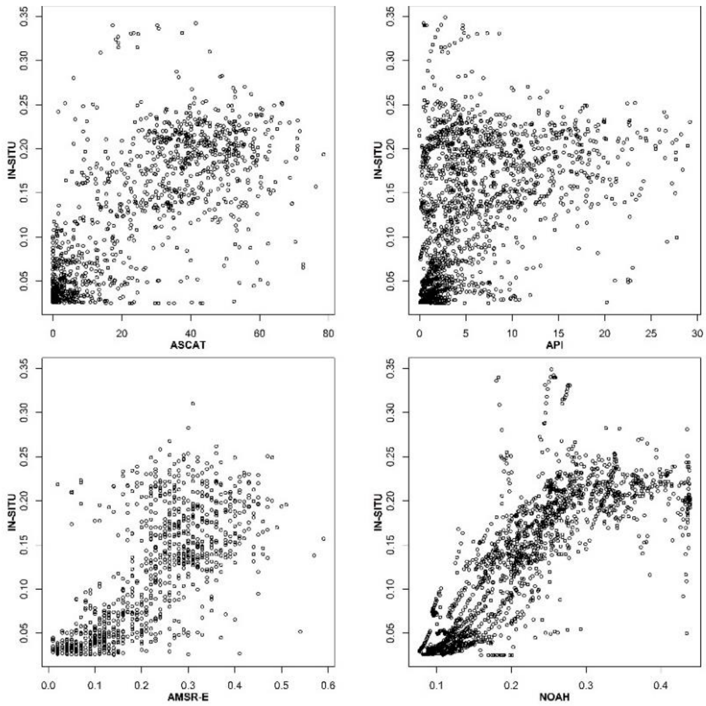

Figure 3.11. Scatterplot of different soil moisture products against WASM over Reynolds Creek watershed

Table 3.6. *The average ratio of low and high frequency soil moisture variance to total time series*

Dataset	*Time series component*			
	Seasonality	*Anomaly*	*Smooth*	*Deviance*
ASCAT	0.31	0.65	0.59	0.27
AMSR-E	0.48	0.48	0.72	0.17
API	0.26	0.7	0.64	0.16
NOAH	0.36	0.62	0.83	0.08
WASM	0.37	0.6	0.74	0.12

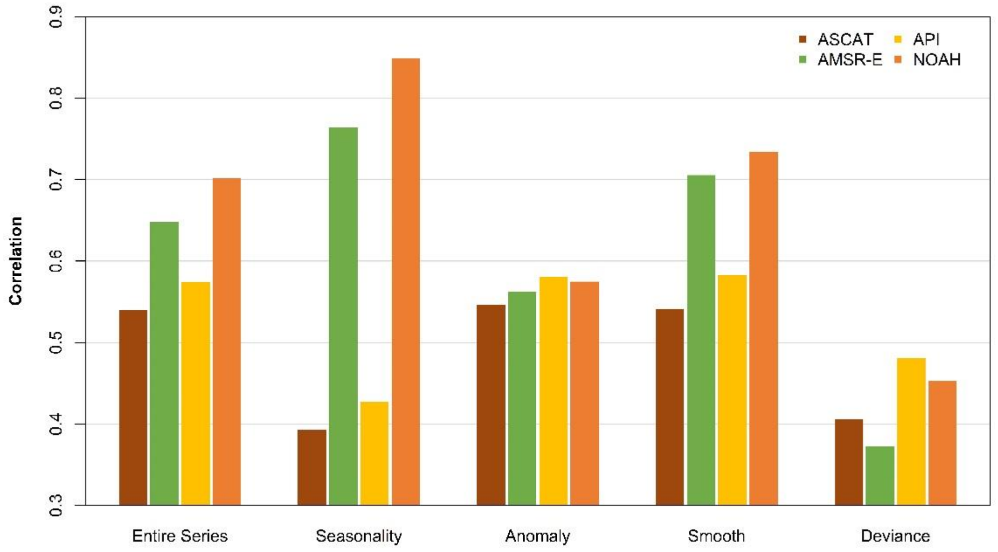

Figure 3.12. The average correlation between WASM and different soil moisture time series components

Here a total of 2880 experiments are performed forming a 6-dimensional resulting matrix. Below results given show only 2-dimensional results obtained by averaging out the remaining four dimensions. For the sake of consistency, one of these two dimensions in these figures are selected as the reference dataset selection (i.e., x-axis) while the other dimension (i.e., y-axis) varied for the remaining 4 dimensions.

The accuracy assessments reflecting the impact of rescaling style selection in a data fusion framework is presented in Figure 3.13. Overall, selection of NOAH as the reference dataset resulted in a more accurate fused product, while this performance was not impacted by the rescaling style (i.e., single/monthly coefficient) selection. The use of more aggressive rescaling style result in degraded fused product accuracy when less accurate reference datasets are selected. In general, higher correlations are associated with the constant rescaling style, while time-varying (i.e., more aggressive) rescaling style selection could not improve the correlation of the final fused product as much particularly when the overall accuracy of the reference product is lower (e.g., ASCAT and API).

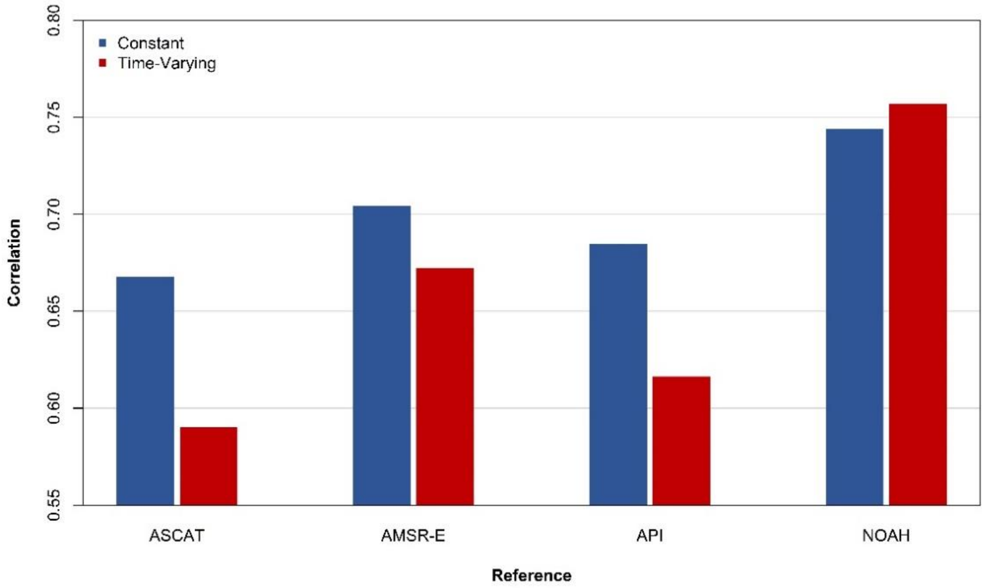

Figure 3.13. Impact of the aggressiveness of rescaling methods and the reference dataset selection on the accuracy of the fused products

On average, the simple fusion of two random noise time series with no error cross-correlation will yield lower variability product (i.e., noise is damped more) than fusion of two random noise products with error cross-correlation (i.e., noise is damped less). Accordingly, in fusion methodologies, it is preferable that the fused products have "real signal" components as similar as possible to each other in some statistical sense, while "real noise" components should get as close as possible to be random and not correlated (i.e., the "real noise" mean and standard deviation to get closer to zero; Figure 3.14).

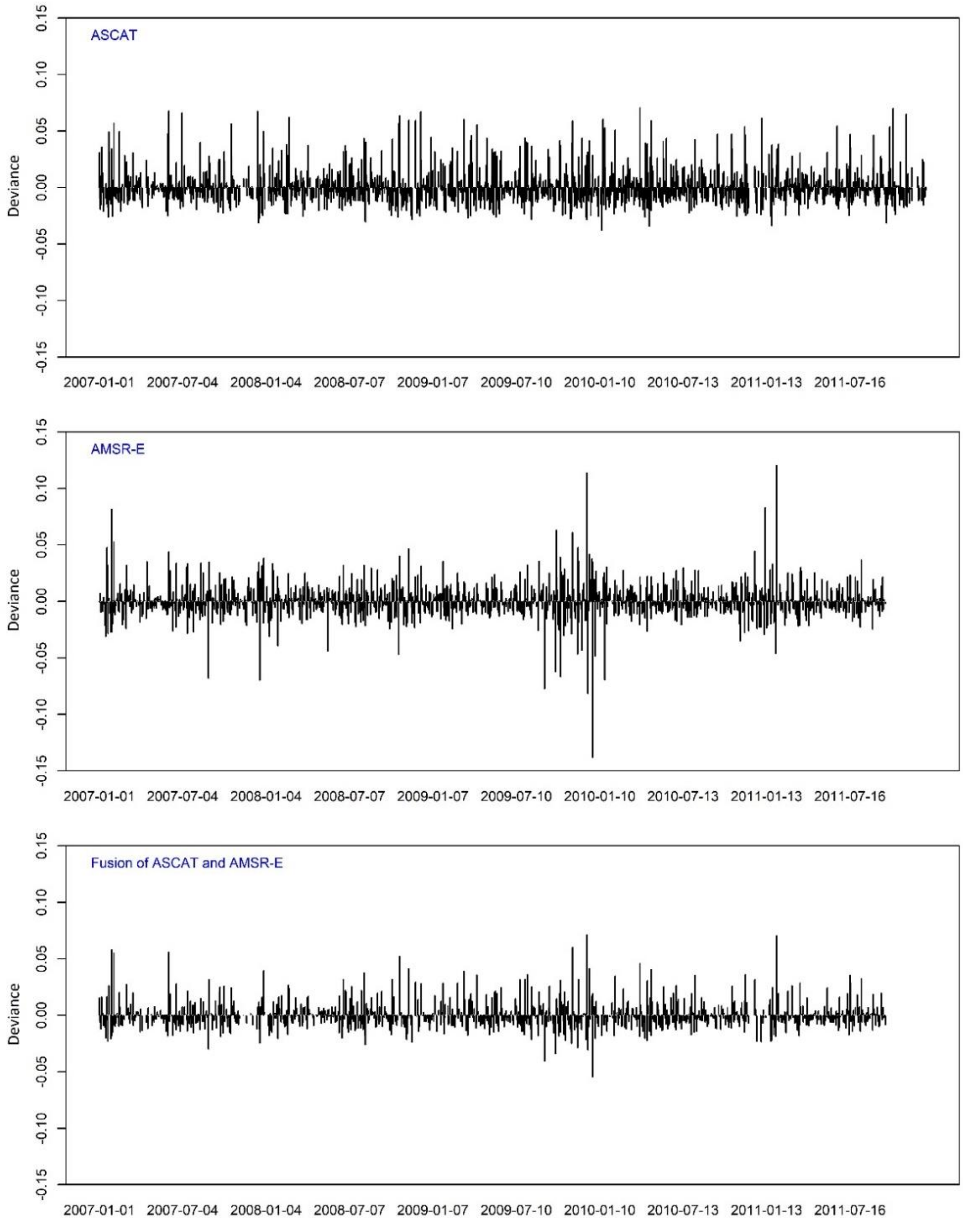

Figure 3.14. Fusion of the deviance component of ASCAT and AMSR-E in NOAH space

The time series can be shown to be a function of the true signal and the noise time series, it is expected that use of different rescaling factors for these components might better reduce the differences between the products. Given the true signal and the real noise components of soil moisture time series cannot be retrieved in practice (i.e., the true signal component may not be retrieved explicitly in many applications), this implementation is not possible. On the other hand, a similar approach can be taken via using different rescaling coefficients for the different time scale components of products (i.e., in this study low/high frequency components, namely seasonality/anomaly & smooth/deviance). It is stressed that the low frequency component does not entirely reflect the truth and the high frequency component does not entirely reflect the noise; instead both the low and the high components carry elements of the truth and the noise. Here, it is important to stress that there is no quarantine that the use of separate rescaling coefficients will yield an improved rescaled product. This usage is beneficial only if different time scale components of products relate to each other differently; if relate similarly, then this usage is not beneficial. However, when the two high/low frequency decomposition methods used in this study (i.e., seasonality/anomaly & smooth/deviance) are compared, the method that obtain low frequency component closer to truth and high frequency component closer to noise might possibly yield better results as we may have more faith in the difference between the rescaling coefficient difference between the truth and the noise than other time scale rescaling coefficient differences.

Given the expectation that independently retrieved products should have quasi-independent errors, having reduced cross-correlation in the high frequency components imply it is closer in nature to noise than the truth and it contains more elements from the real noise than the real true signal. This implies deviance component contains more noise and less truth than anomaly component (*Table 3.7*). At this point, it is plausible that the use of two different rescaling coefficients for two different frequency components of time series that are closer to the truth and the real noise components (respectively) might yield a better fit than use of two different rescaling coefficient for two different components of time series that are mixture of both the truth and the real noise components. Hence, the goal of decomposition efforts should be acquisition of low and high frequency components closer in nature to the truth and the noise, respectively.

Table 3.7. *The average autocorrelation of soil moisture time series and their components*

Dataset	*Time series component*			
	Seasonality	*Anomaly*	*Smooth*	*Deviance*
ASCAT	0.72	1	0.57	0.99
AMSR-E	0.81	1	0.59	0.99
API	0.91	1	0.87	0.99
NOAH	0.96	1	0.94	1
WASM	0.93	1	0.89	0.99

Overall, the deviance components have less cross-correlation (Table 3.8) and lower variability (Table 3.7) than the anomaly components, while smooth components have higher cross-correlation and variability than seasonality. Accordingly, smooth-deviance decomposition is expected to be more beneficial than seasonality-anomaly decomposition. Accordingly, when the variability of decomposition techniques are compared in Table 3, smooth-deviance technique-based low frequency product has lower variability and look more like a random noise than seasonality-anomaly based product (i.e., deviance component is closer to a random noise than anomaly component for the same product). Expectedly, once these components are rescaled and then fused, smooth-deviance decomposition based fused product result in higher accuracy than seasonality-anomaly decomposition based fused product (Figure 3.15).

Table 3.8. *The average cross-correlation between products for different decomposed parts*

Dataset	*Time series component*				
	Entire Series	*Seasonality*	*Anomaly*	*Smooth*	*Deviance*
ASCAT - AMSR-E	0.41	0.092	0.565	0.338	0.43
ASCAT - API	0.514	0.523	0.511	0.561	0.38
ASCAT - NOAH	0.484	0.257	0.51	0.491	0.4
AMSR-E - API	0.312	0.076	0.405	0.29	0.26
AMSR-E - NOAH	0.581	0.737	0.487	0.647	0.33
API - NOAH	0.452	0.324	0.494	0.485	0.35

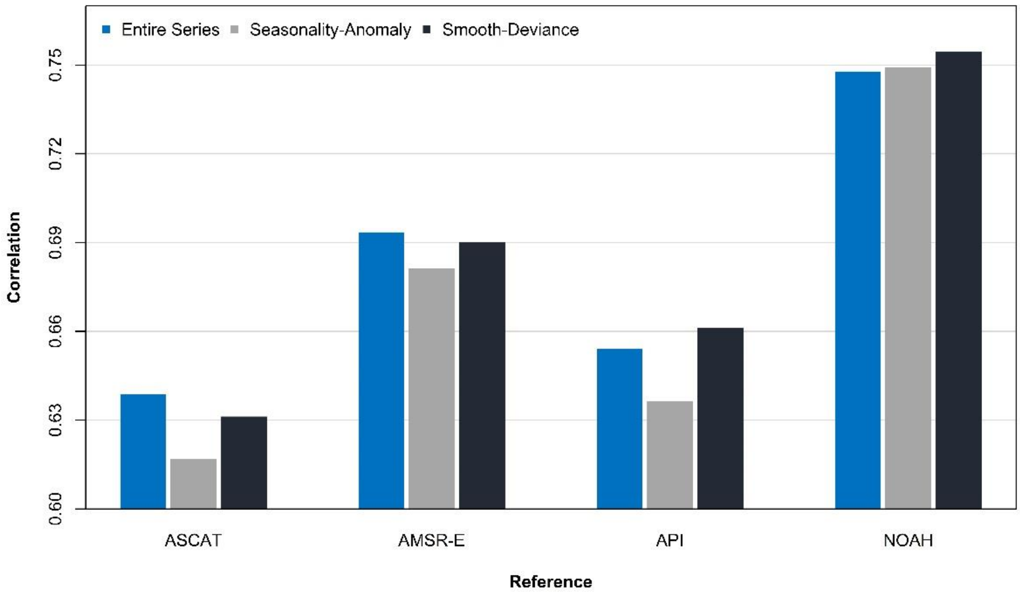

Figure 3.15. Impact of rescaling approach and reference dataset selection on performance of fused products against WASM dataset

Impact of rescaling methods over the accuracy of the fused product is given in Figure 3.16. Overall, the impact of rescaling method selection is more pronounced when the reference dataset is less accurate than more accurate (i.e., difference between the obtained accuracy estimates via various rescaling methods is less for NOAH than ASCAT or AMSR-E). The reference dataset selection also impacts the rescaling method performance: nonlinear MAR and SVM methods yield higher accuracy fused product when NOAH (i.e., higher accuracy product) is used as reference; on the other hand, linear REG and VAR methods yield higher accuracy fused product when less accurate products are used as reference.

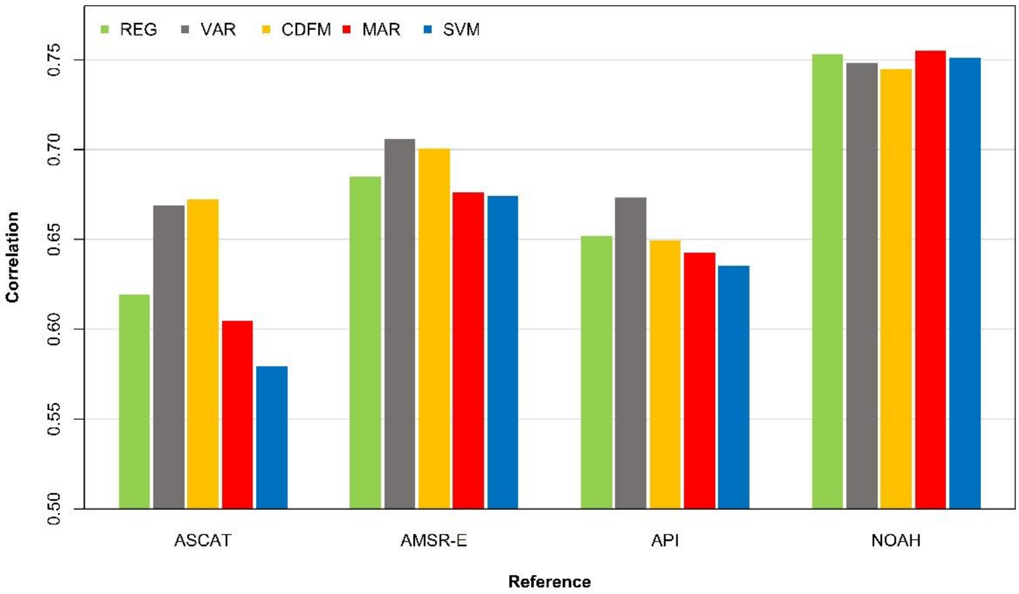

Figure 3.16. Impact of rescaling method and reference dataset selection on performance of fused products against WASM dataset

Investigation of the impact of the parent product selection over the accuracy of the fused product (Figure 3.17) show AMSR-E - API parent couples consistently yield higher accuracy fused estimate than other parent couples regardless of the reference dataset selection. This is perhaps because the mutual information between the products AMSR-E and API is less than the mutual information between other products (i.e., here the mutual linear information is measured using correlation coefficient in Table 3.8). Even though AMSR-E and API products are fused together, results show it is better to rescale both products to the space of NOAH (i.e., third product) first before the fusion to obtain higher accuracy fused estimate (Figure 3.16). Reason for rescaling to a third reference product is because before the fusion of the products their accuracies are low hence rescaling step involve higher sampling errors, which later further propagate to AMSR-E - API fused product. On the other hand, when products are rescaled to the space of a higher quality product first (i.e., to alleviate the differences between the products), then the fusion process becomes more effective via lowered sampling errors added to the fused product.

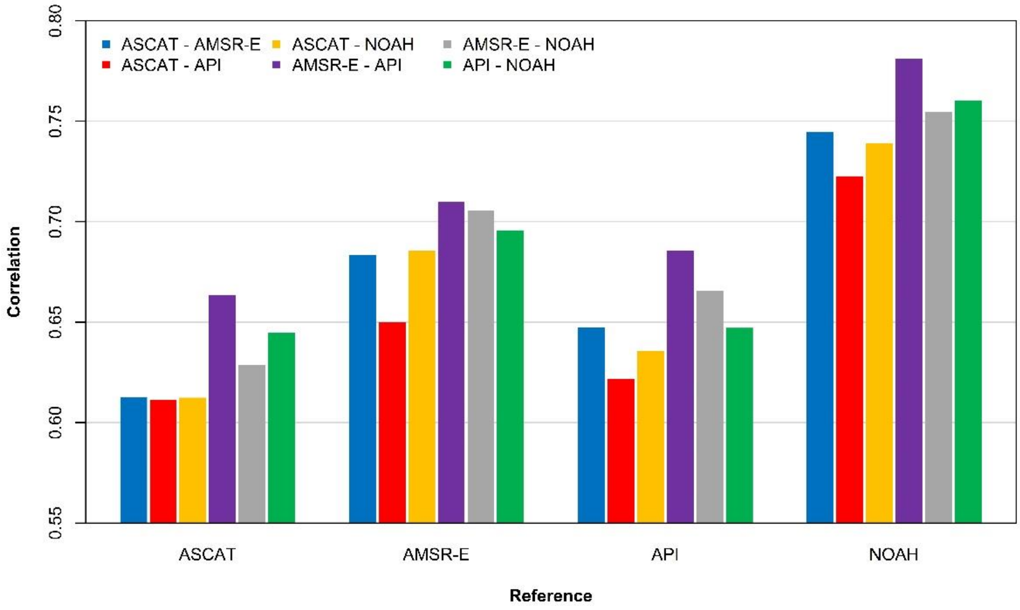

Figure 3.17. Impact of the parent and the reference product selection on fused product accuracy

Given NOAH dataset is globally available, the fused products have better performance when NOAH is selected as the reference dataset, Table 3.9 and Table 3.10 summarizes the correlation statistics of fused products against WASM with considering different parent couples and rescaling methods (i.e., results are related with fusion of ASCAT/AMSR-E/API/NOAH products using NOAH as reference) with using of constant and time-varying application styles. Among the rescaling methods, despite its simplicity REG performs well when it is implemented with smooth-deviance decomposition technique, while VAR and MAR performances are marginally better than other rescaling methods over time-varying application. When the reference dataset selection is changed from NOAH to WASM, it is expected to obtain additional benefit via using of nonlinear methods [i.e., as the reference dataset accuracy increases (Afshar & Yilmaz, 2017)].

Table 3.9. *Impact of rescaling methods and their implementation approaches (with constant application) on performance of fused products (over NOAH reference) using WASM as validation dataset (statistics are averaged over four watersheds)*

Approach	*Fused Product*		*Rescaling Methods*				
			REG	*VAR*	*CDFM*	*MAR*	*SVM*
Smooth-deviance	ASCAT	AMSR-E	**0.78**	0.76	0.75	0.77	0.76
	ASCAT	API	0.69	0.66	0.66	**0.71**	0.7
	ASCAT	NOAH	**0.75**	0.73	0.73	0.74	0.74
	AMSR-E	API	**0.82**	0.81	0.8	0.8	0.8
	AMSR-E	NOAH	0.76	0.76	**0.77**	0.76	0.76
	API	NOAH	**0.76**	0.75	0.75	**0.76**	0.75
Seasonality Anomaly	ASCAT	AMSR-E	0.72	0.71	0.71	**0.75**	0.74
	ASCAT	API	0.71	0.67	0.64	**0.76**	**0.76**
	ASCAT	NOAH	0.74	0.73	0.71	**0.75**	**0.75**
	AMSR-E	API	0.77	0.77	**0.78**	0.77	0.77
	AMSR-E	NOAH	0.75	0.75	0.76	0.75	**0.76**
	API	NOAH	0.76	0.76	0.75	0.77	**0.78**
Entire series	ASCAT	AMSR-E	0.74	0.72	0.71	**0.75**	0.74
	ASCAT	API	0.67	0.65	0.64	**0.7**	0.69
	ASCAT	NOAH	**0.74**	0.72	0.72	**0.74**	**0.74**
	AMSR-E	API	0.79	0.79	0.78	**0.8**	0.79
	AMSR-E	NOAH	**0.76**	**0.76**	**0.76**	**0.76**	**0.76**
	API	NOAH	**0.76**	0.75	0.75	**0.76**	**0.76**

Table 3.10. *Impact of rescaling methods and their implementation approaches (with time-varying application) on performance of fused products (over NOAH reference) using WASM as validation dataset (statistics are averaged over four watersheds)*

Approach	*Fused Product*		*Rescaling Methods*				
			REG	*VAR*	*CDFM*	*MAR*	*SVM*
Smooth-deviance	ASCAT	AMSR-E	**0.76**	**0.76**	**0.76**	0.75	**0.76**
	ASCAT	API	0.76	**0.77**	0.76	0.76	0.75
	ASCAT	NOAH	**0.75**	**0.75**	0.74	0.74	0.74
	AMSR-E	API	0.78	**0.79**	**0.79**	0.77	0.77
	AMSR-E	NOAH	0.75	**0.76**	**0.76**	0.74	0.75
	API	NOAH	0.76	**0.77**	**0.77**	0.75	0.75
Seasonality Anomaly	ASCAT	AMSR-E	0.75	0.74	0.74	**0.76**	0.74
	ASCAT	API	0.76	0.76	0.76	**0.77**	0.75
	ASCAT	NOAH	**0.75**	**0.75**	0.74	**0.75**	0.74
	AMSR-E	API	0.77	**0.78**	**0.78**	0.77	0.76
	AMSR-E	NOAH	**0.75**	**0.75**	**0.75**	**0.75**	**0.75**
	API	NOAH	0.76	**0.77**	**0.77**	0.75	0.75
Entire series	ASCAT	AMSR-E	**0.75**	0.74	0.74	**0.75**	0.74
	ASCAT	API	0.75	**0.76**	**0.76**	**0.76**	0.75
	ASCAT	NOAH	**0.75**	**0.75**	0.74	0.74	0.74
	AMSR-E	API	0.77	**0.78**	**0.78**	**0.78**	0.77
	AMSR-E	NOAH	**0.75**	**0.75**	**0.75**	**0.75**	**0.75**
	API	NOAH	0.76	0.77	**0.78**	0.76	0.75

Among different parent couples, the AMSR-E – API parent couple perform better than others over different rescaling methods and approaches (i.e., both in terms of application style and technique). After AMSR-E – API fusion product, the fusion of ASCAT and AMSR-E gives the highest accuracy among different parent couples. Considering the CDFM method and the REG one with smooth-deviance decomposition application, it can be seen that there is 0.08 correlation improvement with changing the application style and rescaling method from CDFM to REG which implies the utility of smooth-deviance decomposition technique.

The performance of AMSR-E - API parent couple is further investigated over the four WASM datasets separately via comparison of cross-correlations of rescaled products and fused products against WASM over different watersheds using different reference dataset selection (Figure 3.18 to Figure 3.20). Here the fused products are the results of merging AMSR-E and API soil moisture products which are rescaled to different references trough constant application of smooth-deviance decomposition method with considering linear regression as the rescaling method (based on the results of Table 3.9).

On average, the fused product has higher accuracy than all the parent products individually (on average the correlation difference between the fused product and the product having the second highest correlation is 0.12). This result is true for different reference dataset selections that the fusion algorithm shows persistent improvement compared against parent products (e.g., NOAH, AMSR-E, and API). However, there is an exception for this general trend over Reynolds Creek that NOAH has higher correlation than AMSR-E and API fusion; probably because of the poor performance of API due to the mountainous topography of this site (Blanchard et al., 1981), illustrating the neglected importance of API model (particularly over flat areas) and the added utility of proposed smooth-deviance decomposition implementation approach.

On the other hand, when the reference is considered as AMSR-E (Figure 3.19), it can be seen that the usage is of API model for enhancing AMSR-E through data fusion framework while the original correlation of AMSR-E product over Walnut Gulch has been increased more than 0.10 and on average there is an improvement of 0.05 over correlation of AMSR-E soil moisture product over four watersheds. Moreover when the reference is changed from AMSR-E reference to API, and considering this scenario as a very simple assimilation framework, it can be seen that the accuracy of API model by adding AMSR-E information to it can be increased efficiently (~0.12 on average). While this improvement is regardless of the accuracy of rescaled product (e.g., the AMSR-E accuracy has been decreased over Little River and Little Washita watersheds after rescaling).

Overall, it seems that the accuracy of the reference product over data assimilation studies is very important as well. For example, over Walnut Gulch watershed, when the accuracy of API model is slightly higher than other watersheds, the result of data fusion also show higher accuracy and in the case when the reference has less accuracy (Reynolds Creek) the accuracy of final fused product diminishes in comparison to the other fusion scenarios. This once again implies the importance of having a reference product with high accuracy in fusion of soil moisture products.

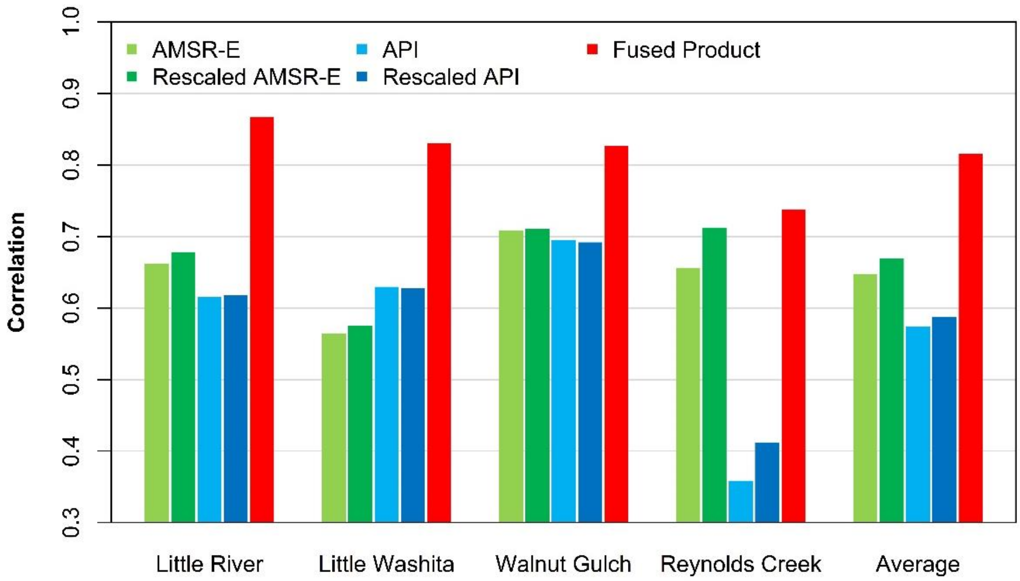

Figure 3.18. Comparison of the accuracy of the unscaled native, the rescaled and the fused products evaluated against WASM datasets over NOAH space

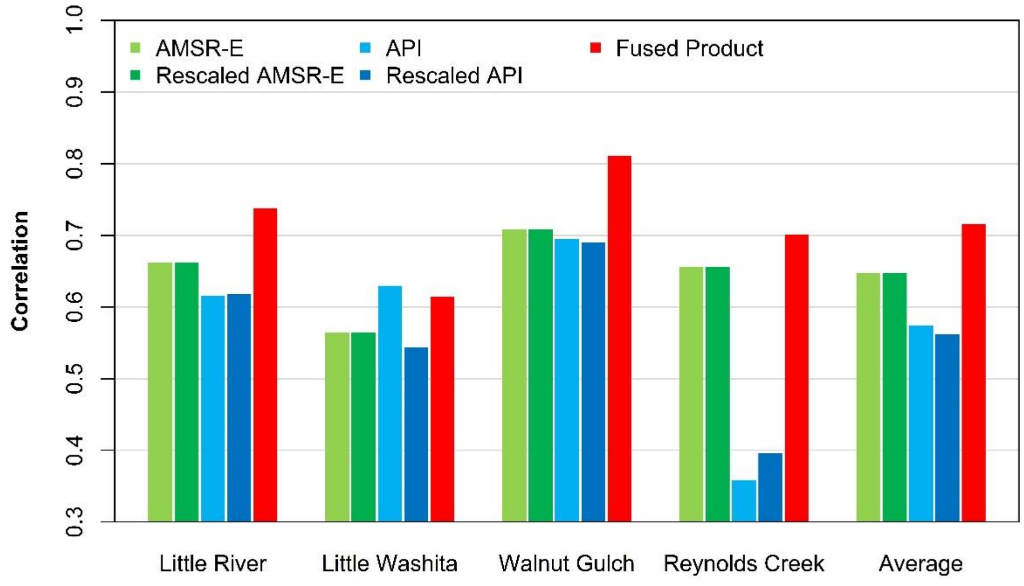

Figure 3.19. Comparison of the accuracy of the unscaled native, the rescaled and the fused products evaluated against WASM datasets over AMSR-E space

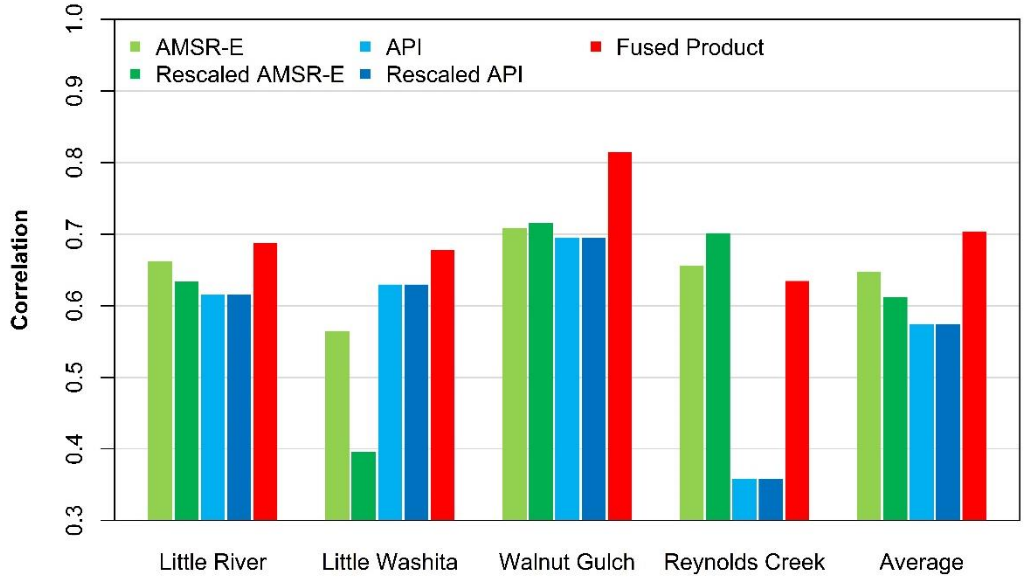

Figure 3.20. Comparison of the accuracy of the unscaled native, the rescaled and the fused products evaluated against WASM datasets over API space

The simple fusion of two products on average improves the correlation of the products by 0.055 (ASCAT 0.115, AMSR-E 0.037, API 0.098, NOAH -0.029) without selecting any particular reference (results are available in appendix 2); but when NOAH is selected as the reference dataset the improvement increases to 0.13 (ASCAT 0.19, AMSR-E 0.11, API 0.18, NOAH 0.05). Comparison of the added value for each individual dataset when NOAH is selected as reference shows ASCAT and API has higher gains (0.19 and 0.18 respectively) while AMSRE and NOAH has relatively lower gains (0.11 and 0.05 respectively). This implies ASCAT and API are less skillful products than AMSR-E and NOAH.

Overall, time-varying rescaling styles assumption (e.g., monthly rescaling styles) clearly results in discontinuities in the soil moisture time series, while constant coefficient assumption does not have such an adverse impact (Figure 3.21 to Figure 3.23). Even though the time-varying rescaling approach results in improved fused products when the reference product is more accurate (Yilmaz et al., 2016), the discontinuities make the time series unrealistic. Briefly, there is a trade-off between the improved accuracy of the fused product and the realism of the time series when the reference dataset accuracy is high. When a relatively less skillful reference dataset is selected, then aggressive implementation of the most nonlinear methods (including the time-varying assumptions) result in reduced fused product skill stemmed from the over-fitting of the unscaled product to the reference product. For such cases, the linear methods are able to remove the systematic differences in the unscaled dataset without compromising the skill of the fused product.

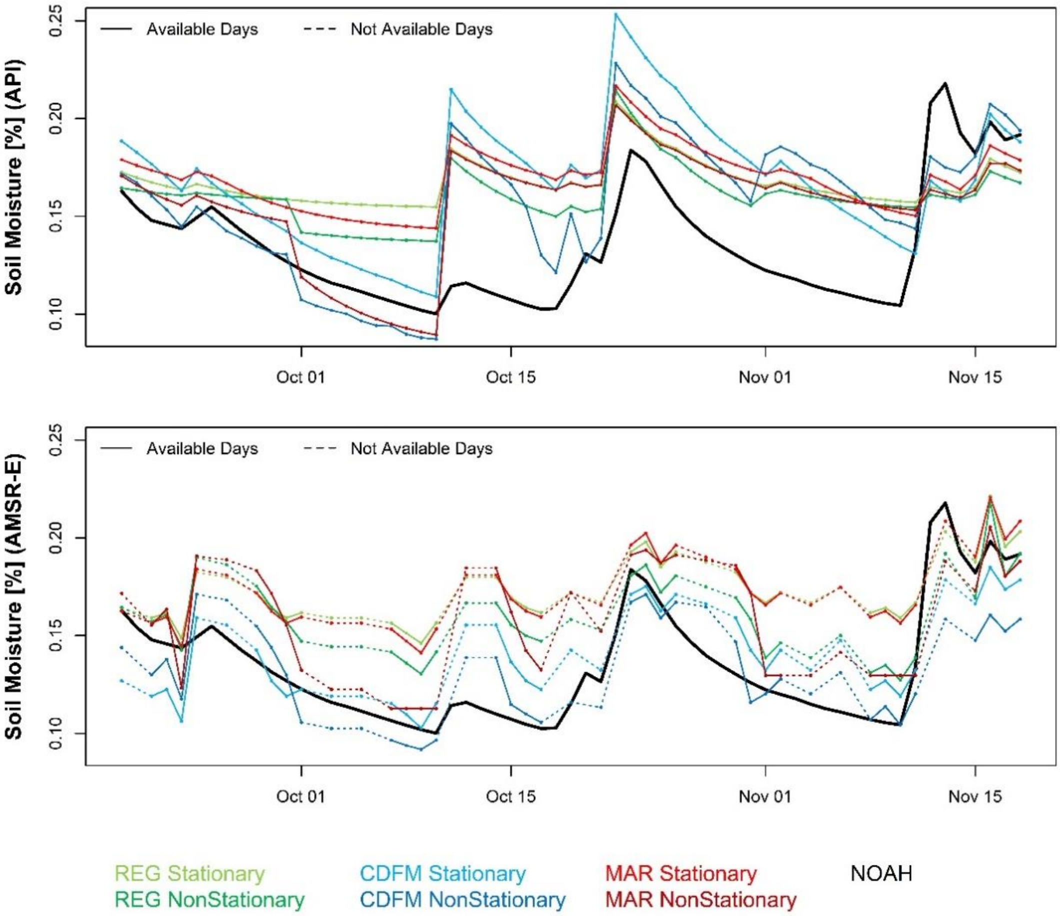

Figure 3.21. Comparison of different rescaling methods and their application style (technique: No-Decomposition), in rescaling of API and AMSR-E soil moisture product to NOAH space over Little Washita watershed between Sept 10 and Nov 20 of year 2010

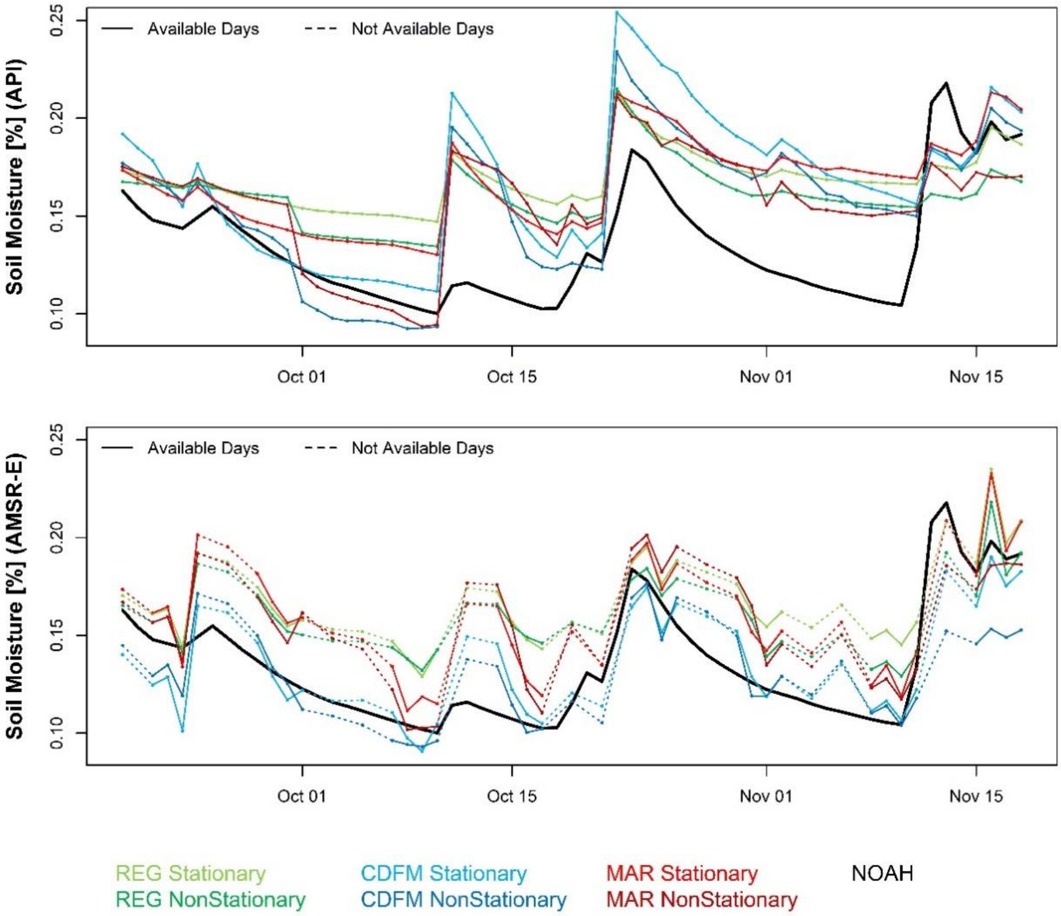

Figure 3.22. Comparison of different rescaling methods and their application style (technique: Seasonality-Anomaly Decomposition), in rescaling of API and AMSR-E soil moisture product to NOAH space over Little Washita watershed between Sept 10 and Nov 20 of year 2010

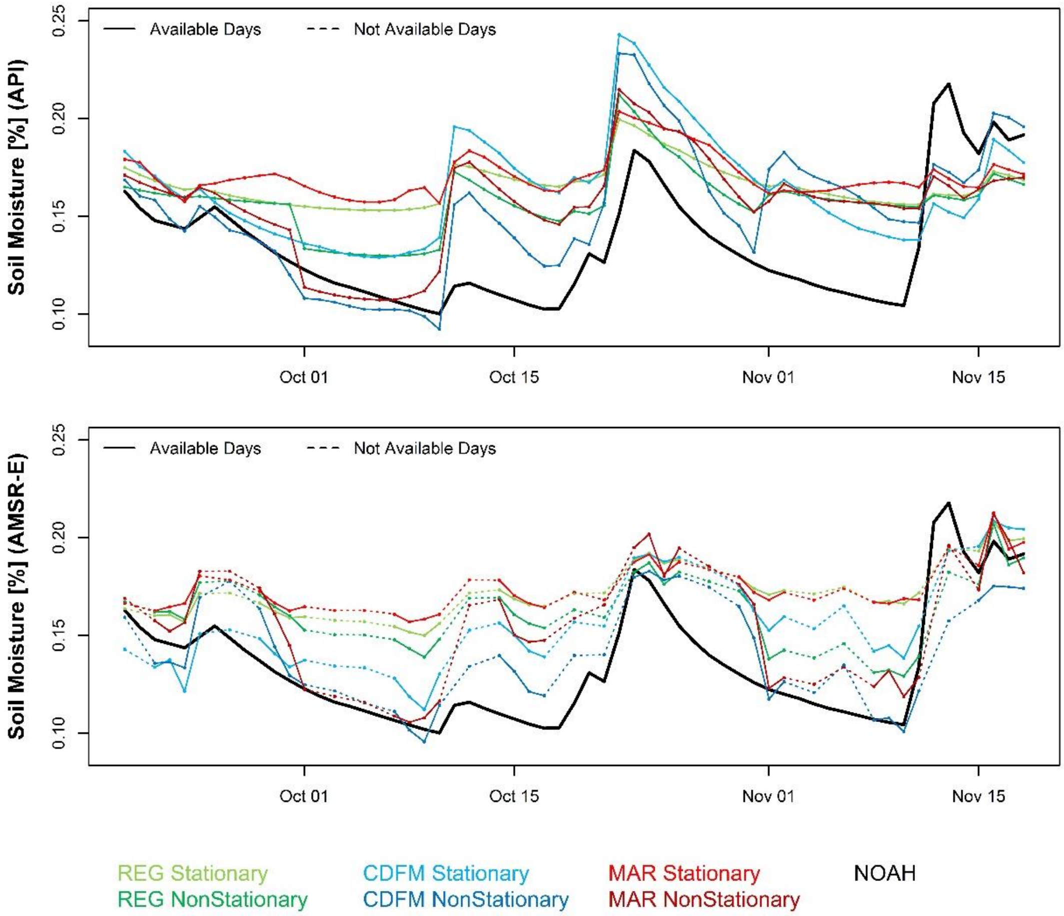

Figure 3.23. Comparison of different rescaling methods and their application style (technique: Smooth-Deviance Decomposition), in rescaling of API and AMSR-E soil moisture product to NOAH space over Little Washita watershed between Sept 10 and Nov 20 of year 2010

The time series of fused products derived from merging of above presented time series (Figure 3.21 to Figure 3.23) are shown in Figure 3.24 to Figure 3.26. Here Figure 3.24 to Figure 3.26 show the performance of fused products over space of WASM (fused products are rescaled to space of WASM using variance-matching method). While the rescaling techniques (i.e., No decomposition, Seasonality-Anomaly decomposition, and Smooth-Deviance decomposition) are separately shown in different figures and each figure is separated to two panels in order to show the impact of different application styles more clear. Overall the discontinuity of rescaled time series that are rescaled by time-varying application style, are also visible in the fused products. Although this discontinuity resulted in low accuracy fused products, but such results, at the same time, show the impact of time-varying approaches in getting close to the reference product more visible. This impact can be very useful if an access to the in-situ measurements is available over regions or at least the reference product is close enough to the real observations.

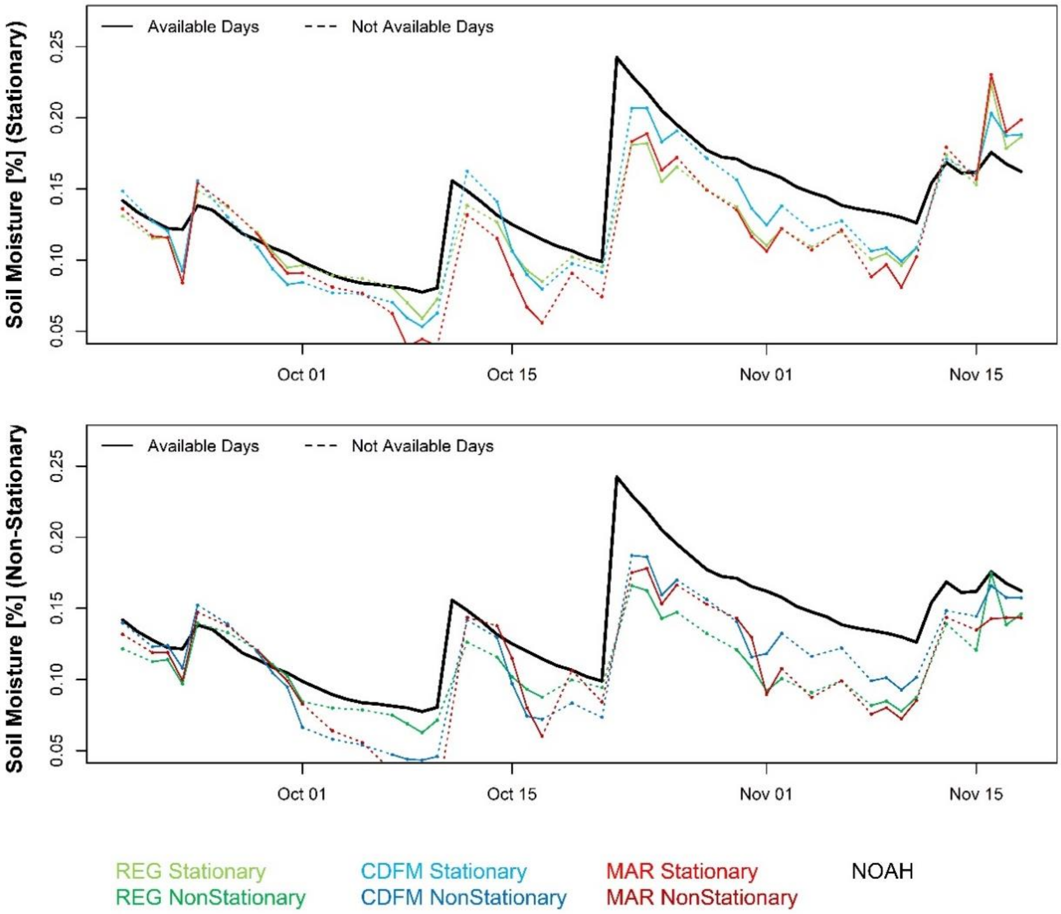

Figure 3.24. Comparison of different rescaling methods and their application style (technique: No Decomposition), in fusion of API and AMSR-E soil moisture product in NOAH space over Little Washita watershed between Sept 10 and Nov 20 of year 2010

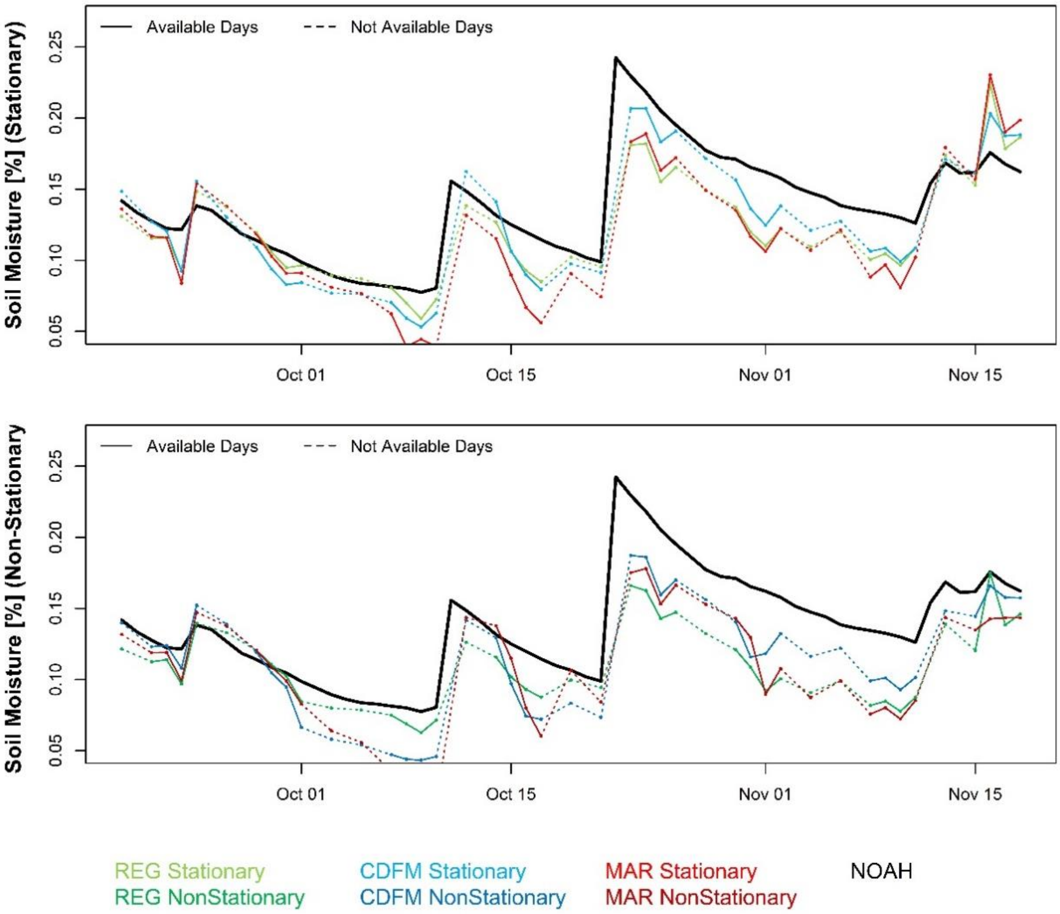

Figure 3.25. Comparison of different rescaling methods and their application style (technique: Seasonality-Anomaly Decomposition), in fusion of API and AMSR-E soil moisture product in NOAH space over Little Washita watershed between Sept 10 and Nov 20 of year 2010

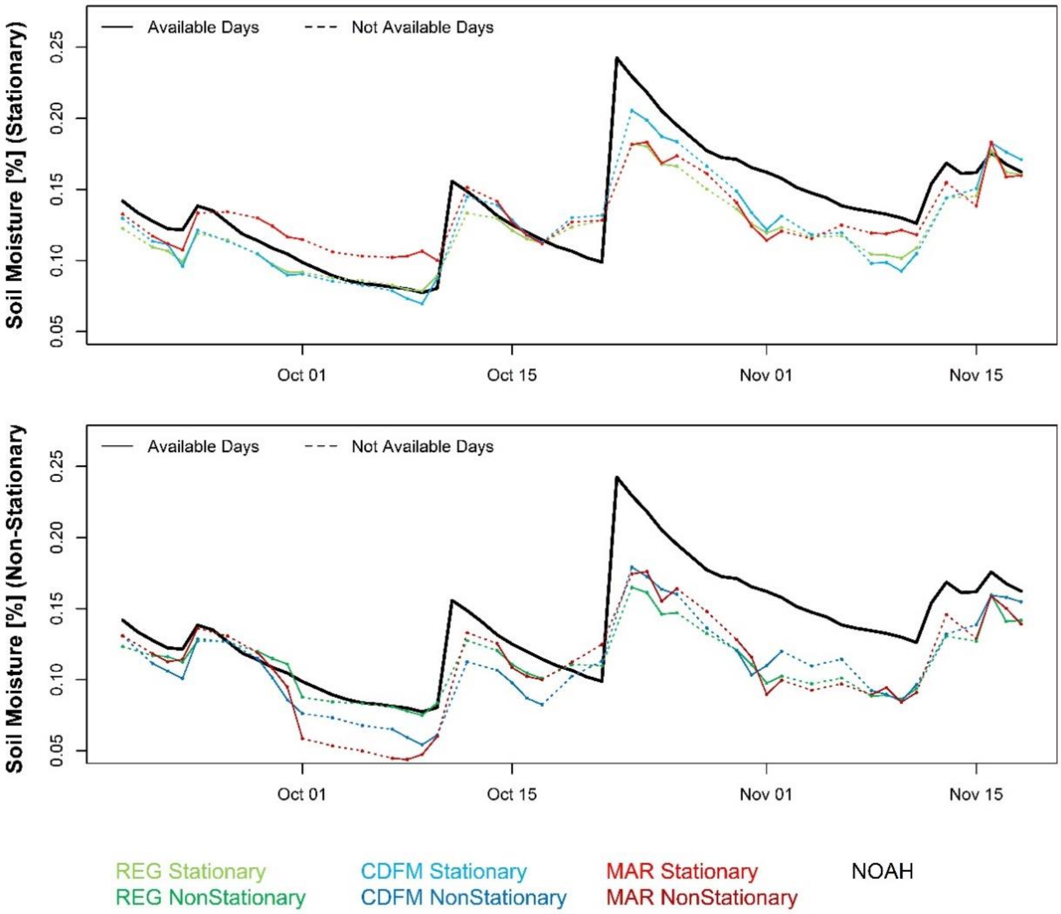

Figure 3.26. Comparison of different rescaling methods and their application style (technique: Smooth-Deviance Decomposition), in fusion of API and AMSR-E soil moisture product in NOAH space over Little Washita watershed between Sept 10 and Nov 20 of year 2010

On the other hand, by concentrating on the lower panel of Figure 3.26, where the rescaling methods are applied to the API and AMSR-E soil moisture products with the smooth-deviance decomposition technique, it can be seen that the usage of smooth-deviance decomposition technique slightly degraded the intensity of this discontinuity. However, this time the constant application of nonlinear methods (MAR) a little bit got away from the main target of data fusion (WASM; shown with black line in both panels)

Moreover, by paying attention to the difference of methods in upper panel of each rescaling technique, it can be seen that over very simple rescaling technique (Figure

3.24; considering no decomposition), the final fused products are very close to each other. However, by applying decomposition methods, the impact of rescaling methods also change. For example, over Seasonality-Anomaly decomposition (Figure 3.25), the nonlinear rescaling method produces a drier soil moisture product in comparison to the CDFM and REG methods (within the presented time interval). While this pattern is not happening over the Smooth-Deviance decomposition method. This difference in accuracy and the shape of rescaled products when they are rescaled by using the same methodology and different techniques or applying different styles implies the importance of rescaling techniques and also their application style one more time, beside the importance of rescaling methods.

CHAPTER 4

CONCLUSIONS

While some soil moisture applications require a soil moisture product with low bias, majority of the applications are in need of a soil moisture product with a good accuracy [i.e., high correlation with ground measurements; (Entekhabi, Reichle, et al., 2010; Koster et al., 2009)]. For such studies, an improved soil moisture datasets can be obtained via handling the systematic differences between the products and merging them with a proper methodology (i.e., simple fusion, data assimilation). However, the approach taken during the removal of systematic differences (i.e., rescaling) affect the final fused product skill. In this study, two different case studies are evaluated. The first case study has focused on the reducing of the systematic differences among datasets with rescaling of AMSR-E to the WASM datasets over four USDA ARS watersheds. While the second case study has focused on impact of rescaling methods in the frame work of data fusion. Both case studies are the first to perform a comprehensive comparison of the performances of various linear (REG, VAR, TCA) and nonlinear (CDFM, MAR, GP, SVM, ANN, and copula) methods (total 18 methods); the first to use the MAR, GP, SVM, and ANN methods to explicitly rescale the soil moisture datasets in the framework of soil moisture rescaling; and the first to comprehensively investigate the added utility of rescaling methods and their implementation approaches in the fusion of rescaled soil moisture products.

The relative performances of methods using training and validation datasets are consistent; the rescaling method that results in a more accurate rescaled product using training data also results in a more accurate rescaled product using validation data, and the best performing method using the training datasets yields better results than any other individual method that uses the validation datasets. Although the actual performances of the rescaling methods might change for different datasets, it is viable that a similar consistency would also exist for other datasets that are not used in this study. Such a consistency between the training and validation results gives confidence to the user in their selection of the rescaling method, particularly in the operational implementation of rescaling methods.

A large majority of the related variability between products are due to first-order linear relations. Although multiple linear regression-based rescaling methods slightly improve the rescaled product statistics, the training and the validation statistics consistently show that nonlinear methods resulted in a more accurate rescaled product than linear methods. Overall, GP and ELMAN ANN improved independent validation dataset correlations the best (on average 0.05), whereas improvements reached as high as 0.14 at individual locations (ELMAN ANN over RC).

Among nonlinear methods, ELMAN ANN exhibits superior performance, particularly when the datasets are highly autocorrelated (over RC), whereas the GP and SVM methods exhibit superior performance when the lagged observations are also used as predictors (over LR and LW). Although lagged observations improve the rescaled product statistics when datasets are rescaled linearly, nonlinear methods yield better statistics than linear methods. This highlights that lagged observations, which contain valuable information in the soil moisture rescaling framework as in the TCA framework (W. T. Crow et al., 2015; Chun-Hsu Su, Ryu, Crow, & Western, 2014; Zwieback, Dorigo, & Wagner, 2013). Nonlinear methods have higher added utility potential than linear methods in using lagged observations, in addition to their overall higher rescaling potential compared to the linear methods.

The higher rescaling potential of nonlinear methods compared to linear methods clearly show that the soil moisture datasets used in this study have nonlinear relations that cannot be modeled using linear methods. It is also viable that such nonlinear relationships may exist between other soil moisture datasets that are not used in this study. These results imply that the soil moisture inter-comparison studies (Clement Albergel et al., 2012; Brocca et al., 2011; Hain et al., 2011; Mladenova et al., 2014; Parinussa et al., 2015) and non-data assimilation type blending studies (Leroux et al., 2014) may benefit from these nonlinear rescaling methods, given the key results in this study. The performance metrics (ρ, σ_ε, and AMB) can be considerably (in some cases statistically significantly) improved via such nonlinear methods, whereas their degree of improvements may be dataset specific.

Overall, it is likely that more accurate nonlinearly rescaled products will improve applications that are better related to studies using linearly rescaled products. For example, assimilation experiments require observations to be rescaled into model space before they can be merged. By definition, an assimilation of more accurate observations (e.g., obtained via nonlinearly rescaling methods) in models always results in a more accurate analysis than the assimilation of less accurate observations (unless the underlying assumptions are not met). On the one hand, Yilmaz and Crow (2013) show an assimilation analysis accuracy that depends on the degree to which the smooth component of observations should be rescaled to the smooth component of the model, rather than the overall product differences that are alleviated directly, as done in this study. Similarly, Su et al. (2014) and Zwieback et al. (2016) show that matching this smooth component is also very important for error characterization. Consistently, Yilmaz and Crow (2013) demonstrate TCA matching of the smooth components of the datasets and a better rescaling method than REG in the assimilation framework.

Moreover the results based on the second case study as well show that linear rescaling methods could only improve the bias, while nonlinear methods increase the correlation of the rescaled product with the reference product in addition to the bias removal. However, this advantage of nonlinear approaches is effective when the reference product has high accuracy; else, in the presence of a degraded reference product, the nonlinear rescaling approaches will lead in loss of rescaled product skill.

Among rescaling approaches, the implementation of linear regression method with smooth-deviance decomposition approach resulted in the best fused product, while time-varying application of the rescaling methods could not improve the performance of final fused product and sometimes degraded the performance of them by leading the rescaled products to over fit to the reference product and to lose its continuity during rescaling procedure.

Overall, the variability due to reference dataset selection (under the same other rescaling related conditions) result in the highest variability in the fused product accuracy (i.e., reference dataset selection matters the most). After the reference dataset selection, the parent dataset selection matters the most. Once the reference and the parent dataset selections are made, then rescaling method, style, and technique selection matters with decreasing impact over the accuracy of the fused product. In the absence of appropriate reference dataset selection, better rescaling methodology selection does not yield fused product with the highest accuracy.

On the other hand, based on the results of parent couples analysis during data fusion and also studies that highlight the utility of simple API models compared to more complex models (W. T. Crow, Kumar, & Bolten, 2012; Han et al., 2014), it can be concluded that the simple API models, particularly over flat areas where such models perform good enough and provide worthy information about soil moisture, can be added to the parent products of data fusion in fusing of soil moisture products. Recent studies also highlight the utility of simple API models compared to more complex models, particularly in studies aiming to methodologically improve current techniques (W. T. Crow & Yilmaz, 2014; Yilmaz & Crow, 2013). Given that such simple models have better skills in drought studies (W. T. Crow et al., 2012), such models can be used to create long and homogenous time series, expanding to historical dates, where precipitation observations are available. To ensure the consistency of the units of the model values with traditional ground observations, this model time series could be rescaled to available ground observations, relying on the consistency found between the training and the validation datasets, where mutually available datasets can be used to retrieve the necessary parameters.

Overall, it is likely that each soil moisture application requires its own rescaling strategy. For example removing systematic differences among soil moisture time series require a nonlinear method rather than a linear method (Afshar & Yilmaz, 2017), or the assimilation techniques based on their nature require TCA types of rescaling [e.g., linear variance matching, CDFM, polynomial CDFM (Yilmaz et al., 2016)]. But so far, based on the results of this study, it can be concluded that among rescaling approaches, the implementation of REG does not yield the highest accuracy fused product; however, it gives close enough skill that justifies the use of this method (with smooth-deviance decomposition approach) given its ease of implementation. Additionally, the results of present study verify that the reference dataset selection matters almost as much as the dataset selection. Hence, it is better to rescale the parent products to a more accurate product (e.g., NOAH) to reduce the sampling errors, even if this reference product is not one of the merged products..

There are many ground station-based soil moisture observations that are used for validation of satellite- and model-based soil moisture estimates or the products obtained after merging of these estimates. The error statistics (error standard deviation, bias, etc.) of the soil moisture estimates, however, are impacted from the rescaling methodologies, styles, techniques as well as reference product selection used to alleviate the differences between products. On the other hand, many studies chose a simple rescaling approach and do not consider the alternatives that might yield better accuracy product. Compared to limited number of rescaling approach options that are widely used in the literature, this study lays out the relative skills of variety of rescaling approaches for estimation of superior fused products. Here, the validation of such fused products are performed using various ground station-based observations (e.g., ISMN, Western Mesonet Soil Moisture Network in Turkey, etc.), hence the rescaling approaches introduced in this study also contributes to the efforts to better utilize these observations. For example, soil moisture conditions describe part of the boundary conditions that Global Circulation Models use in weather predictions that accurate prediction of feedback mechanisms between the land and the atmosphere impact the accuracy of the predictions; the studies focusing on soil moisture data assimilation/insertion into such models may benefit from the methodologies introduced in this study..

REFERENCES

Afshar, M. H., & Yilmaz, M. T. (2017). The added utility of nonlinear methods compared to linear methods in rescaling soil moisture products. *Remote Sensing of Environment*, *196*, 224–237. https://doi.org/10.1016/J.RSE.2017.05.017

Al-Yaari, A., Wigneron, J. P., Kerr, Y., de Jeu, R., Rodriguez-Fernandez, N., van der Schalie, R., … Ducharne, A. (2016). Testing regression equations to derive long-term global soil moisture datasets from passive microwave observations. *Remote Sensing of Environment*, *180*, 453–464. https://doi.org/10.1016/J.RSE.2015.11.022

Albergel, C., de Rosnay, P., Gruhier, C., Muñoz-Sabater, J., Hasenauer, S., Isaksen, L., … Wagner, W. (2012). Evaluation of remotely sensed and modelled soil moisture products using global ground-based in situ observations. *Remote Sensing of Environment*, *118*, 215–226. https://doi.org/10.1016/j.rse.2011.11.017

Albergel, C., Rüdiger, C., Carrer, D., Calvet, J.-C., Fritz, N., Naeimi, V., … Hasenauer, S. (2009). An evaluation of ASCAT surface soil moisture products with in-situ observations in Southwestern France. *Hydrology and Earth System Sciences*, *13*(2), 115–124. https://doi.org/10.5194/hess-13-115-2009

Anderson, M. C., Zolin, C. A., Hain, C. R., Semmens, K., Yilmaz, M. T., & Gao, F. (2015). Comparison of satellite-derived LAI and precipitation anomalies over Brazil with a thermal infrared-based Evaporative Stress Index for 2003–2013. *Journal of Hydrology*, *526*, 287–302.

Anderson, M. C., Zolin, C. A., Sentelhas, P. C., Hain, C. R., Semmens, K., Yilmaz, M. T., … Tetrault, R. (2016). The Evaporative Stress Index as an indicator of agricultural drought in Brazil: An assessment based on crop yield impacts. *Remote Sensing of Environment*, *174*, 82–99.

Andrés Suárez, J., Lorca Fernández, P., Cos Juez, F. J. de, & Sánchez Lasheras, F. (2011). Bankruptcy forecasting: A hybrid approach using Fuzzy c-means clustering and Multivariate Adaptive Regression Splines (MARS). *Scopus*.

Bartalis, Z., Wagner, W., Naeimi, V., Hasenauer, S., Scipal, K., Bonekamp, H., … Anderson, C. (2007). Initial soil moisture retrievals from the METOP-A Advanced Scatterometer (ASCAT). *Geophysical Research Letters*, *34*(20), L20401. https://doi.org/10.1029/2007GL031088

Bergmeir, C. N., & Benítez Sánchez, J. M. (2012). Neural Networks in R Using the Stuttgart Neural Network Simulator: RSNNS.

Blanchard, B. J., McFarland, M. J., Schmugge, T. J., & Rhoades, E. (1981). Estimation of Soil-Moisture With Api Algorithms and Microwave Emission. *Water Resources Bulletin*, *17*(5), 767–774. https://doi.org/10.1111/j.1752-1688.1981.tb01296.x

Bosch, D. D., Sheridan, J. M., & Marshall, L. K. (2007). Precipitation, soil moisture, and climate database, Little River Experimental Watershed, Georgia, United States. *Water Resources Research*, *43*(9). https://doi.org/10.1029/2006WR005834

Brocca, L., Hasenauer, S., Lacava, T., Melone, F., Moramarco, T., Wagner, W., … Bittelli, M. (2011). Soil moisture estimation through ASCAT and AMSR-E sensors: An intercomparison and validation study across Europe. *Remote Sensing of Environment*, *115*(12), 3390–3408. https://doi.org/10.1016/j.rse.2011.08.003

Chen, F., Mitchell, K., Schaake, J., Xue, Y., Pan, H.-L., Koren, V., … Betts, A. (1996). Modeling of land surface evaporation by four schemes and comparison with FIFE observations. *Journal of Geophysical Research: Atmospheres*, *101*(D3), 7251–7268. https://doi.org/10.1029/95JD02165

Chen, S., & Billings, S. A. (1992). Neural networks for nonlinear dynamic system modelling and identification. *International Journal of Control*, *56*(2), 319–346. https://doi.org/10.1080/00207179208934317

Chow, V. T. (1964). Handbook of Applied Hydrology. In *Handbook of Applied Hydrology* (p. (21): 1-5). New York: McGraw-HiU Book Company, Inc.

CLAYTON, D. G. (1978). A model for association in bivariate life tables and its application in epidemiological studies of familial tendency in chronic disease incidence. *Biometrika*, *65*(1), 141–151. https://doi.org/10.1093/biomet/65.1.141

Colliander, A., Jackson, T. J., Bindlish, R., Chan, S., Das, N., Kim, S. B., … Yueh, S. (2017). Validation of SMAP surface soil moisture products with core validation sites. *Remote Sensing of Environment*, *191*, 215–231. https://doi.org/10.1016/J.RSE.2017.01.021

Cosh, M. H., Jackson, T. J., Starks, P., & Heathman, G. (2006). Temporal stability of surface soil moisture in the Little Washita River watershed and its applications in satellite soil moisture product validation. *Journal of Hydrology*, *323*(1–4), 168–177. https://doi.org/10.1016/j.jhydrol.2005.08.020

Crow, W. T., Kumar, S. V., & Bolten, J. D. (2012). On the utility of land surface models for agricultural drought monitoring. *Hydrology and Earth System Sciences*, *16*(9), 3451–3460. https://doi.org/10.5194/hess-16-3451-2012

Crow, W. T., & Ryu, D. (2009). A new data assimilation approach for improving runoff prediction using remotely-sensed soil moisture retrievals. *Hydrology and Earth System Sciences*, *13*(1), 1–16. https://doi.org/10.5194/hess-13-1-2009

Crow, W. T., Su, C.-H., Ryu, D., & Yilmaz, M. T. (2015). Optimal averaging of soil moisture predictions from ensemble land surface model simulations. *Water Resources Research*, *51*(11), 9273–9289. https://doi.org/10.1002/2015WR016944

Crow, W. T., & Wood, E. F. (2003). The assimilation of remotely sensed soil brightness temperature imagery into a land surface model using Ensemble Kalman filtering: a case study based on ESTAR measurements during SGP97. *Advances in Water Resources*, *26*(2), 137–149. https://doi.org/https://doi.org/10.1016/S0309-1708(02)00088-X

Crow, W. T., & Yilmaz, M. T. (2014). The Auto-Tuned Land Data Assimilation System (ATLAS). *Water Resources Research*, *50*(1), 371–385. https://doi.org/10.1002/2013WR014550

Crow, W. T., & Zhan, X. (2007). Continental-Scale Evaluation of Remotely Sensed Soil Moisture Products. *IEEE Geoscience and Remote Sensing Letters*, *4*(3), 451–455. https://doi.org/10.1109/LGRS.2007.896533

Dirmeyer, P. A., Guo, Z., Gao, X., Dirmeyer, P. A., Guo, Z., & Gao, X. (2004). Comparison, Validation, and Transferability of Eight Multiyear Global Soil Wetness Products. *Journal of Hydrometeorology*, *5*(6), 1011–1033. https://doi.org/10.1175/JHM-388.1

Dorigo, W. A., Wagner, W., Hohensinn, R., Hahn, S., Paulik, C., Xaver, A., … Jackson, T. (2011). The International Soil Moisture Network: a data hosting facility for global in situ soil moisture measurements. *Hydrology and Earth System Sciences*, *15*(5), 1675–1698. https://doi.org/10.5194/hess-15-1675-2011

Dorigo, W., de Jeu, R., Chung, D., Parinussa, R., Liu, Y., Wagner, W., & Fernández-Prieto, D. (2012). Evaluating global trends (1988-2010) in harmonized multi-satellite surface soil moisture. *Geophysical Research Letters*, *39*(18), n/a-n/a. https://doi.org/10.1029/2012GL052988

Dorigo, W., Wagner, W., Albergel, C., Albrecht, F., Balsamo, G., Brocca, L., … Lecomte, P. (2017). ESA CCI Soil Moisture for improved Earth system understanding: State-of-the art and future directions. *Remote Sensing of Environment*, *203*, 185–215. https://doi.org/10.1016/j.rse.2017.07.001

Draper, C. S., Walker, J. P., Steinle, P. J., de Jeu, R. A. M., & Holmes, T. R. H. (2009). An evaluation of AMSR–E derived soil moisture over Australia. *Remote Sensing of Environment*, *113*(4), 703–710. https://doi.org/10.1016/j.rse.2008.11.011

Ek, M. B., Mitchell, K. E., Lin, Y., Rogers, E., Grunmann, P., Koren, V., … Tarpley, J. D. (2003). Implementation of Noah land surface model advances in the National Centers for Environmental Prediction operational mesoscale Eta model. *Journal of Geophysical Research*, *108*(D22), 8851. https://doi.org/10.1029/2002JD003296

Elman, J. L. (1990). Finding structure in time. *Cognitive Science*, *14*(2), 179–211. https://doi.org/10.1016/0364-0213(90)90002-E

Entekhabi, D., Njoku, E. G., O'Neill, P. E., Kellogg, K. H., Crow, W. T., Edelstein, W. N., … Johnson, J. (2010). The soil moisture active passive (SMAP) mission. *Proceedings of the IEEE*, *98*(5), 704–716.

Entekhabi, D., Reichle, R. H., Koster, R. D., Crow, W. T., Entekhabi, D., Reichle, R. H., … Crow, W. T. (2010). Performance Metrics for Soil Moisture Retrievals and Application Requirements. *Journal of Hydrometeorology*, *11*(3), 832–840. https://doi.org/10.1175/2010JHM1223.1

Flasch, O., Mersmann, O., Bartz-Beielstein, T., Stork, J., & Zaefferer, M. (2015). R genetic programming framework. R package version 0.4-1.

Frahm, G., Junker, M., & Szimayer, A. (2003). *Elliptical copulas: applicability and limitations*. *Statistics & Probability Letters* (Vol. 63). https://doi.org/10.1016/S0167-7152(03)00092-0

Friedman, J. H. (1991). Multivariate Adaptive Regression Splines. *The Annals of Statistics*, *19*(1), 1–67. https://doi.org/10.1214/aos/1176347963

Genest, C. (1987). Frank's family of bivariate distributions. *Biometrika*, *74*(3), 549–555. https://doi.org/10.1093/biomet/74.3.549

Genest, C., & Favre, A.-C. (2007). Everything You Always Wanted to Know about Copula Modeling but Were Afraid to Ask. *Journal of Hydrologic Engineering*, *12*(4), 347–368. https://doi.org/10.1061/(ASCE)1084-0699(2007)12:4(347)

Gruber, A., Dorigo, W. A., Crow, W., & Wagner, W. (2017). Triple Collocation-Based Merging of Satellite Soil Moisture Retrievals. *IEEE Transactions on Geoscience and Remote Sensing*, *55*(12), 6780–6792. https://doi.org/10.1109/TGRS.2017.2734070

Guang-Bin Huang, & Babri, H. A. (1998). Upper bounds on the number of hidden neurons in feedforward networks with arbitrary bounded nonlinear activation functions. *IEEE Transactions on Neural Networks*, *9*(1), 224–229. https://doi.org/10.1109/72.655045

Gumbel, E. J. (1960). *Distributions des valeurs extrˆemes en plusieurs dimensions*. *Publications de l'Institut de Statistique de l'Universit´e de Paris* (Vol. 9). Paris, France: Distributions des valeurs extrˆemes en plusieurs dimensions.

Hain, C. R., Crow, W. T., Mecikalski, J. R., Anderson, M. C., & Holmes, T. (2011). An intercomparison of available soil moisture estimates from thermal infrared and passive microwave remote sensing and land surface modeling. *Journal of Geophysical Research Atmospheres*, *116*(15), 1–18. https://doi.org/10.1029/2011JD015633

Han, E., Crow, W. T., Holmes, T., & Bolten, J. (2014). Benchmarking a Soil Moisture Data Assimilation System for Agricultural Drought Monitoring. *Journal of Hydrometeorology*, *15*(2010), 1117–1134. https://doi.org/10.1175/JHM-D-13-0125.1

Hastie, T., Tibshirani, R., & Friedman, J. (2009). *The Elements of Statistical Learning*. New York, NY: Springer New York. https://doi.org/10.1007/978-0-387-84858-7

Hernández, N., Kiralj, R., Ferreira, M. M. C., & Talavera, I. (2009). Critical comparative analysis, validation and interpretation of SVM and PLS regression models in a QSAR study on HIV-1 protease inhibitors. *Chemometrics and Intelligent Laboratory Systems*, *98*(1), 65–77. https://doi.org/10.1016/j.chemolab.2009.04.012

Hesami Afshar, M., Sorman, A., & Yilmaz, M. (2016). Conditional Copula-Based Spatial–Temporal Drought Characteristics Analysis—A Case Study over Turkey. *Water*, *8*(10), 426. https://doi.org/10.3390/w8100426

Hofert, M., Kojadinovic, I., Maechler, M., & Yan, J. (2012). Copula: Multivariate Dependence with Copulas. R package version 0.999-13. Retrieved from http://cran.r-project.org/package=copula

Houser, P. R., Harlow, C., Shuttleworth, W. J., Keefer, T. O., Emmerich, W. E., & Goodrich, D. C. (1998). Evaluation of multiple flux measurement techniques using water balance information at a semi-arid site. In *Special Symposium in Hydrology* (pp. 84–87).

Huffman, G. J., Bolvin, D. T., Nelkin, E. J., Wolff, D. B., Adler, R. F., Gu, G., … Stocker, E. F. (2007). The TRMM multisatellite precipitation analysis (TMPA): Quasi-global, multiyear, combined-sensor precipitation estimates at fine scales. *Journal of Hydrometeorology*, *8*(1), 38–55.

Jackson, T. J., Bindlish, R., Cosh, M. H., Zhao, T., Starks, P. J., Bosch, D. D., … Leroux, D. (2012). Validation of Soil Moisture and Ocean Salinity (SMOS) Soil Moisture Over Watershed Networks in the U.S. *IEEE Transactions on Geoscience and Remote Sensing*, *50*(5), 1530–1543. https://doi.org/10.1109/TGRS.2011.2168533

Jackson, T. J., Cosh, M. H., Bindlish, R., Starks, P. J., Bosch, D. D., Seyfried, M., … Du, J. (2010). Validation of Advanced Microwave Scanning Radiometer Soil Moisture Products. *IEEE Transactions on Geoscience and Remote Sensing*, *48*(12), 4256–4272. https://doi.org/10.1109/TGRS.2010.2051035

Joe, H. (1997). *Multivariate models and multivariate dependence concepts*. US: CRC Press.

Jordan, M. I. (1997). Serial Order: A Parallel Distributed Processing Approach (pp.

471–495). North-Holland/Elsevier Science Publishers. https://doi.org/10.1016/S0166-4115(97)80111-2

Karsoliya, S. (2012). Approximating Number of Hidden layer neurons in Multiple Hidden Layer BPNN Architecture. *International Journal of Engineering Trends and Technology*, *3*(6), 714–717.

Kentel, E. (2009). Estimation of river flow by artificial neural networks and identification of input vectors susceptible to producing unreliable flow estimates. *Journal of Hydrology*, *375*(3), 481–488. https://doi.org/10.1016/j.jhydrol.2009.06.051

Kerr, Y. H., Waldteufel, P., Wigneron, J.-P., Martinuzzi, J., Font, J., & Berger, M. (2001). Soil moisture retrieval from space: The Soil Moisture and Ocean Salinity (SMOS) mission. *IEEE Transactions on Geoscience and Remote Sensing*, *39*(8), 1729–1735.

Koren, V., Schaake, J., Mitchell, K., Duan, Q.-Y., Chen, F., & Baker, J. M. (1999). A parameterization of snowpack and frozen ground intended for NCEP weather and climate models. *Journal of Geophysical Research: Atmospheres*, *104*(D16), 19569–19585. https://doi.org/10.1029/1999JD900232

Koster, R. D., Dirmeyer, P. A., Guo, Z., Bonan, G., Chan, E., Cox, P., … Yamada, T. (2004). Regions of Strong Coupling Between Soil Moisture and Precipitation. *Science*, *305*(5687), 1138–1140. https://doi.org/10.1126/science.1100217

Koster, R. D., Guo, Z., Yang, R., Dirmeyer, P. A., Mitchell, K., Puma, M. J., … Puma, M. J. (2009). On the Nature of Soil Moisture in Land Surface Models. *Journal of Climate*, *22*(16), 4322–4335. https://doi.org/10.1175/2009JCLI2832.1

Koza, J. (1994). Genetic programming as a means for programming computers by natural selection. *Statistics and Computing*, *4*(2), 87–112. https://doi.org/10.1007/BF00175355

Lawrence, J. E., & Hornberger, G. M. (2007). Soil moisture variability across climate zones. *Geophysical Research Letters*, *34*(20), 1–5. https://doi.org/10.1029/2007GL031382

Leroux, D. J., Kerr, Y. H., Wood, E. F., Sahoo, A. K., Bindlish, R., & Jackson, T. J. (2014). An Approach to Constructing a Homogeneous Time Series of Soil Moisture Using SMOS. *IEEE Transactions on Geoscience and Remote Sensing*, *52*(1), 393–405. https://doi.org/10.1109/TGRS.2013.2240691

Lievens, H., Tomer, S. K., Al Bitar, A., De Lannoy, G. J. M., Drusch, M., Dumedah, G., … Pan, M. (2015). SMOS soil moisture assimilation for improved hydrologic simulation in the Murray Darling Basin, Australia. *Remote Sensing of Environment*, *168*, 146–162.

Lindsey, R. K., Kohler, Jr., M. A., & Paulhus, J. L. (1949). *Applied Hydrology*. New

York: McGraw-Hill Book Company, Inc.

Liu, Y. Y., Dorigo, W. A., Parinussa, R. M., de Jeu, R. A. M., Wagner, W., McCabe, M. F., … van Dijk, A. I. J. M. (2012). Trend-preserving blending of passive and active microwave soil moisture retrievals. *Remote Sensing of Environment*, *123*, 280–297. https://doi.org/10.1016/j.rse.2012.03.014

Liu, Y. Y., Parinussa, R. M., Dorigo, W. A., De Jeu, R. A. M., Wagner, W., van Dijk, A. I. J. M., … Evans, J. P. (2011). Developing an improved soil moisture dataset by blending passive and active microwave satellite-based retrievals. *Hydrology and Earth System Sciences*, *15*(2), 425–436. https://doi.org/10.5194/hess-15-425-2011

McFarland, M. J., & Blanchard, B. J. (1977). Temporal Cone lation of Antecedent Precipitation With Nimbus 5 ESMR Brightness Temperatures. In *Second Conference on Hydrometeorology* (pp. 311–315). Toronto, Ontario, Canada.

Meyer, D., Dimitriadou, E., Hornik, K., Weingessel, A., Leisch, F., Chang, C., & Lin, C. (2015). Misc Functions of the Department of Statistics, Probability Theory Group (Formerly: E1071), R package version 1.6-7. TU Wien.

Milborrow, S. (2016). earth: Multivariate Adaptive Regression Spline Models, 2009. *URL Http://CRAN. R-Project. Org/Package= Earth. R Package Version*, 2–4.

Miralles, D. G., De Jeu, R. A. M., Gash, J. H., Holmes, T. R. H., & Dolman, A. J. (2011). Magnitude and variability of land evaporation and its components at the global scale. *Hydrology and Earth System Sciences*, *15*(3), 967–981. https://doi.org/10.5194/hess-15-967-2011

Mladenova, I. E., Jackson, T. J., Njoku, E., Bindlish, R., Chan, S., Cosh, M. H., … Santi, E. (2014). Remote monitoring of soil moisture using passive microwave-based techniques — Theoretical basis and overview of selected algorithms for AMSR-E. *Remote Sensing of Environment*, *144*, 197–213. https://doi.org/10.1016/J.RSE.2014.01.013

Murata, N., Yoshizawa, S., & Amari, S. (1994). Network information criterion-determining the number of hidden units for an artificial neural network model. *IEEE Transactions on Neural Networks*, *5*(6), 865–872. https://doi.org/10.1109/72.329683

Mutlu, E., Chaubey, I., Hexmoor, H., & Bajwa, S. G. (2008). Comparison of artificial neural network models for hydrologic predictions at multiple gauging stations in an agricultural watershed. *Hydrological Processes*, *22*(26), 5097–5106. https://doi.org/10.1002/hyp.7136

Nelsen, R. B. (1999). *An Introduction to Copulas* (Vol. 139). New York, NY: Springer New York. https://doi.org/10.1007/978-1-4757-3076-0

Olson, D. L., & Delen, D. (2008). *Advanced data mining techniques*. Springer.

Owe, M., de Jeu, R., & Holmes, T. (2008). Multisensor historical climatology of satellite-derived global land surface moisture. *Journal of Geophysical Research*, *113*(F1), F01002. https://doi.org/10.1029/2007JF000769

Owe, M., de Jeu, R., & Walker, J. (2001). A methodology for surface soil moisture and vegetation optical depth retrieval using the microwave polarization difference index. *IEEE Transactions on Geoscience and Remote Sensing*, *39*(8), 1643–1654. https://doi.org/10.1109/36.942542

Parinussa, R. M., Holmes, T. R. H., Wanders, N., Dorigo, W. A., de Jeu, R. A. M., Parinussa, R. M., … Jeu, R. A. M. de. (2015). A Preliminary Study toward Consistent Soil Moisture from AMSR2. *Journal of Hydrometeorology*, *16*(2), 932–947. https://doi.org/10.1175/JHM-D-13-0200.1

Pasolli, L., Notarnicola, C., & Bruzzone, L. (2011). Estimating soil moisture with the support vector regression technique. *IEEE Geoscience and Remote Sensing Letters*, *8*(6), 1080–1084.

Poggio, T., & Girosi, F. (1990). Networks for approximation and learning. *Proceedings of the IEEE*, *78*(9), 1481–1497. https://doi.org/10.1109/5.58326

Principe, J. C., Rathie, A., & Kuo, J.-M. (1992). PREDICTION OF CHAOTIC TIME SERIES WITH NEURAL NETWORKS AND THE ISSUE OF DYNAMIC MODELING. *International Journal of Bifurcation and Chaos*, *02*(04), 989–996. https://doi.org/10.1142/S0218127492000598

R Core Team. (2015). R: A language and environment for statistical computing. R Foundation for Statistical Computing. Vienna. Austria. Retrieved from http://www.r-project.org/

Reichle, R. H., Crow, W. T., Koster, R. D., Sharif, H. O., & Mahanama, S. P. P. (2008). Contribution of soil moisture retrievals to land data assimilation products. *Geophysical Research Letters*, *35*(1), L01404. https://doi.org/10.1029/2007GL031986

Reichle, R. H., & Koster, R. D. (2004). Bias reduction in short records of satellite soil moisture. *Geophysical Research Letters*, *31*(19), L19501. https://doi.org/10.1029/2004GL020938

Renard, K. G., Nichols, M. H., Woolhiser, D. A., & Osborn, H. B. (2008). A brief background on the U.S. Department of Agriculture Agricultural Research Service Walnut Gulch Experimental Watershed. *Water Resources Research*, *44*(5). https://doi.org/10.1029/2006WR005691

Rodell, M., Houser, P. R., Jambor, U., Gottschalck, J., Mitchell, K., Meng, C.-J., … Toll, D. (2004). The Global Land Data Assimilation System. *Bulletin of the American Meteorological Society*, *85*(3), 381–394. https://doi.org/10.1175/BAMS-85-3-381

Rodríguez-Fernández, N., Kerr, Y., van der Schalie, R., Al-Yaari, A., Wigneron, J.-P., de Jeu, R., … Drusch, M. (2016). Long Term Global Surface Soil Moisture Fields Using an SMOS-Trained Neural Network Applied to AMSR-E Data. *Remote Sensing*, *8*(11), 959. https://doi.org/10.3390/rs8110959

Rosenblatt, F. (1958). The perceptron: A probabilistic model for information storage and organization in the brain. *Psychological Review*, *65*(6), 386–408. https://doi.org/10.1037/h0042519

Scipal, K., Holmes, T., de Jeu, R., Naeimi, V., & Wagner, W. (2008). A possible solution for the problem of estimating the error structure of global soil moisture data sets. *Geophysical Research Letters*, *35*(24), L24403. https://doi.org/10.1029/2008GL035599

Sharda, V. N., Prasher, S. O., Patel, R. M., Ojasvi, P. R., & Prakash, C. (2008). Performance of Multivariate Adaptive Regression Splines (MARS) in predicting runoff in mid-Himalayan micro-watersheds with limited data. *Hydrological Sciences Journal-Journal Des Sciences Hydrologiques*, *53*(6), 1165–1175. https://doi.org/10.1623/hysj.53.6.1165

Sheela, K. G., Deepa, S. N., Sheela, K. G., & Deepa, S. N. (2013). Review on Methods to Fix Number of Hidden Neurons in Neural Networks. *Mathematical Problems in Engineering*, *2013*, 1–11. https://doi.org/10.1155/2013/425740

Sklar, A. (1959). *Fonctions de Répartition à n Dimensions et Leurs Marges*. Publications de l'Institut de Statistique de L'Université de Paris.

Slaughter, C. W., Marks, D., Flerchinger, G. N., Van Vactor, S. S., & Burgess, M. (2001). *Thirty-five years of research data collection at the Reynolds Creek Experimental Watershed, Idaho, United States*. *WATER RESOURCES RESEARCH* (Vol. 37). https://doi.org/10.1029/2001WR000413

Smola, A. J., & Schölkopf, B. (2004). A tutorial on support vector regression. *Statistics and Computing*, *14*(3), 199–222. https://doi.org/10.1023/B:STCO.0000035301.49549.88

Stoffelen, A. (1998). Toward the true near-surface wind speed: Error modeling and calibration using triple collocation. *Journal of Geophysical Research: Oceans*, *103*(C4), 7755–7766. https://doi.org/10.1029/97JC03180

Su, C.-H., & Ryu, D. (2015). Multi-scale analysis of bias correction of soil moisture. *Hydrology and Earth System Sciences*, *19*(1), 17–31. https://doi.org/10.5194/hess-19-17-2015

Su, C.-H., Ryu, D., Crow, W. T., & Western, A. W. (2014). Beyond triple collocation: Applications to soil moisture monitoring. *Journal of Geophysical Research: Atmospheres*, *119*(11), 6419–6439. https://doi.org/10.1002/2013JD021043

van der Schalie, R., de Jeu, R. A. M., Kerr, Y. H., Wigneron, J. P., Rodríguez-

Fernández, N. J., Al-Yaari, A., … Drusch, M. (2017). The merging of radiative transfer based surface soil moisture data from SMOS and AMSR-E. *Remote Sensing of Environment*, *189*, 180–193. https://doi.org/10.1016/J.RSE.2016.11.026

Vapnik, V. N. (1998). *Statistical learning theory*. Wiley.

Vapnik, V. N., & Chervonenkis, A. Y. (1974). *Theory of Pattern Recognition [in Russian]*. Nauka, USSR.

Vladislavleva, E. J., Smits, G. F., & den Hertog, D. (2009). Order of Nonlinearity as a Complexity Measure for Models Generated by Symbolic Regression via Pareto Genetic Programming. *IEEE Transactions on Evolutionary Computation*, *13*(2), 333–349. https://doi.org/10.1109/TEVC.2008.926486

Wagner, W., Blöschl, G., Pampaloni, P., Calvet, J.-C., Bizzarri, B., Wigneron, J.-P., & Kerr, Y. (2007). Operational readiness of microwave remote sensing of soil moisture for hydrologic applications. *Hydrology Research*, *38*(1), 1–20. https://doi.org/10.2166/nh.2007.029

Wagner, W., Dorigo, W., de Jeu, R., Fernandez, D., Benveniste, J., Haas, E., & Ertl, M. (2012). Fusion of Active and Passive Microwave Observations To Create an Essential Climate Variable Data Record on Soil Moisture. *ISPRS Annals of Photogrammetry, Remote Sensing and Spatial Information Sciences*, *I-7*(September), 315–321. https://doi.org/10.5194/isprsannals-I-7-315-2012

Wagner, W., Lemoine, G., & Rott, H. (1999). A Method for Estimating Soil Moisture from ERS Scatterometer and Soil Data. *Remote Sensing of Environment*, *70*(2), 191–207. https://doi.org/10.1016/S0034-4257(99)00036-X

Xu, S., & Chen, L. (2008). A novel approach for determining the optimal number of hidden layer neurons for FNN's and its application in data mining.

Yilmaz, M. T., & Crow, W. T. (2013). The Optimality of Potential Rescaling Approaches in Land Data Assimilation. *Journal of Hydrometeorology*, *14*(2), 650–660. https://doi.org/10.1175/JHM-D-12-052.1

Yilmaz, M. T., & Crow, W. T. (2014). Evaluation of Assumptions in Soil Moisture Triple Collocation Analysis. *Journal of Hydrometeorology*, *15*(3), 1293–1302. https://doi.org/10.1175/JHM-D-13-0158.1

Yilmaz, M. T., Crow, W. T., Anderson, M. C., & Hain, C. (2012). An objective methodology for merging satellite- and model-based soil moisture products. *Water Resources Research*, *48*(11), n/a-n/a. https://doi.org/10.1029/2011WR011682

Yilmaz, M. T., Crow, W. T., Ryu, D., Yilmaz, M. T., Crow, W. T., & Ryu, D. (2016). Impact of Model Relative Accuracy in Framework of Rescaling Observations in Hydrological Data Assimilation Studies. *Journal of Hydrometeorology*, *17*(8), 2245–2257. https://doi.org/10.1175/JHM-D-15-0206.1

Yilmaz, M. T., DelSole, T., & Houser, P. R. (2011). Improving land data assimilation performance with a water budget constraint. *Journal of Hydrometeorology*, *12*(5), 1040–1055.

Yin, J., Zhan, X., Zheng, Y., Liu, J., Hain, C. R., & Fang, L. (2014). Impact of quality control of satellite soil moisture data on their assimilation into land surface model. *Geophysical Research Letters*, *41*(20), 7159–7166. https://doi.org/10.1002/2014GL060659

Zheng, D., van der Velde, R., Su, Z., Wang, X., Wen, J., Booij, M. J., … Chen, Y. (2015). Augmentations to the Noah model physics for application to the Yellow River source area. Part I: Soil water flow. *Journal of Hydrometeorology*, *16*(6), 2659–2676.

Zwieback, S., Dorigo, W., & Wagner, W. (2013). Estimation of the temporal autocorrelation structure by the collocation technique with an emphasis on soil moisture studies. *Hydrological Sciences Journal*, *58*(8), 1729–1747. https://doi.org/10.1080/02626667.2013.839876

Zwieback, S., Su, C.-H., Gruber, A., Dorigo, W. A., Wagner, W., Zwieback, S., … Wagner, W. (2016). The Impact of Quadratic Nonlinear Relations between Soil Moisture Products on Uncertainty Estimates from Triple Collocation Analysis and Two Quadratic Extensions. Journal of Hydrometeorology, 17(6), 1725–1743. https://doi.org/10.1175/JHM-D-15-0213.1

APPENDICES

A. Comparison of the impact of rescaling approaches over the accuracy of rescaled products (results are averages over four watersheds)

ID	Unscaled Product	Rescalin g Method	Rescaling Technique	Application Style	Ref	Cor (Ref)	Cor (WASM)
1	ASCAT	REG	ND	Constant	ASCAT	1	0.54
2	ASCAT	REG	ND	Constant	AMSR-E	0.41	0.54
3	ASCAT	REG	ND	Constant	API	0.51	0.54
4	ASCAT	REG	ND	Constant	NOAH	0.48	0.54
5	ASCAT	REG	ND	Constant	WASM	0.54	0.54
6	ASCAT	REG	ND	TV	ASCAT	1	0.54
7	ASCAT	REG	ND	TV	AMSR-E	0.83	0.61
8	ASCAT	REG	ND	TV	API	0.72	0.54
9	ASCAT	REG	ND	TV	NOAH	0.76	0.71
10	ASCAT	REG	ND	TV	WASM	0.78	0.78
11	ASCAT	REG	SA	Constant	ASCAT	1	0.54
12	ASCAT	REG	SA	Constant	AMSR-E	0.52	0.5
13	ASCAT	REG	SA	Constant	API	0.56	0.54
14	ASCAT	REG	SA	Constant	NOAH	0.56	0.57
15	ASCAT	REG	SA	Constant	WASM	0.6	0.6
16	ASCAT	REG	SA	TV	ASCAT	1	0.54
17	ASCAT	REG	SA	TV	AMSR-E	0.84	0.62
18	ASCAT	REG	SA	TV	API	0.73	0.55
19	ASCAT	REG	SA	TV	NOAH	0.78	0.71
20	ASCAT	REG	SA	TV	WASM	0.79	0.79
21	ASCAT	REG	SD	Constant	ASCAT	1	0.54
22	ASCAT	REG	SD	Constant	AMSR-E	0.44	0.48
23	ASCAT	REG	SD	Constant	API	0.55	0.56
24	ASCAT	REG	SD	Constant	NOAH	0.52	0.57
25	ASCAT	REG	SD	Constant	WASM	0.57	0.57
26	ASCAT	REG	SD	TV	ASCAT	1	0.54
27	ASCAT	REG	SD	TV	AMSR-E	0.85	0.63
28	ASCAT	REG	SD	TV	API	0.74	0.57
29	ASCAT	REG	SD	TV	NOAH	0.81	0.72
30	ASCAT	REG	SD	TV	WASM	0.81	0.81
31	ASCAT	VAR	ND	Constant	ASCAT	1	0.54
32	ASCAT	VAR	ND	Constant	AMSR-E	0.41	0.54

ID	Unscaled Product	Rescaling Method	Rescaling Technique	Application Style	Ref	Cor (Ref)	Cor (WASM)
33	ASCAT	VAR	ND	Constant	API	0.51	0.54
34	ASCAT	VAR	ND	Constant	NOAH	0.48	0.54
35	ASCAT	VAR	ND	Constant	WASM	0.54	0.54
36	ASCAT	VAR	ND	TV	ASCAT	1	0.54
37	ASCAT	VAR	ND	TV	AMSR-E	0.78	0.62
38	ASCAT	VAR	ND	TV	API	0.67	0.54
39	ASCAT	VAR	ND	TV	NOAH	0.72	0.68
40	ASCAT	VAR	ND	TV	WASM	0.73	0.73
41	ASCAT	VAR	SA	Constant	ASCAT	1	0.54
42	ASCAT	VAR	SA	Constant	AMSR-E	0.33	0.48
43	ASCAT	VAR	SA	Constant	API	0.56	0.53
44	ASCAT	VAR	SA	Constant	NOAH	0.5	0.56
45	ASCAT	VAR	SA	Constant	WASM	0.54	0.54
46	ASCAT	VAR	SA	TV	ASCAT	1	0.54
47	ASCAT	VAR	SA	TV	AMSR-E	0.79	0.63
48	ASCAT	VAR	SA	TV	API	0.68	0.55
49	ASCAT	VAR	SA	TV	NOAH	0.72	0.69
50	ASCAT	VAR	SA	TV	WASM	0.74	0.74
51	ASCAT	VAR	SD	Constant	ASCAT	1	0.54
52	ASCAT	VAR	SD	Constant	AMSR-E	0.39	0.54
53	ASCAT	VAR	SD	Constant	API	0.54	0.54
54	ASCAT	VAR	SD	Constant	NOAH	0.51	0.56
55	ASCAT	VAR	SD	Constant	WASM	0.55	0.55
56	ASCAT	VAR	SD	TV	ASCAT	1	0.54
57	ASCAT	VAR	SD	TV	AMSR-E	0.79	0.63
58	ASCAT	VAR	SD	TV	API	0.7	0.56
59	ASCAT	VAR	SD	TV	NOAH	0.77	0.71
60	ASCAT	VAR	SD	TV	WASM	0.76	0.76
61	ASCAT	CDFM	ND	Constant	ASCAT	1	0.54
62	ASCAT	CDFM	ND	Constant	AMSR-E	0.2	0.3
63	ASCAT	CDFM	ND	Constant	API	0.5	0.53
64	ASCAT	CDFM	ND	Constant	NOAH	0.45	0.5
65	ASCAT	CDFM	ND	Constant	WASM	0.51	0.51
66	ASCAT	CDFM	ND	TV	ASCAT	1	0.54
67	ASCAT	CDFM	ND	TV	AMSR-E	0.71	0.55
68	ASCAT	CDFM	ND	TV	API	0.66	0.48
69	ASCAT	CDFM	ND	TV	NOAH	0.72	0.66
70	ASCAT	CDFM	ND	TV	WASM	0.73	0.73
71	ASCAT	CDFM	SA	Constant	ASCAT	1	0.54

ID	Unscaled Product	Rescaling Method	Rescaling Technique	Application Style	Ref	Cor (Ref)	Cor (WASM)
72	ASCAT	CDFM	SA	Constant	AMSR-E	0.14	0.29
73	ASCAT	CDFM	SA	Constant	API	0.5	0.53
74	ASCAT	CDFM	SA	Constant	NOAH	0.45	0.48
75	ASCAT	CDFM	SA	Constant	WASM	0.49	0.49
76	ASCAT	CDFM	SA	TV	ASCAT	1	0.54
77	ASCAT	CDFM	SA	TV	AMSR-E	0.74	0.56
78	ASCAT	CDFM	SA	TV	API	0.66	0.5
79	ASCAT	CDFM	SA	TV	NOAH	0.73	0.67
80	ASCAT	CDFM	SA	TV	WASM	0.74	0.74
81	ASCAT	CDFM	SD	Constant	ASCAT	1	0.54
82	ASCAT	CDFM	SD	Constant	AMSR-E	0.18	0.34
83	ASCAT	CDFM	SD	Constant	API	0.52	0.51
84	ASCAT	CDFM	SD	Constant	NOAH	0.5	0.54
85	ASCAT	CDFM	SD	Constant	WASM	0.54	0.54
86	ASCAT	CDFM	SD	TV	ASCAT	1	0.54
87	ASCAT	CDFM	SD	TV	AMSR-E	0.75	0.56
88	ASCAT	CDFM	SD	TV	API	0.72	0.55
89	ASCAT	CDFM	SD	TV	NOAH	0.77	0.68
90	ASCAT	CDFM	SD	TV	WASM	0.77	0.77
91	ASCAT	MAR	ND	Constant	ASCAT	1	0.54
92	ASCAT	MAR	ND	Constant	AMSR-E	0.51	0.53
93	ASCAT	MAR	ND	Constant	API	0.55	0.56
94	ASCAT	MAR	ND	Constant	NOAH	0.56	0.58
95	ASCAT	MAR	ND	Constant	WASM	0.59	0.59
96	ASCAT	MAR	ND	TV	ASCAT	1	0.54
97	ASCAT	MAR	ND	TV	AMSR-E	0.86	0.62
98	ASCAT	MAR	ND	TV	API	0.74	0.55
99	ASCAT	MAR	ND	TV	NOAH	0.79	0.71
100	ASCAT	MAR	ND	TV	WASM	0.8	0.8
101	ASCAT	MAR	SA	Constant	ASCAT	1	0.54
102	ASCAT	MAR	SA	Constant	AMSR-E	0.69	0.61
103	ASCAT	MAR	SA	Constant	API	0.66	0.56
104	ASCAT	MAR	SA	Constant	NOAH	0.66	0.66
105	ASCAT	MAR	SA	Constant	WASM	0.7	0.7
106	ASCAT	MAR	SA	TV	ASCAT	1	0.54
107	ASCAT	MAR	SA	TV	AMSR-E	0.86	0.62
108	ASCAT	MAR	SA	TV	API	0.76	0.56
109	ASCAT	MAR	SA	TV	NOAH	0.8	0.72
110	ASCAT	MAR	SA	TV	WASM	0.81	0.81

ID	Unscaled Product	Rescaling Method	Rescaling Technique	Application Style	Ref	Cor (Ref)	Cor (WASM)
111	ASCAT	MAR	SD	Constant	ASCAT	1	0.54
112	ASCAT	MAR	SD	Constant	AMSR-E	0.61	0.54
113	ASCAT	MAR	SD	Constant	API	0.62	0.58
114	ASCAT	MAR	SD	Constant	NOAH	0.63	0.63
115	ASCAT	MAR	SD	Constant	WASM	0.65	0.65
116	ASCAT	MAR	SD	TV	ASCAT	1	0.54
117	ASCAT	MAR	SD	TV	AMSR-E	0.87	0.64
118	ASCAT	MAR	SD	TV	API	0.81	0.58
119	ASCAT	MAR	SD	TV	NOAH	0.84	0.72
120	ASCAT	MAR	SD	TV	WASM	0.84	0.84
121	ASCAT	SVM	ND	Constant	ASCAT	1	0.54
122	ASCAT	SVM	ND	Constant	AMSR-E	0.51	0.52
123	ASCAT	SVM	ND	Constant	API	0.55	0.56
124	ASCAT	SVM	ND	Constant	NOAH	0.56	0.57
125	ASCAT	SVM	ND	Constant	WASM	0.58	0.58
126	ASCAT	SVM	ND	TV	ASCAT	1	0.54
127	ASCAT	SVM	ND	TV	AMSR-E	0.86	0.63
128	ASCAT	SVM	ND	TV	API	0.73	0.51
129	ASCAT	SVM	ND	TV	NOAH	0.78	0.7
130	ASCAT	SVM	ND	TV	WASM	0.8	0.8
131	ASCAT	SVM	SA	Constant	ASCAT	1	0.54
132	ASCAT	SVM	SA	Constant	AMSR-E	0.67	0.6
133	ASCAT	SVM	SA	Constant	API	0.64	0.55
134	ASCAT	SVM	SA	Constant	NOAH	0.66	0.65
135	ASCAT	SVM	SA	Constant	WASM	0.7	0.7
136	ASCAT	SVM	SA	TV	ASCAT	1	0.53
137	ASCAT	SVM	SA	TV	AMSR-E	0.86	0.63
138	ASCAT	SVM	SA	TV	API	0.75	0.52
139	ASCAT	SVM	SA	TV	NOAH	0.8	0.7
140	ASCAT	SVM	SA	TV	WASM	0.81	0.81
141	ASCAT	SVM	SD	Constant	ASCAT	1	0.54
142	ASCAT	SVM	SD	Constant	AMSR-E	0.59	0.51
143	ASCAT	SVM	SD	Constant	API	0.6	0.58
144	ASCAT	SVM	SD	Constant	NOAH	0.62	0.61
145	ASCAT	SVM	SD	Constant	WASM	0.64	0.64
146	ASCAT	SVM	SD	TV	ASCAT	1	0.54
147	ASCAT	SVM	SD	TV	AMSR-E	0.87	0.64
148	ASCAT	SVM	SD	TV	API	0.78	0.56
149	ASCAT	SVM	SD	TV	NOAH	0.84	0.71

ID	Unscaled Product	Rescalin g Method	Rescaling Technique	Application Style	Ref	Cor (Ref)	Cor (WASM)
150	ASCAT	SVM	SD	TV	WASM	0.84	0.84
151	AMSR-E	REG	ND	Constant	ASCAT	0.41	0.65
152	AMSR-E	REG	ND	Constant	AMSR-E	1	0.65
153	AMSR-E	REG	ND	Constant	API	0.32	0.65
154	AMSR-E	REG	ND	Constant	NOAH	0.58	0.65
155	AMSR-E	REG	ND	Constant	WASM	0.65	0.65
156	AMSR-E	REG	ND	TV	ASCAT	0.77	0.55
157	AMSR-E	REG	ND	TV	AMSR-E	1	0.65
158	AMSR-E	REG	ND	TV	API	0.64	0.56
159	AMSR-E	REG	ND	TV	NOAH	0.76	0.71
160	AMSR-E	REG	ND	TV	WASM	0.78	0.78
161	AMSR-E	REG	SA	Constant	ASCAT	0.56	0.46
162	AMSR-E	REG	SA	Constant	AMSR-E	1	0.65
163	AMSR-E	REG	SA	Constant	API	0.42	0.52
164	AMSR-E	REG	SA	Constant	NOAH	0.62	0.65
165	AMSR-E	REG	SA	Constant	WASM	0.66	0.66
166	AMSR-E	REG	SA	TV	ASCAT	0.78	0.54
167	AMSR-E	REG	SA	TV	AMSR-E	1	0.65
168	AMSR-E	REG	SA	TV	API	0.66	0.57
169	AMSR-E	REG	SA	TV	NOAH	0.76	0.71
170	AMSR-E	REG	SA	TV	WASM	0.8	0.8
171	AMSR-E	REG	SD	Constant	ASCAT	0.48	0.42
172	AMSR-E	REG	SD	Constant	AMSR-E	1	0.65
173	AMSR-E	REG	SD	Constant	API	0.33	0.61
174	AMSR-E	REG	SD	Constant	NOAH	0.61	0.67
175	AMSR-E	REG	SD	Constant	WASM	0.67	0.67
176	AMSR-E	REG	SD	TV	ASCAT	0.79	0.55
177	AMSR-E	REG	SD	TV	AMSR-E	1	0.65
178	AMSR-E	REG	SD	TV	API	0.68	0.59
179	AMSR-E	REG	SD	TV	NOAH	0.82	0.74
180	AMSR-E	REG	SD	TV	WASM	0.81	0.81
181	AMSR-E	VAR	ND	Constant	ASCAT	0.41	0.65
182	AMSR-E	VAR	ND	Constant	AMSR-E	1	0.65
183	AMSR-E	VAR	ND	Constant	API	0.32	0.65
184	AMSR-E	VAR	ND	Constant	NOAH	0.58	0.65
185	AMSR-E	VAR	ND	Constant	WASM	0.65	0.65
186	AMSR-E	VAR	ND	TV	ASCAT	0.73	0.57
187	AMSR-E	VAR	ND	TV	AMSR-E	1	0.65
188	AMSR-E	VAR	ND	TV	API	0.59	0.57

ID	Unscaled Product	Rescalin g Method	Rescaling Technique	Application Style	Ref	Cor (Ref)	Cor (WASM)
189	AMSR-E	VAR	ND	TV	NOAH	0.72	0.69
190	AMSR-E	VAR	ND	TV	WASM	0.75	0.75
191	AMSR-E	VAR	SA	Constant	ASCAT	0.48	0.65
192	AMSR-E	VAR	SA	Constant	AMSR-E	1	0.65
193	AMSR-E	VAR	SA	Constant	API	0.36	0.6
194	AMSR-E	VAR	SA	Constant	NOAH	0.6	0.64
195	AMSR-E	VAR	SA	Constant	WASM	0.65	0.65
196	AMSR-E	VAR	SA	TV	ASCAT	0.73	0.57
197	AMSR-E	VAR	SA	TV	AMSR-E	1	0.65
198	AMSR-E	VAR	SA	TV	API	0.6	0.57
199	AMSR-E	VAR	SA	TV	NOAH	0.72	0.69
200	AMSR-E	VAR	SA	TV	WASM	0.75	0.75
201	AMSR-E	VAR	SD	Constant	ASCAT	0.44	0.63
202	AMSR-E	VAR	SD	Constant	AMSR-E	1	0.65
203	AMSR-E	VAR	SD	Constant	API	0.32	0.64
204	AMSR-E	VAR	SD	Constant	NOAH	0.61	0.67
205	AMSR-E	VAR	SD	Constant	WASM	0.66	0.66
206	AMSR-E	VAR	SD	TV	ASCAT	0.74	0.56
207	AMSR-E	VAR	SD	TV	AMSR-E	1	0.65
208	AMSR-E	VAR	SD	TV	API	0.62	0.59
209	AMSR-E	VAR	SD	TV	NOAH	0.77	0.72
210	AMSR-E	VAR	SD	TV	WASM	0.78	0.78
211	AMSR-E	CDFM	ND	Constant	ASCAT	0.42	0.65
212	AMSR-E	CDFM	ND	Constant	AMSR-E	1	0.65
213	AMSR-E	CDFM	ND	Constant	API	0.32	0.66
214	AMSR-E	CDFM	ND	Constant	NOAH	0.59	0.66
215	AMSR-E	CDFM	ND	Constant	WASM	0.66	0.66
216	AMSR-E	CDFM	ND	TV	ASCAT	0.7	0.48
217	AMSR-E	CDFM	ND	TV	AMSR-E	1	0.65
218	AMSR-E	CDFM	ND	TV	API	0.6	0.48
219	AMSR-E	CDFM	ND	TV	NOAH	0.73	0.68
220	AMSR-E	CDFM	ND	TV	WASM	0.74	0.74
221	AMSR-E	CDFM	SA	Constant	ASCAT	0.42	0.65
222	AMSR-E	CDFM	SA	Constant	AMSR-E	1	0.65
223	AMSR-E	CDFM	SA	Constant	API	0.17	0.5
224	AMSR-E	CDFM	SA	Constant	NOAH	0.6	0.62
225	AMSR-E	CDFM	SA	Constant	WASM	0.61	0.61
226	AMSR-E	CDFM	SA	TV	ASCAT	0.7	0.49
227	AMSR-E	CDFM	SA	TV	AMSR-E	1	0.65

ID	Unscaled Product	Rescaling Method	Rescaling Technique	Application Style	Ref	Cor (Ref)	Cor (WASM)
228	AMSR-E	CDFM	SA	TV	API	0.61	0.49
229	AMSR-E	CDFM	SA	TV	NOAH	0.73	0.7
230	AMSR-E	CDFM	SA	TV	WASM	0.75	0.75
231	AMSR-E	CDFM	SD	Constant	ASCAT	0.41	0.66
232	AMSR-E	CDFM	SD	Constant	AMSR-E	1	0.65
233	AMSR-E	CDFM	SD	Constant	API	0.26	0.6
234	AMSR-E	CDFM	SD	Constant	NOAH	0.6	0.66
235	AMSR-E	CDFM	SD	Constant	WASM	0.67	0.67
236	AMSR-E	CDFM	SD	TV	ASCAT	0.74	0.55
237	AMSR-E	CDFM	SD	TV	AMSR-E	1	0.65
238	AMSR-E	CDFM	SD	TV	API	0.61	0.54
239	AMSR-E	CDFM	SD	TV	NOAH	0.79	0.72
240	AMSR-E	CDFM	SD	TV	WASM	0.8	0.8
241	AMSR-E	MAR	ND	Constant	ASCAT	0.56	0.46
242	AMSR-E	MAR	ND	Constant	AMSR-E	1	0.65
243	AMSR-E	MAR	ND	Constant	API	0.35	0.61
244	AMSR-E	MAR	ND	Constant	NOAH	0.62	0.66
245	AMSR-E	MAR	ND	Constant	WASM	0.68	0.68
246	AMSR-E	MAR	ND	TV	ASCAT	0.83	0.54
247	AMSR-E	MAR	ND	TV	AMSR-E	1	0.65
248	AMSR-E	MAR	ND	TV	API	0.68	0.58
249	AMSR-E	MAR	ND	TV	NOAH	0.78	0.72
250	AMSR-E	MAR	ND	TV	WASM	0.82	0.82
251	AMSR-E	MAR	SA	Constant	ASCAT	0.71	0.52
252	AMSR-E	MAR	SA	Constant	AMSR-E	1	0.65
253	AMSR-E	MAR	SA	Constant	API	0.57	0.57
254	AMSR-E	MAR	SA	Constant	NOAH	0.68	0.68
255	AMSR-E	MAR	SA	Constant	WASM	0.73	0.73
256	AMSR-E	MAR	SA	TV	ASCAT	0.83	0.53
257	AMSR-E	MAR	SA	TV	AMSR-E	1	0.65
258	AMSR-E	MAR	SA	TV	API	0.69	0.57
259	AMSR-E	MAR	SA	TV	NOAH	0.78	0.72
260	AMSR-E	MAR	SA	TV	WASM	0.83	0.83
261	AMSR-E	MAR	SD	Constant	ASCAT	0.64	0.5
262	AMSR-E	MAR	SD	Constant	AMSR-E	1	0.65
263	AMSR-E	MAR	SD	Constant	API	0.46	0.58
264	AMSR-E	MAR	SD	Constant	NOAH	0.66	0.68
265	AMSR-E	MAR	SD	Constant	WASM	0.71	0.71
266	AMSR-E	MAR	SD	TV	ASCAT	0.84	0.58

ID	Unscaled Product	Rescaling Method	Rescaling Technique	Application Style	Ref	Cor (Ref)	Cor (WASM)
267	AMSR-E	MAR	SD	TV	AMSR-E	1	0.65
268	AMSR-E	MAR	SD	TV	API	0.74	0.6
269	AMSR-E	MAR	SD	TV	NOAH	0.84	0.74
270	AMSR-E	MAR	SD	TV	WASM	0.87	0.87
271	AMSR-E	SVM	ND	Constant	ASCAT	0.57	0.4
272	AMSR-E	SVM	ND	Constant	AMSR-E	1	0.65
273	AMSR-E	SVM	ND	Constant	API	0.33	0.54
274	AMSR-E	SVM	ND	Constant	NOAH	0.62	0.66
275	AMSR-E	SVM	ND	Constant	WASM	0.68	0.68
276	AMSR-E	SVM	ND	TV	ASCAT	0.82	0.52
277	AMSR-E	SVM	ND	TV	AMSR-E	0.99	0.65
278	AMSR-E	SVM	ND	TV	API	0.7	0.56
279	AMSR-E	SVM	ND	TV	NOAH	0.78	0.71
280	AMSR-E	SVM	ND	TV	WASM	0.82	0.82
281	AMSR-E	SVM	SA	Constant	ASCAT	0.69	0.49
282	AMSR-E	SVM	SA	Constant	AMSR-E	0.99	0.65
283	AMSR-E	SVM	SA	Constant	API	0.55	0.53
284	AMSR-E	SVM	SA	Constant	NOAH	0.68	0.68
285	AMSR-E	SVM	SA	Constant	WASM	0.72	0.72
286	AMSR-E	SVM	SA	TV	ASCAT	0.82	0.52
287	AMSR-E	SVM	SA	TV	AMSR-E	0.99	0.66
288	AMSR-E	SVM	SA	TV	API	0.7	0.56
289	AMSR-E	SVM	SA	TV	NOAH	0.79	0.72
290	AMSR-E	SVM	SA	TV	WASM	0.83	0.83
291	AMSR-E	SVM	SD	Constant	ASCAT	0.62	0.42
292	AMSR-E	SVM	SD	Constant	AMSR-E	1	0.65
293	AMSR-E	SVM	SD	Constant	API	0.4	0.51
294	AMSR-E	SVM	SD	Constant	NOAH	0.66	0.68
295	AMSR-E	SVM	SD	Constant	WASM	0.7	0.7
296	AMSR-E	SVM	SD	TV	ASCAT	0.84	0.55
297	AMSR-E	SVM	SD	TV	AMSR-E	0.99	0.66
298	AMSR-E	SVM	SD	TV	API	0.73	0.6
299	AMSR-E	SVM	SD	TV	NOAH	0.84	0.73
300	AMSR-E	SVM	SD	TV	WASM	0.85	0.85
301	API	REG	ND	Constant	ASCAT	0.51	0.57
302	API	REG	ND	Constant	AMSR-E	0.32	0.57
303	API	REG	ND	Constant	API	1	0.57
304	API	REG	ND	Constant	NOAH	0.45	0.57
305	API	REG	ND	Constant	WASM	0.57	0.57

ID	Unscaled Product	Rescaling Method	Rescaling Technique	Application Style	Ref	Cor (Ref)	Cor (WASM)
306	API	REG	ND	TV	ASCAT	0.75	0.55
307	API	REG	ND	TV	AMSR-E	0.8	0.62
308	API	REG	ND	TV	API	1	0.57
309	API	REG	ND	TV	NOAH	0.75	0.73
310	API	REG	ND	TV	WASM	0.82	0.82
311	API	REG	SA	Constant	ASCAT	0.52	0.6
312	API	REG	SA	Constant	AMSR-E	0.44	0.52
313	API	REG	SA	Constant	API	1	0.57
314	API	REG	SA	Constant	NOAH	0.5	0.61
315	API	REG	SA	Constant	WASM	0.61	0.61
316	API	REG	SA	TV	ASCAT	0.75	0.55
317	API	REG	SA	TV	AMSR-E	0.81	0.62
318	API	REG	SA	TV	API	1	0.57
319	API	REG	SA	TV	NOAH	0.76	0.74
320	API	REG	SA	TV	WASM	0.82	0.82
321	API	REG	SD	Constant	ASCAT	0.52	0.58
322	API	REG	SD	Constant	AMSR-E	0.33	0.56
323	API	REG	SD	Constant	API	1	0.57
324	API	REG	SD	Constant	NOAH	0.48	0.59
325	API	REG	SD	Constant	WASM	0.59	0.59
326	API	REG	SD	TV	ASCAT	0.76	0.55
327	API	REG	SD	TV	AMSR-E	0.81	0.62
328	API	REG	SD	TV	API	1	0.57
329	API	REG	SD	TV	NOAH	0.78	0.74
330	API	REG	SD	TV	WASM	0.82	0.82
331	API	VAR	ND	Constant	ASCAT	0.51	0.57
332	API	VAR	ND	Constant	AMSR-E	0.32	0.57
333	API	VAR	ND	Constant	API	1	0.57
334	API	VAR	ND	Constant	NOAH	0.45	0.57
335	API	VAR	ND	Constant	WASM	0.57	0.57
336	API	VAR	ND	TV	ASCAT	0.7	0.58
337	API	VAR	ND	TV	AMSR-E	0.74	0.66
338	API	VAR	ND	TV	API	1	0.57
339	API	VAR	ND	TV	NOAH	0.7	0.72
340	API	VAR	ND	TV	WASM	0.78	0.78
341	API	VAR	SA	Constant	ASCAT	0.52	0.59
342	API	VAR	SA	Constant	AMSR-E	0.28	0.53
343	API	VAR	SA	Constant	API	1	0.57
344	API	VAR	SA	Constant	NOAH	0.49	0.6

ID	Unscaled Product	Rescaling Method	Rescaling Technique	Application Style	Ref	Cor (Ref)	Cor (WASM)
345	API	VAR	SA	Constant	WASM	0.58	0.58
346	API	VAR	SA	TV	ASCAT	0.7	0.58
347	API	VAR	SA	TV	AMSR-E	0.74	0.65
348	API	VAR	SA	TV	API	1	0.57
349	API	VAR	SA	TV	NOAH	0.7	0.72
350	API	VAR	SA	TV	WASM	0.78	0.78
351	API	VAR	SD	Constant	ASCAT	0.51	0.56
352	API	VAR	SD	Constant	AMSR-E	0.32	0.57
353	API	VAR	SD	Constant	API	1	0.57
354	API	VAR	SD	Constant	NOAH	0.48	0.58
355	API	VAR	SD	Constant	WASM	0.58	0.58
356	API	VAR	SD	TV	ASCAT	0.7	0.56
357	API	VAR	SD	TV	AMSR-E	0.73	0.65
358	API	VAR	SD	TV	API	1	0.57
359	API	VAR	SD	TV	NOAH	0.72	0.73
360	API	VAR	SD	TV	WASM	0.79	0.79
361	API	CDFM	ND	Constant	ASCAT	0.32	0.41
362	API	CDFM	ND	Constant	AMSR-E	0.19	0.32
363	API	CDFM	ND	Constant	API	1	0.57
364	API	CDFM	ND	Constant	NOAH	0.48	0.58
365	API	CDFM	ND	Constant	WASM	0.56	0.56
366	API	CDFM	ND	TV	ASCAT	0.6	0.52
367	API	CDFM	ND	TV	AMSR-E	0.7	0.61
368	API	CDFM	ND	TV	API	1	0.57
369	API	CDFM	ND	TV	NOAH	0.73	0.74
370	API	CDFM	ND	TV	WASM	0.81	0.81
371	API	CDFM	SA	Constant	ASCAT	0.37	0.42
372	API	CDFM	SA	Constant	AMSR-E	0.19	0.32
373	API	CDFM	SA	Constant	API	1	0.57
374	API	CDFM	SA	Constant	NOAH	0.5	0.6
375	API	CDFM	SA	Constant	WASM	0.58	0.58
376	API	CDFM	SA	TV	ASCAT	0.61	0.5
377	API	CDFM	SA	TV	AMSR-E	0.72	0.59
378	API	CDFM	SA	TV	API	1	0.57
379	API	CDFM	SA	TV	NOAH	0.72	0.73
380	API	CDFM	SA	TV	WASM	0.8	0.8
381	API	CDFM	SD	Constant	ASCAT	0.36	0.44
382	API	CDFM	SD	Constant	AMSR-E	0.21	0.4
383	API	CDFM	SD	Constant	API	1	0.57

ID	Unscaled Product	Rescaling Method	Rescaling Technique	Application Style	Ref	Cor (Ref)	Cor (WASM)
384	API	CDFM	SD	Constant	NOAH	0.5	0.6
385	API	CDFM	SD	Constant	WASM	0.58	0.58
386	API	CDFM	SD	TV	ASCAT	0.64	0.5
387	API	CDFM	SD	TV	AMSR-E	0.78	0.62
388	API	CDFM	SD	TV	API	1	0.57
389	API	CDFM	SD	TV	NOAH	0.73	0.74
390	API	CDFM	SD	TV	WASM	0.82	0.82
391	API	MAR	ND	Constant	ASCAT	0.56	0.58
392	API	MAR	ND	Constant	AMSR-E	0.38	0.54
393	API	MAR	ND	Constant	API	1	0.57
394	API	MAR	ND	Constant	NOAH	0.49	0.6
395	API	MAR	ND	Constant	WASM	0.62	0.62
396	API	MAR	ND	TV	ASCAT	0.78	0.55
397	API	MAR	ND	TV	AMSR-E	0.83	0.64
398	API	MAR	ND	TV	API	1	0.57
399	API	MAR	ND	TV	NOAH	0.8	0.74
400	API	MAR	ND	TV	WASM	0.86	0.86
401	API	MAR	SA	Constant	ASCAT	0.66	0.59
402	API	MAR	SA	Constant	AMSR-E	0.64	0.55
403	API	MAR	SA	Constant	API	1	0.57
404	API	MAR	SA	Constant	NOAH	0.6	0.69
405	API	MAR	SA	Constant	WASM	0.72	0.72
406	API	MAR	SA	TV	ASCAT	0.78	0.54
407	API	MAR	SA	TV	AMSR-E	0.84	0.63
408	API	MAR	SA	TV	API	1	0.57
409	API	MAR	SA	TV	NOAH	0.8	0.74
410	API	MAR	SA	TV	WASM	0.86	0.86
411	API	MAR	SD	Constant	ASCAT	0.58	0.59
412	API	MAR	SD	Constant	AMSR-E	0.42	0.53
413	API	MAR	SD	Constant	API	1	0.57
414	API	MAR	SD	Constant	NOAH	0.52	0.6
415	API	MAR	SD	Constant	WASM	0.64	0.64
416	API	MAR	SD	TV	ASCAT	0.79	0.56
417	API	MAR	SD	TV	AMSR-E	0.84	0.64
418	API	MAR	SD	TV	API	1	0.57
419	API	MAR	SD	TV	NOAH	0.82	0.74
420	API	MAR	SD	TV	WASM	0.87	0.87
421	API	SVM	ND	Constant	ASCAT	0.56	0.57
422	API	SVM	ND	Constant	AMSR-E	0.38	0.54

ID	Unscaled Product	Rescalin g Method	Rescaling Technique	Application Style	Ref	Cor (Ref)	Cor (WASM)
423	API	SVM	ND	Constant	API	1	0.58
424	API	SVM	ND	Constant	NOAH	0.49	0.6
425	API	SVM	ND	Constant	WASM	0.62	0.62
426	API	SVM	ND	TV	ASCAT	0.78	0.51
427	API	SVM	ND	TV	AMSR-E	0.83	0.64
428	API	SVM	ND	TV	API	1	0.57
429	API	SVM	ND	TV	NOAH	0.79	0.73
430	API	SVM	ND	TV	WASM	0.84	0.84
431	API	SVM	SA	Constant	ASCAT	0.64	0.58
432	API	SVM	SA	Constant	AMSR-E	0.63	0.53
433	API	SVM	SA	Constant	API	1	0.58
434	API	SVM	SA	Constant	NOAH	0.59	0.69
435	API	SVM	SA	Constant	WASM	0.72	0.72
436	API	SVM	SA	TV	ASCAT	0.78	0.5
437	API	SVM	SA	TV	AMSR-E	0.83	0.64
438	API	SVM	SA	TV	API	1	0.57
439	API	SVM	SA	TV	NOAH	0.8	0.72
440	API	SVM	SA	TV	WASM	0.85	0.85
441	API	SVM	SD	Constant	ASCAT	0.58	0.58
442	API	SVM	SD	Constant	AMSR-E	0.4	0.48
443	API	SVM	SD	Constant	API	1	0.58
444	API	SVM	SD	Constant	NOAH	0.52	0.6
445	API	SVM	SD	Constant	WASM	0.63	0.63
446	API	SVM	SD	TV	ASCAT	0.78	0.53
447	API	SVM	SD	TV	AMSR-E	0.84	0.64
448	API	SVM	SD	TV	API	0.99	0.58
449	API	SVM	SD	TV	NOAH	0.81	0.73
450	API	SVM	SD	TV	WASM	0.86	0.86
451	NOAH	REG	ND	Constant	ASCAT	0.48	0.7
452	NOAH	REG	ND	Constant	AMSR-E	0.58	0.7
453	NOAH	REG	ND	Constant	API	0.45	0.7
454	NOAH	REG	ND	Constant	NOAH	1	0.7
455	NOAH	REG	ND	Constant	WASM	0.7	0.7
456	NOAH	REG	ND	TV	ASCAT	0.75	0.53
457	NOAH	REG	ND	TV	AMSR-E	0.82	0.64
458	NOAH	REG	ND	TV	API	0.72	0.55
459	NOAH	REG	ND	TV	NOAH	1	0.7
460	NOAH	REG	ND	TV	WASM	0.8	0.8
461	NOAH	REG	SA	Constant	ASCAT	0.54	0.55

ID	Unscaled Product	Rescaling Method	Rescaling Technique	Application Style	Ref	Cor (Ref)	Cor (WASM)
462	NOAH	REG	SA	Constant	AMSR-E	0.65	0.69
463	NOAH	REG	SA	Constant	API	0.47	0.62
464	NOAH	REG	SA	Constant	NOAH	1	0.7
465	NOAH	REG	SA	Constant	WASM	0.72	0.72
466	NOAH	REG	SA	TV	ASCAT	0.76	0.52
467	NOAH	REG	SA	TV	AMSR-E	0.82	0.64
468	NOAH	REG	SA	TV	API	0.73	0.55
469	NOAH	REG	SA	TV	NOAH	1	0.7
470	NOAH	REG	SA	TV	WASM	0.81	0.81
471	NOAH	REG	SD	Constant	ASCAT	0.53	0.66
472	NOAH	REG	SD	Constant	AMSR-E	0.58	0.7
473	NOAH	REG	SD	Constant	API	0.46	0.7
474	NOAH	REG	SD	Constant	NOAH	1	0.7
475	NOAH	REG	SD	Constant	WASM	0.7	0.7
476	NOAH	REG	SD	TV	ASCAT	0.76	0.52
477	NOAH	REG	SD	TV	AMSR-E	0.82	0.64
478	NOAH	REG	SD	TV	API	0.73	0.56
479	NOAH	REG	SD	TV	NOAH	1	0.7
480	NOAH	REG	SD	TV	WASM	0.81	0.81
481	NOAH	VAR	ND	Constant	ASCAT	0.48	0.7
482	NOAH	VAR	ND	Constant	AMSR-E	0.58	0.7
483	NOAH	VAR	ND	Constant	API	0.45	0.7
484	NOAH	VAR	ND	Constant	NOAH	1	0.7
485	NOAH	VAR	ND	Constant	WASM	0.7	0.7
486	NOAH	VAR	ND	TV	ASCAT	0.7	0.57
487	NOAH	VAR	ND	TV	AMSR-E	0.77	0.66
488	NOAH	VAR	ND	TV	API	0.67	0.56
489	NOAH	VAR	ND	TV	NOAH	1	0.7
490	NOAH	VAR	ND	TV	WASM	0.77	0.77
491	NOAH	VAR	SA	Constant	ASCAT	0.48	0.7
492	NOAH	VAR	SA	Constant	AMSR-E	0.63	0.69
493	NOAH	VAR	SA	Constant	API	0.46	0.64
494	NOAH	VAR	SA	Constant	NOAH	1	0.7
495	NOAH	VAR	SA	Constant	WASM	0.7	0.7
496	NOAH	VAR	SA	TV	ASCAT	0.7	0.56
497	NOAH	VAR	SA	TV	AMSR-E	0.77	0.66
498	NOAH	VAR	SA	TV	API	0.68	0.56
499	NOAH	VAR	SA	TV	NOAH	1	0.7
500	NOAH	VAR	SA	TV	WASM	0.78	0.78

ID	Unscaled Product	Rescaling Method	Rescaling Technique	Application Style	Ref	Cor (Ref)	Cor (WASM)
501	NOAH	VAR	SD	Constant	ASCAT	0.51	0.67
502	NOAH	VAR	SD	Constant	AMSR-E	0.57	0.68
503	NOAH	VAR	SD	Constant	API	0.46	0.68
504	NOAH	VAR	SD	Constant	NOAH	1	0.7
505	NOAH	VAR	SD	Constant	WASM	0.7	0.7
506	NOAH	VAR	SD	TV	ASCAT	0.71	0.55
507	NOAH	VAR	SD	TV	AMSR-E	0.76	0.65
508	NOAH	VAR	SD	TV	API	0.68	0.56
509	NOAH	VAR	SD	TV	NOAH	1	0.7
510	NOAH	VAR	SD	TV	WASM	0.78	0.78
511	NOAH	CDFM	ND	Constant	ASCAT	0.32	0.58
512	NOAH	CDFM	ND	Constant	AMSR-E	0.56	0.51
513	NOAH	CDFM	ND	Constant	API	0.46	0.64
514	NOAH	CDFM	ND	Constant	NOAH	1	0.7
515	NOAH	CDFM	ND	Constant	WASM	0.7	0.7
516	NOAH	CDFM	ND	TV	ASCAT	0.61	0.48
517	NOAH	CDFM	ND	TV	AMSR-E	0.72	0.57
518	NOAH	CDFM	ND	TV	API	0.69	0.54
519	NOAH	CDFM	ND	TV	NOAH	1	0.7
520	NOAH	CDFM	ND	TV	WASM	0.78	0.78
521	NOAH	CDFM	SA	Constant	ASCAT	0.34	0.6
522	NOAH	CDFM	SA	Constant	AMSR-E	0.6	0.53
523	NOAH	CDFM	SA	Constant	API	0.47	0.59
524	NOAH	CDFM	SA	Constant	NOAH	1	0.7
525	NOAH	CDFM	SA	Constant	WASM	0.7	0.7
526	NOAH	CDFM	SA	TV	ASCAT	0.61	0.49
527	NOAH	CDFM	SA	TV	AMSR-E	0.72	0.57
528	NOAH	CDFM	SA	TV	API	0.69	0.54
529	NOAH	CDFM	SA	TV	NOAH	1	0.7
530	NOAH	CDFM	SA	TV	WASM	0.79	0.79
531	NOAH	CDFM	SD	Constant	ASCAT	0.35	0.64
532	NOAH	CDFM	SD	Constant	AMSR-E	0.6	0.6
533	NOAH	CDFM	SD	Constant	API	0.47	0.64
534	NOAH	CDFM	SD	Constant	NOAH	1	0.7
535	NOAH	CDFM	SD	Constant	WASM	0.71	0.71
536	NOAH	CDFM	SD	TV	ASCAT	0.66	0.51
537	NOAH	CDFM	SD	TV	AMSR-E	0.76	0.62
538	NOAH	CDFM	SD	TV	API	0.7	0.56
539	NOAH	CDFM	SD	TV	NOAH	1	0.7

ID	Unscaled Product	Rescaling Method	Rescaling Technique	Application Style	Ref	Cor (Ref)	Cor (WASM)
540	NOAH	CDFM	SD	TV	WASM	0.8	0.8
541	NOAH	MAR	ND	Constant	ASCAT	0.58	0.62
542	NOAH	MAR	ND	Constant	AMSR-E	0.65	0.66
543	NOAH	MAR	ND	Constant	API	0.55	0.66
544	NOAH	MAR	ND	Constant	NOAH	1	0.7
545	NOAH	MAR	ND	Constant	WASM	0.73	0.73
546	NOAH	MAR	ND	TV	ASCAT	0.79	0.53
547	NOAH	MAR	ND	TV	AMSR-E	0.83	0.64
548	NOAH	MAR	ND	TV	API	0.77	0.56
549	NOAH	MAR	ND	TV	NOAH	1	0.7
550	NOAH	MAR	ND	TV	WASM	0.84	0.84
551	NOAH	MAR	SA	Constant	ASCAT	0.63	0.48
552	NOAH	MAR	SA	Constant	AMSR-E	0.72	0.65
553	NOAH	MAR	SA	Constant	API	0.58	0.56
554	NOAH	MAR	SA	Constant	NOAH	1	0.7
555	NOAH	MAR	SA	Constant	WASM	0.74	0.74
556	NOAH	MAR	SA	TV	ASCAT	0.79	0.52
557	NOAH	MAR	SA	TV	AMSR-E	0.84	0.62
558	NOAH	MAR	SA	TV	API	0.77	0.56
559	NOAH	MAR	SA	TV	NOAH	1	0.7
560	NOAH	MAR	SA	TV	WASM	0.84	0.84
561	NOAH	MAR	SD	Constant	ASCAT	0.6	0.6
562	NOAH	MAR	SD	Constant	AMSR-E	0.66	0.66
563	NOAH	MAR	SD	Constant	API	0.57	0.68
564	NOAH	MAR	SD	Constant	NOAH	1	0.7
565	NOAH	MAR	SD	Constant	WASM	0.74	0.74
566	NOAH	MAR	SD	TV	ASCAT	0.81	0.54
567	NOAH	MAR	SD	TV	AMSR-E	0.86	0.64
568	NOAH	MAR	SD	TV	API	0.81	0.58
569	NOAH	MAR	SD	TV	NOAH	1	0.7
570	NOAH	MAR	SD	TV	WASM	0.87	0.87
571	NOAH	SVM	ND	Constant	ASCAT	0.58	0.58
572	NOAH	SVM	ND	Constant	AMSR-E	0.64	0.66
573	NOAH	SVM	ND	Constant	API	0.52	0.65
574	NOAH	SVM	ND	Constant	NOAH	1	0.7
575	NOAH	SVM	ND	Constant	WASM	0.73	0.73
576	NOAH	SVM	ND	TV	ASCAT	0.78	0.5
577	NOAH	SVM	ND	TV	AMSR-E	0.83	0.65
578	NOAH	SVM	ND	TV	API	0.74	0.53

ID	Unscaled Product	Rescaling Method	Rescaling Technique	Application Style	Ref	Cor (Ref)	Cor (WASM)
579	NOAH	SVM	ND	TV	NOAH	1	0.7
580	NOAH	SVM	ND	TV	WASM	0.83	0.83
581	NOAH	SVM	SA	Constant	ASCAT	0.62	0.4
582	NOAH	SVM	SA	Constant	AMSR-E	0.71	0.63
583	NOAH	SVM	SA	Constant	API	0.55	0.53
584	NOAH	SVM	SA	Constant	NOAH	1	0.7
585	NOAH	SVM	SA	Constant	WASM	0.74	0.74
586	NOAH	SVM	SA	TV	ASCAT	0.79	0.5
587	NOAH	SVM	SA	TV	AMSR-E	0.84	0.64
588	NOAH	SVM	SA	TV	API	0.76	0.52
589	NOAH	SVM	SA	TV	NOAH	1	0.7
590	NOAH	SVM	SA	TV	WASM	0.84	0.84
591	NOAH	SVM	SD	Constant	ASCAT	0.58	0.56
592	NOAH	SVM	SD	Constant	AMSR-E	0.66	0.66
593	NOAH	SVM	SD	Constant	API	0.54	0.68
594	NOAH	SVM	SD	Constant	NOAH	1	0.7
595	NOAH	SVM	SD	Constant	WASM	0.73	0.73
596	NOAH	SVM	SD	TV	ASCAT	0.8	0.51
597	NOAH	SVM	SD	TV	AMSR-E	0.85	0.64
598	NOAH	SVM	SD	TV	API	0.78	0.56
599	NOAH	SVM	SD	TV	NOAH	1	0.7
600	NOAH	SVM	SD	TV	WASM	0.85	0.85
601	WASM	REG	ND	Constant	ASCAT	0.54	1
602	WASM	REG	ND	Constant	AMSR-E	0.65	1
603	WASM	REG	ND	Constant	API	0.57	1
604	WASM	REG	ND	Constant	NOAH	0.7	1
605	WASM	REG	ND	Constant	WASM	1	1
606	WASM	REG	ND	TV	ASCAT	0.77	0.71
607	WASM	REG	ND	TV	AMSR-E	0.84	0.77
608	WASM	REG	ND	TV	API	0.77	0.74
609	WASM	REG	ND	TV	NOAH	0.79	0.89
610	WASM	REG	ND	TV	WASM	1	1
611	WASM	REG	SA	Constant	ASCAT	0.6	0.9
612	WASM	REG	SA	Constant	AMSR-E	0.7	0.94
613	WASM	REG	SA	Constant	API	0.63	0.93
614	WASM	REG	SA	Constant	NOAH	0.73	0.97
615	WASM	REG	SA	Constant	WASM	1	1
616	WASM	REG	SA	TV	ASCAT	0.78	0.7
617	WASM	REG	SA	TV	AMSR-E	0.84	0.77

ID	Unscaled Product	Rescaling Method	Rescaling Technique	Application Style	Ref	Cor (Ref)	Cor (WASM)
618	WASM	REG	SA	TV	API	0.78	0.74
619	WASM	REG	SA	TV	NOAH	0.8	0.88
620	WASM	REG	SA	TV	WASM	1	1
621	WASM	REG	SD	Constant	ASCAT	0.57	0.96
622	WASM	REG	SD	Constant	AMSR-E	0.66	0.99
623	WASM	REG	SD	Constant	API	0.58	1
624	WASM	REG	SD	Constant	NOAH	0.72	0.99
625	WASM	REG	SD	Constant	WASM	1	1
626	WASM	REG	SD	TV	ASCAT	0.78	0.7
627	WASM	REG	SD	TV	AMSR-E	0.84	0.76
628	WASM	REG	SD	TV	API	0.78	0.74
629	WASM	REG	SD	TV	NOAH	0.81	0.88
630	WASM	REG	SD	TV	WASM	1	1
631	WASM	VAR	ND	Constant	ASCAT	0.54	1
632	WASM	VAR	ND	Constant	AMSR-E	0.65	1
633	WASM	VAR	ND	Constant	API	0.57	1
634	WASM	VAR	ND	Constant	NOAH	0.7	1
635	WASM	VAR	ND	Constant	WASM	1	1
636	WASM	VAR	ND	TV	ASCAT	0.72	0.81
637	WASM	VAR	ND	TV	AMSR-E	0.8	0.85
638	WASM	VAR	ND	TV	API	0.73	0.81
639	WASM	VAR	ND	TV	NOAH	0.76	0.93
640	WASM	VAR	ND	TV	WASM	1	1
641	WASM	VAR	SA	Constant	ASCAT	0.54	1
642	WASM	VAR	SA	Constant	AMSR-E	0.68	0.97
643	WASM	VAR	SA	Constant	API	0.61	0.96
644	WASM	VAR	SA	Constant	NOAH	0.71	0.99
645	WASM	VAR	SA	Constant	WASM	1	1
646	WASM	VAR	SA	TV	ASCAT	0.72	0.8
647	WASM	VAR	SA	TV	AMSR-E	0.8	0.85
648	WASM	VAR	SA	TV	API	0.73	0.8
649	WASM	VAR	SA	TV	NOAH	0.76	0.92
650	WASM	VAR	SA	TV	WASM	1	1
651	WASM	VAR	SD	Constant	ASCAT	0.55	0.98
652	WASM	VAR	SD	Constant	AMSR-E	0.64	1
653	WASM	VAR	SD	Constant	API	0.58	1
654	WASM	VAR	SD	Constant	NOAH	0.71	1
655	WASM	VAR	SD	Constant	WASM	1	1
656	WASM	VAR	SD	TV	ASCAT	0.73	0.79

ID	Unscaled Product	Rescaling Method	Rescaling Technique	Application Style	Ref	Cor (Ref)	Cor (WASM)
657	WASM	VAR	SD	TV	AMSR-E	0.8	0.85
658	WASM	VAR	SD	TV	API	0.73	0.8
659	WASM	VAR	SD	TV	NOAH	0.76	0.92
660	WASM	VAR	SD	TV	WASM	1	1
661	WASM	CDFM	ND	Constant	ASCAT	0.34	0.97
662	WASM	CDFM	ND	Constant	AMSR-E	0.61	0.96
663	WASM	CDFM	ND	Constant	API	0.57	0.94
664	WASM	CDFM	ND	Constant	NOAH	0.71	0.98
665	WASM	CDFM	ND	Constant	WASM	1	1
666	WASM	CDFM	ND	TV	ASCAT	0.61	0.7
667	WASM	CDFM	ND	TV	AMSR-E	0.74	0.8
668	WASM	CDFM	ND	TV	API	0.76	0.72
669	WASM	CDFM	ND	TV	NOAH	0.76	0.89
670	WASM	CDFM	ND	TV	WASM	1	1
671	WASM	CDFM	SA	Constant	ASCAT	0.42	0.92
672	WASM	CDFM	SA	Constant	AMSR-E	0.59	0.87
673	WASM	CDFM	SA	Constant	API	0.64	0.94
674	WASM	CDFM	SA	Constant	NOAH	0.73	0.97
675	WASM	CDFM	SA	Constant	WASM	1	1
676	WASM	CDFM	SA	TV	ASCAT	0.63	0.7
677	WASM	CDFM	SA	TV	AMSR-E	0.72	0.78
678	WASM	CDFM	SA	TV	API	0.76	0.72
679	WASM	CDFM	SA	TV	NOAH	0.76	0.89
680	WASM	CDFM	SA	TV	WASM	1	1
681	WASM	CDFM	SD	Constant	ASCAT	0.37	0.91
682	WASM	CDFM	SD	Constant	AMSR-E	0.64	0.92
683	WASM	CDFM	SD	Constant	API	0.56	0.96
684	WASM	CDFM	SD	Constant	NOAH	0.71	0.98
685	WASM	CDFM	SD	Constant	WASM	1	1
686	WASM	CDFM	SD	TV	ASCAT	0.65	0.67
687	WASM	CDFM	SD	TV	AMSR-E	0.76	0.78
688	WASM	CDFM	SD	TV	API	0.75	0.74
689	WASM	CDFM	SD	TV	NOAH	0.76	0.89
690	WASM	CDFM	SD	TV	WASM	1	1
691	WASM	MAR	ND	Constant	ASCAT	0.6	0.89
692	WASM	MAR	ND	Constant	AMSR-E	0.72	0.9
693	WASM	MAR	ND	Constant	API	0.66	0.87
694	WASM	MAR	ND	Constant	NOAH	0.73	0.97
695	WASM	MAR	ND	Constant	WASM	1	1

ID	Unscaled Product	Rescaling Method	Rescaling Technique	Application Style	Ref	Cor (Ref)	Cor (WASM)
696	WASM	MAR	ND	TV	ASCAT	0.8	0.66
697	WASM	MAR	ND	TV	AMSR-E	0.86	0.74
698	WASM	MAR	ND	TV	API	0.82	0.69
699	WASM	MAR	ND	TV	NOAH	0.82	0.86
700	WASM	MAR	ND	TV	WASM	1	1
701	WASM	MAR	SA	Constant	ASCAT	0.68	0.8
702	WASM	MAR	SA	Constant	AMSR-E	0.78	0.84
703	WASM	MAR	SA	Constant	API	0.73	0.8
704	WASM	MAR	SA	Constant	NOAH	0.76	0.94
705	WASM	MAR	SA	Constant	WASM	1	1
706	WASM	MAR	SA	TV	ASCAT	0.8	0.66
707	WASM	MAR	SA	TV	AMSR-E	0.86	0.75
708	WASM	MAR	SA	TV	API	0.82	0.69
709	WASM	MAR	SA	TV	NOAH	0.82	0.85
710	WASM	MAR	SA	TV	WASM	1	1
711	WASM	MAR	SD	Constant	ASCAT	0.64	0.87
712	WASM	MAR	SD	Constant	AMSR-E	0.73	0.9
713	WASM	MAR	SD	Constant	API	0.68	0.86
714	WASM	MAR	SD	Constant	NOAH	0.74	0.96
715	WASM	MAR	SD	Constant	WASM	1	1
716	WASM	MAR	SD	TV	ASCAT	0.82	0.68
717	WASM	MAR	SD	TV	AMSR-E	0.87	0.74
718	WASM	MAR	SD	TV	API	0.84	0.7
719	WASM	MAR	SD	TV	NOAH	0.85	0.84
720	WASM	MAR	SD	TV	WASM	1	1
721	WASM	SVM	ND	Constant	ASCAT	0.6	0.84
722	WASM	SVM	ND	Constant	AMSR-E	0.71	0.9
723	WASM	SVM	ND	Constant	API	0.65	0.85
724	WASM	SVM	ND	Constant	NOAH	0.73	0.96
725	WASM	SVM	ND	Constant	WASM	1	1
726	WASM	SVM	ND	TV	ASCAT	0.8	0.63
727	WASM	SVM	ND	TV	AMSR-E	0.86	0.74
728	WASM	SVM	ND	TV	API	0.8	0.67
729	WASM	SVM	ND	TV	NOAH	0.82	0.84
730	WASM	SVM	ND	TV	WASM	1	1
731	WASM	SVM	SA	Constant	ASCAT	0.66	0.77
732	WASM	SVM	SA	Constant	AMSR-E	0.78	0.82
733	WASM	SVM	SA	Constant	API	0.71	0.8
734	WASM	SVM	SA	Constant	NOAH	0.75	0.94

ID	Unscaled Product	Rescaling Method	Rescaling Technique	Application Style	Ref	Cor (Ref)	Cor (WASM)
735	WASM	SVM	SA	Constant	WASM	1	1
736	WASM	SVM	SA	TV	ASCAT	0.81	0.64
737	WASM	SVM	SA	TV	AMSR-E	0.86	0.75
738	WASM	SVM	SA	TV	API	0.81	0.68
739	WASM	SVM	SA	TV	NOAH	0.82	0.84
740	WASM	SVM	SA	TV	WASM	1	1
741	WASM	SVM	SD	Constant	ASCAT	0.62	0.83
742	WASM	SVM	SD	Constant	AMSR-E	0.73	0.9
743	WASM	SVM	SD	Constant	API	0.66	0.86
744	WASM	SVM	SD	Constant	NOAH	0.74	0.96
745	WASM	SVM	SD	Constant	WASM	1	1
746	WASM	SVM	SD	TV	ASCAT	0.8	0.64
747	WASM	SVM	SD	TV	AMSR-E	0.86	0.74
748	WASM	SVM	SD	TV	API	0.82	0.68
749	WASM	SVM	SD	TV	NOAH	0.84	0.83
750	WASM	SVM	SD	TV	WASM	1	1

B. Comparison of the impact of rescaling approaches over the accuracy of fused products (results are averages over four watersheds)

ID	Parent Couples	Rescaling Method	Rescaling Technique	Application Style	Reference	Cor (WASM)
1	ASCAT AMSR-E	REG	ND	Constant	ASCAT	0.62
2	ASCAT AMSR-E	REG	ND	Constant	AMSR-E	0.71
3	ASCAT AMSR-E	REG	ND	Constant	API	0.69
4	ASCAT AMSR-E	REG	ND	Constant	NOAH	0.74
5	ASCAT AMSR-E	REG	ND	Constant	WASM	0.74
6	ASCAT AMSR-E	REG	ND	TV	ASCAT	0.59
7	ASCAT AMSR-E	REG	ND	TV	AMSR-E	0.66
8	ASCAT AMSR-E	REG	ND	TV	API	0.61
9	ASCAT AMSR-E	REG	ND	TV	NOAH	0.75
10	ASCAT AMSR-E	REG	ND	TV	WASM	0.81
11	ASCAT AMSR-E	REG	SA	Constant	ASCAT	0.58
12	ASCAT AMSR-E	REG	SA	Constant	AMSR-E	0.69
13	ASCAT AMSR-E	REG	SA	Constant	API	0.65
14	ASCAT AMSR-E	REG	SA	Constant	NOAH	0.72
15	ASCAT AMSR-E	REG	SA	Constant	WASM	0.75
16	ASCAT AMSR-E	REG	SA	TV	ASCAT	0.58
17	ASCAT AMSR-E	REG	SA	TV	AMSR-E	0.66
18	ASCAT AMSR-E	REG	SA	TV	API	0.62
19	ASCAT AMSR-E	REG	SA	TV	NOAH	0.75
20	ASCAT AMSR-E	REG	SA	TV	WASM	0.83
21	ASCAT AMSR-E	REG	SD	Constant	ASCAT	0.59
22	ASCAT AMSR-E	REG	SD	Constant	AMSR-E	0.7
23	ASCAT AMSR-E	REG	SD	Constant	API	0.7
24	ASCAT AMSR-E	REG	SD	Constant	NOAH	0.78
25	ASCAT AMSR-E	REG	SD	Constant	WASM	0.78
26	ASCAT AMSR-E	REG	SD	TV	ASCAT	0.59
27	ASCAT AMSR-E	REG	SD	TV	AMSR-E	0.66
28	ASCAT AMSR-E	REG	SD	TV	API	0.63
29	ASCAT AMSR-E	REG	SD	TV	NOAH	0.76
30	ASCAT AMSR-E	REG	SD	TV	WASM	0.84
31	ASCAT AMSR-E	VAR	ND	Constant	ASCAT	0.72
32	ASCAT AMSR-E	VAR	ND	Constant	AMSR-E	0.72
33	ASCAT AMSR-E	VAR	ND	Constant	API	0.72
34	ASCAT AMSR-E	VAR	ND	Constant	NOAH	0.72
35	ASCAT AMSR-E	VAR	ND	Constant	WASM	0.72
36	ASCAT AMSR-E	VAR	ND	TV	ASCAT	0.61

ID	Parent Couples	Rescaling Method	Rescaling Technique	Application Style	Reference	Cor (WASM)
37	ASCAT AMSR-E	VAR	ND	TV	AMSR-E	0.67
38	ASCAT AMSR-E	VAR	ND	TV	API	0.63
39	ASCAT AMSR-E	VAR	ND	TV	NOAH	0.74
40	ASCAT AMSR-E	VAR	ND	TV	WASM	0.79
41	ASCAT AMSR-E	VAR	SA	Constant	ASCAT	0.7
42	ASCAT AMSR-E	VAR	SA	Constant	AMSR-E	0.71
43	ASCAT AMSR-E	VAR	SA	Constant	API	0.69
44	ASCAT AMSR-E	VAR	SA	Constant	NOAH	0.71
45	ASCAT AMSR-E	VAR	SA	Constant	WASM	0.72
46	ASCAT AMSR-E	VAR	SA	TV	ASCAT	0.6
47	ASCAT AMSR-E	VAR	SA	TV	AMSR-E	0.68
48	ASCAT AMSR-E	VAR	SA	TV	API	0.64
49	ASCAT AMSR-E	VAR	SA	TV	NOAH	0.74
50	ASCAT AMSR-E	VAR	SA	TV	WASM	0.8
51	ASCAT AMSR-E	VAR	SD	Constant	ASCAT	0.7
52	ASCAT AMSR-E	VAR	SD	Constant	AMSR-E	0.73
53	ASCAT AMSR-E	VAR	SD	Constant	API	0.73
54	ASCAT AMSR-E	VAR	SD	Constant	NOAH	0.76
55	ASCAT AMSR-E	VAR	SD	Constant	WASM	0.75
56	ASCAT AMSR-E	VAR	SD	TV	ASCAT	0.6
57	ASCAT AMSR-E	VAR	SD	TV	AMSR-E	0.68
58	ASCAT AMSR-E	VAR	SD	TV	API	0.65
59	ASCAT AMSR-E	VAR	SD	TV	NOAH	0.76
60	ASCAT AMSR-E	VAR	SD	TV	WASM	0.82
61	ASCAT AMSR-E	CDFM	ND	Constant	ASCAT	0.7
62	ASCAT AMSR-E	CDFM	ND	Constant	AMSR-E	0.59
63	ASCAT AMSR-E	CDFM	ND	Constant	API	0.68
64	ASCAT AMSR-E	CDFM	ND	Constant	NOAH	0.7
65	ASCAT AMSR-E	CDFM	ND	Constant	WASM	0.69
66	ASCAT AMSR-E	CDFM	ND	TV	ASCAT	0.56
67	ASCAT AMSR-E	CDFM	ND	TV	AMSR-E	0.64
68	ASCAT AMSR-E	CDFM	ND	TV	API	0.54
69	ASCAT AMSR-E	CDFM	ND	TV	NOAH	0.72
70	ASCAT AMSR-E	CDFM	ND	TV	WASM	0.77
71	ASCAT AMSR-E	CDFM	SA	Constant	ASCAT	0.71
72	ASCAT AMSR-E	CDFM	SA	Constant	AMSR-E	0.63
73	ASCAT AMSR-E	CDFM	SA	Constant	API	0.66
74	ASCAT AMSR-E	CDFM	SA	Constant	NOAH	0.69
75	ASCAT AMSR-E	CDFM	SA	Constant	WASM	0.7

ID	Parent Couples	Rescaling Method	Rescaling Technique	Application Style	Reference	Cor (WASM)
76	ASCAT AMSR-E	CDFM	SA	TV	ASCAT	0.57
77	ASCAT AMSR-E	CDFM	SA	TV	AMSR-E	0.65
78	ASCAT AMSR-E	CDFM	SA	TV	API	0.56
79	ASCAT AMSR-E	CDFM	SA	TV	NOAH	0.73
80	ASCAT AMSR-E	CDFM	SA	TV	WASM	0.79
81	ASCAT AMSR-E	CDFM	SD	Constant	ASCAT	0.72
82	ASCAT AMSR-E	CDFM	SD	Constant	AMSR-E	0.67
83	ASCAT AMSR-E	CDFM	SD	Constant	API	0.69
84	ASCAT AMSR-E	CDFM	SD	Constant	NOAH	0.74
85	ASCAT AMSR-E	CDFM	SD	Constant	WASM	0.74
86	ASCAT AMSR-E	CDFM	SD	TV	ASCAT	0.59
87	ASCAT AMSR-E	CDFM	SD	TV	AMSR-E	0.65
88	ASCAT AMSR-E	CDFM	SD	TV	API	0.62
89	ASCAT AMSR-E	CDFM	SD	TV	NOAH	0.75
90	ASCAT AMSR-E	CDFM	SD	TV	WASM	0.83
91	ASCAT AMSR-E	MAR	ND	Constant	ASCAT	0.59
92	ASCAT AMSR-E	MAR	ND	Constant	AMSR-E	0.7
93	ASCAT AMSR-E	MAR	ND	Constant	API	0.68
94	ASCAT AMSR-E	MAR	ND	Constant	NOAH	0.75
95	ASCAT AMSR-E	MAR	ND	Constant	WASM	0.76
96	ASCAT AMSR-E	MAR	ND	TV	ASCAT	0.58
97	ASCAT AMSR-E	MAR	ND	TV	AMSR-E	0.66
98	ASCAT AMSR-E	MAR	ND	TV	API	0.61
99	ASCAT AMSR-E	MAR	ND	TV	NOAH	0.75
100	ASCAT AMSR-E	MAR	ND	TV	WASM	0.84
101	ASCAT AMSR-E	MAR	SA	Constant	ASCAT	0.59
102	ASCAT AMSR-E	MAR	SA	Constant	AMSR-E	0.69
103	ASCAT AMSR-E	MAR	SA	Constant	API	0.65
104	ASCAT AMSR-E	MAR	SA	Constant	NOAH	0.75
105	ASCAT AMSR-E	MAR	SA	Constant	WASM	0.79
106	ASCAT AMSR-E	MAR	SA	TV	ASCAT	0.58
107	ASCAT AMSR-E	MAR	SA	TV	AMSR-E	0.66
108	ASCAT AMSR-E	MAR	SA	TV	API	0.61
109	ASCAT AMSR-E	MAR	SA	TV	NOAH	0.76
110	ASCAT AMSR-E	MAR	SA	TV	WASM	0.86
111	ASCAT AMSR-E	MAR	SD	Constant	ASCAT	0.59
112	ASCAT AMSR-E	MAR	SD	Constant	AMSR-E	0.68
113	ASCAT AMSR-E	MAR	SD	Constant	API	0.69
114	ASCAT AMSR-E	MAR	SD	Constant	NOAH	0.77

ID	Parent Couples	Rescaling Method	Rescaling Technique	Application Style	Reference	Cor (WASM)
115	ASCAT AMSR-E	MAR	SD	Constant	WASM	0.79
116	ASCAT AMSR-E	MAR	SD	TV	ASCAT	0.6
117	ASCAT AMSR-E	MAR	SD	TV	AMSR-E	0.67
118	ASCAT AMSR-E	MAR	SD	TV	API	0.62
119	ASCAT AMSR-E	MAR	SD	TV	NOAH	0.75
120	ASCAT AMSR-E	MAR	SD	TV	WASM	0.89
121	ASCAT AMSR-E	SVM	ND	Constant	ASCAT	0.56
122	ASCAT AMSR-E	SVM	ND	Constant	AMSR-E	0.7
123	ASCAT AMSR-E	SVM	ND	Constant	API	0.64
124	ASCAT AMSR-E	SVM	ND	Constant	NOAH	0.74
125	ASCAT AMSR-E	SVM	ND	Constant	WASM	0.75
126	ASCAT AMSR-E	SVM	ND	TV	ASCAT	0.57
127	ASCAT AMSR-E	SVM	ND	TV	AMSR-E	0.66
128	ASCAT AMSR-E	SVM	ND	TV	API	0.59
129	ASCAT AMSR-E	SVM	ND	TV	NOAH	0.74
130	ASCAT AMSR-E	SVM	ND	TV	WASM	0.84
131	ASCAT AMSR-E	SVM	SA	Constant	ASCAT	0.58
132	ASCAT AMSR-E	SVM	SA	Constant	AMSR-E	0.69
133	ASCAT AMSR-E	SVM	SA	Constant	API	0.64
134	ASCAT AMSR-E	SVM	SA	Constant	NOAH	0.74
135	ASCAT AMSR-E	SVM	SA	Constant	WASM	0.78
136	ASCAT AMSR-E	SVM	SA	TV	ASCAT	0.56
137	ASCAT AMSR-E	SVM	SA	TV	AMSR-E	0.66
138	ASCAT AMSR-E	SVM	SA	TV	API	0.6
139	ASCAT AMSR-E	SVM	SA	TV	NOAH	0.74
140	ASCAT AMSR-E	SVM	SA	TV	WASM	0.85
141	ASCAT AMSR-E	SVM	SD	Constant	ASCAT	0.57
142	ASCAT AMSR-E	SVM	SD	Constant	AMSR-E	0.67
143	ASCAT AMSR-E	SVM	SD	Constant	API	0.65
144	ASCAT AMSR-E	SVM	SD	Constant	NOAH	0.76
145	ASCAT AMSR-E	SVM	SD	Constant	WASM	0.78
146	ASCAT AMSR-E	SVM	SD	TV	ASCAT	0.58
147	ASCAT AMSR-E	SVM	SD	TV	AMSR-E	0.67
148	ASCAT AMSR-E	SVM	SD	TV	API	0.64
149	ASCAT AMSR-E	SVM	SD	TV	NOAH	0.76
150	ASCAT AMSR-E	SVM	SD	TV	WASM	0.87
151	ASCAT API	REG	ND	Constant	ASCAT	0.63
152	ASCAT API	REG	ND	Constant	AMSR-E	0.67
153	ASCAT API	REG	ND	Constant	API	0.64

ID	Parent Couples	Rescaling Method	Rescaling Technique	Application Style	Reference	Cor (WASM)
154	ASCAT API	REG	ND	Constant	NOAH	0.67
155	ASCAT API	REG	ND	Constant	WASM	0.67
156	ASCAT API	REG	ND	TV	ASCAT	0.58
157	ASCAT API	REG	ND	TV	AMSR-E	0.64
158	ASCAT API	REG	ND	TV	API	0.61
159	ASCAT API	REG	ND	TV	NOAH	0.75
160	ASCAT API	REG	ND	TV	WASM	0.83
161	ASCAT API	REG	SA	Constant	ASCAT	0.64
162	ASCAT API	REG	SA	Constant	AMSR-E	0.63
163	ASCAT API	REG	SA	Constant	API	0.63
164	ASCAT API	REG	SA	Constant	NOAH	0.71
165	ASCAT API	REG	SA	Constant	WASM	0.71
166	ASCAT API	REG	SA	TV	ASCAT	0.58
167	ASCAT API	REG	SA	TV	AMSR-E	0.64
168	ASCAT API	REG	SA	TV	API	0.61
169	ASCAT API	REG	SA	TV	NOAH	0.76
170	ASCAT API	REG	SA	TV	WASM	0.84
171	ASCAT API	REG	SD	Constant	ASCAT	0.63
172	ASCAT API	REG	SD	Constant	AMSR-E	0.68
173	ASCAT API	REG	SD	Constant	API	0.64
174	ASCAT API	REG	SD	Constant	NOAH	0.69
175	ASCAT API	REG	SD	Constant	WASM	0.69
176	ASCAT API	REG	SD	TV	ASCAT	0.58
177	ASCAT API	REG	SD	TV	AMSR-E	0.65
178	ASCAT API	REG	SD	TV	API	0.61
179	ASCAT API	REG	SD	TV	NOAH	0.76
180	ASCAT API	REG	SD	TV	WASM	0.85
181	ASCAT API	VAR	ND	Constant	ASCAT	0.65
182	ASCAT API	VAR	ND	Constant	AMSR-E	0.65
183	ASCAT API	VAR	ND	Constant	API	0.65
184	ASCAT API	VAR	ND	Constant	NOAH	0.65
185	ASCAT API	VAR	ND	Constant	WASM	0.65
186	ASCAT API	VAR	ND	TV	ASCAT	0.61
187	ASCAT API	VAR	ND	TV	AMSR-E	0.68
188	ASCAT API	VAR	ND	TV	API	0.61
189	ASCAT API	VAR	ND	TV	NOAH	0.76
190	ASCAT API	VAR	ND	TV	WASM	0.82
191	ASCAT API	VAR	SA	Constant	ASCAT	0.65
192	ASCAT API	VAR	SA	Constant	AMSR-E	0.58

ID	Parent Couples	Rescaling Method	Rescaling Technique	Application Style	Reference	Cor (WASM)
193	ASCAT API	VAR	SA	Constant	API	0.63
194	ASCAT API	VAR	SA	Constant	NOAH	0.67
195	ASCAT API	VAR	SA	Constant	WASM	0.65
196	ASCAT API	VAR	SA	TV	ASCAT	0.61
197	ASCAT API	VAR	SA	TV	AMSR-E	0.68
198	ASCAT API	VAR	SA	TV	API	0.61
199	ASCAT API	VAR	SA	TV	NOAH	0.76
200	ASCAT API	VAR	SA	TV	WASM	0.82
201	ASCAT API	VAR	SD	Constant	ASCAT	0.64
202	ASCAT API	VAR	SD	Constant	AMSR-E	0.64
203	ASCAT API	VAR	SD	Constant	API	0.64
204	ASCAT API	VAR	SD	Constant	NOAH	0.66
205	ASCAT API	VAR	SD	Constant	WASM	0.66
206	ASCAT API	VAR	SD	TV	ASCAT	0.6
207	ASCAT API	VAR	SD	TV	AMSR-E	0.68
208	ASCAT API	VAR	SD	TV	API	0.62
209	ASCAT API	VAR	SD	TV	NOAH	0.77
210	ASCAT API	VAR	SD	TV	WASM	0.83
211	ASCAT API	CDFM	ND	Constant	ASCAT	0.51
212	ASCAT API	CDFM	ND	Constant	AMSR-E	0.32
213	ASCAT API	CDFM	ND	Constant	API	0.63
214	ASCAT API	CDFM	ND	Constant	NOAH	0.64
215	ASCAT API	CDFM	ND	Constant	WASM	0.63
216	ASCAT API	CDFM	ND	TV	ASCAT	0.55
217	ASCAT API	CDFM	ND	TV	AMSR-E	0.64
218	ASCAT API	CDFM	ND	TV	API	0.6
219	ASCAT API	CDFM	ND	TV	NOAH	0.76
220	ASCAT API	CDFM	ND	TV	WASM	0.83
221	ASCAT API	CDFM	SA	Constant	ASCAT	0.51
222	ASCAT API	CDFM	SA	Constant	AMSR-E	0.33
223	ASCAT API	CDFM	SA	Constant	API	0.64
224	ASCAT API	CDFM	SA	Constant	NOAH	0.65
225	ASCAT API	CDFM	SA	Constant	WASM	0.63
226	ASCAT API	CDFM	SA	TV	ASCAT	0.55
227	ASCAT API	CDFM	SA	TV	AMSR-E	0.61
228	ASCAT API	CDFM	SA	TV	API	0.6
229	ASCAT API	CDFM	SA	TV	NOAH	0.76
230	ASCAT API	CDFM	SA	TV	WASM	0.84
231	ASCAT API	CDFM	SD	Constant	ASCAT	0.55

ID	Parent Couples	Rescaling Method	Rescaling Technique	Application Style	Reference	Cor (WASM)
232	ASCAT API	CDFM	SD	Constant	AMSR-E	0.39
233	ASCAT API	CDFM	SD	Constant	API	0.63
234	ASCAT API	CDFM	SD	Constant	NOAH	0.65
235	ASCAT API	CDFM	SD	Constant	WASM	0.64
236	ASCAT API	CDFM	SD	TV	ASCAT	0.55
237	ASCAT API	CDFM	SD	TV	AMSR-E	0.64
238	ASCAT API	CDFM	SD	TV	API	0.61
239	ASCAT API	CDFM	SD	TV	NOAH	0.76
240	ASCAT API	CDFM	SD	TV	WASM	0.85
241	ASCAT API	MAR	ND	Constant	ASCAT	0.63
242	ASCAT API	MAR	ND	Constant	AMSR-E	0.66
243	ASCAT API	MAR	ND	Constant	API	0.64
244	ASCAT API	MAR	ND	Constant	NOAH	0.7
245	ASCAT API	MAR	ND	Constant	WASM	0.71
246	ASCAT API	MAR	ND	TV	ASCAT	0.58
247	ASCAT API	MAR	ND	TV	AMSR-E	0.65
248	ASCAT API	MAR	ND	TV	API	0.61
249	ASCAT API	MAR	ND	TV	NOAH	0.76
250	ASCAT API	MAR	ND	TV	WASM	0.86
251	ASCAT API	MAR	SA	Constant	ASCAT	0.61
252	ASCAT API	MAR	SA	Constant	AMSR-E	0.65
253	ASCAT API	MAR	SA	Constant	API	0.63
254	ASCAT API	MAR	SA	Constant	NOAH	0.76
255	ASCAT API	MAR	SA	Constant	WASM	0.78
256	ASCAT API	MAR	SA	TV	ASCAT	0.58
257	ASCAT API	MAR	SA	TV	AMSR-E	0.65
258	ASCAT API	MAR	SA	TV	API	0.61
259	ASCAT API	MAR	SA	TV	NOAH	0.77
260	ASCAT API	MAR	SA	TV	WASM	0.87
261	ASCAT API	MAR	SD	Constant	ASCAT	0.63
262	ASCAT API	MAR	SD	Constant	AMSR-E	0.65
263	ASCAT API	MAR	SD	Constant	API	0.64
264	ASCAT API	MAR	SD	Constant	NOAH	0.71
265	ASCAT API	MAR	SD	Constant	WASM	0.74
266	ASCAT API	MAR	SD	TV	ASCAT	0.58
267	ASCAT API	MAR	SD	TV	AMSR-E	0.66
268	ASCAT API	MAR	SD	TV	API	0.61
269	ASCAT API	MAR	SD	TV	NOAH	0.76
270	ASCAT API	MAR	SD	TV	WASM	0.89

ID	Parent Couples	Rescaling Method	Rescaling Technique	Application Style	Reference	Cor (WASM)
271	ASCAT API	SVM	ND	Constant	ASCAT	0.62
272	ASCAT API	SVM	ND	Constant	AMSR-E	0.64
273	ASCAT API	SVM	ND	Constant	API	0.64
274	ASCAT API	SVM	ND	Constant	NOAH	0.69
275	ASCAT API	SVM	ND	Constant	WASM	0.71
276	ASCAT API	SVM	ND	TV	ASCAT	0.56
277	ASCAT API	SVM	ND	TV	AMSR-E	0.65
278	ASCAT API	SVM	ND	TV	API	0.59
279	ASCAT API	SVM	ND	TV	NOAH	0.75
280	ASCAT API	SVM	ND	TV	WASM	0.86
281	ASCAT API	SVM	SA	Constant	ASCAT	0.61
282	ASCAT API	SVM	SA	Constant	AMSR-E	0.64
283	ASCAT API	SVM	SA	Constant	API	0.63
284	ASCAT API	SVM	SA	Constant	NOAH	0.76
285	ASCAT API	SVM	SA	Constant	WASM	0.78
286	ASCAT API	SVM	SA	TV	ASCAT	0.55
287	ASCAT API	SVM	SA	TV	AMSR-E	0.65
288	ASCAT API	SVM	SA	TV	API	0.6
289	ASCAT API	SVM	SA	TV	NOAH	0.75
290	ASCAT API	SVM	SA	TV	WASM	0.87
291	ASCAT API	SVM	SD	Constant	ASCAT	0.62
292	ASCAT API	SVM	SD	Constant	AMSR-E	0.62
293	ASCAT API	SVM	SD	Constant	API	0.64
294	ASCAT API	SVM	SD	Constant	NOAH	0.7
295	ASCAT API	SVM	SD	Constant	WASM	0.74
296	ASCAT API	SVM	SD	TV	ASCAT	0.57
297	ASCAT API	SVM	SD	TV	AMSR-E	0.66
298	ASCAT API	SVM	SD	TV	API	0.61
299	ASCAT API	SVM	SD	TV	NOAH	0.75
300	ASCAT API	SVM	SD	TV	WASM	0.88
301	ASCAT NOAH	REG	ND	Constant	ASCAT	0.64
302	ASCAT NOAH	REG	ND	Constant	AMSR-E	0.74
303	ASCAT NOAH	REG	ND	Constant	API	0.72
304	ASCAT NOAH	REG	ND	Constant	NOAH	0.74
305	ASCAT NOAH	REG	ND	Constant	WASM	0.74
306	ASCAT NOAH	REG	ND	TV	ASCAT	0.57
307	ASCAT NOAH	REG	ND	TV	AMSR-E	0.65
308	ASCAT NOAH	REG	ND	TV	API	0.58
309	ASCAT NOAH	REG	ND	TV	NOAH	0.75

ID	Parent Couples	Rescaling Method	Rescaling Technique	Application Style	Reference	Cor (WASM)
310	ASCAT NOAH	REG	ND	TV	WASM	0.83
311	ASCAT NOAH	REG	SA	Constant	ASCAT	0.6
312	ASCAT NOAH	REG	SA	Constant	AMSR-E	0.73
313	ASCAT NOAH	REG	SA	Constant	API	0.68
314	ASCAT NOAH	REG	SA	Constant	NOAH	0.74
315	ASCAT NOAH	REG	SA	Constant	WASM	0.77
316	ASCAT NOAH	REG	SA	TV	ASCAT	0.57
317	ASCAT NOAH	REG	SA	TV	AMSR-E	0.65
318	ASCAT NOAH	REG	SA	TV	API	0.58
319	ASCAT NOAH	REG	SA	TV	NOAH	0.75
320	ASCAT NOAH	REG	SA	TV	WASM	0.84
321	ASCAT NOAH	REG	SD	Constant	ASCAT	0.63
322	ASCAT NOAH	REG	SD	Constant	AMSR-E	0.73
323	ASCAT NOAH	REG	SD	Constant	API	0.72
324	ASCAT NOAH	REG	SD	Constant	NOAH	0.75
325	ASCAT NOAH	REG	SD	Constant	WASM	0.75
326	ASCAT NOAH	REG	SD	TV	ASCAT	0.57
327	ASCAT NOAH	REG	SD	TV	AMSR-E	0.65
328	ASCAT NOAH	REG	SD	TV	API	0.59
329	ASCAT NOAH	REG	SD	TV	NOAH	0.75
330	ASCAT NOAH	REG	SD	TV	WASM	0.84
331	ASCAT NOAH	VAR	ND	Constant	ASCAT	0.72
332	ASCAT NOAH	VAR	ND	Constant	AMSR-E	0.72
333	ASCAT NOAH	VAR	ND	Constant	API	0.72
334	ASCAT NOAH	VAR	ND	Constant	NOAH	0.72
335	ASCAT NOAH	VAR	ND	Constant	WASM	0.72
336	ASCAT NOAH	VAR	ND	TV	ASCAT	0.6
337	ASCAT NOAH	VAR	ND	TV	AMSR-E	0.68
338	ASCAT NOAH	VAR	ND	TV	API	0.6
339	ASCAT NOAH	VAR	ND	TV	NOAH	0.75
340	ASCAT NOAH	VAR	ND	TV	WASM	0.81
341	ASCAT NOAH	VAR	SA	Constant	ASCAT	0.72
342	ASCAT NOAH	VAR	SA	Constant	AMSR-E	0.71
343	ASCAT NOAH	VAR	SA	Constant	API	0.69
344	ASCAT NOAH	VAR	SA	Constant	NOAH	0.73
345	ASCAT NOAH	VAR	SA	Constant	WASM	0.73
346	ASCAT NOAH	VAR	SA	TV	ASCAT	0.6
347	ASCAT NOAH	VAR	SA	TV	AMSR-E	0.69
348	ASCAT NOAH	VAR	SA	TV	API	0.6

ID	Parent Couples	Rescaling Method	Rescaling Technique	Application Style	Reference	Cor (WASM)
349	ASCAT NOAH	VAR	SA	TV	NOAH	0.75
350	ASCAT NOAH	VAR	SA	TV	WASM	0.82
351	ASCAT NOAH	VAR	SD	Constant	ASCAT	0.7
352	ASCAT NOAH	VAR	SD	Constant	AMSR-E	0.71
353	ASCAT NOAH	VAR	SD	Constant	API	0.71
354	ASCAT NOAH	VAR	SD	Constant	NOAH	0.73
355	ASCAT NOAH	VAR	SD	Constant	WASM	0.72
356	ASCAT NOAH	VAR	SD	TV	ASCAT	0.59
357	ASCAT NOAH	VAR	SD	TV	AMSR-E	0.68
358	ASCAT NOAH	VAR	SD	TV	API	0.6
359	ASCAT NOAH	VAR	SD	TV	NOAH	0.75
360	ASCAT NOAH	VAR	SD	TV	WASM	0.83
361	ASCAT NOAH	CDFM	ND	Constant	ASCAT	0.62
362	ASCAT NOAH	CDFM	ND	Constant	AMSR-E	0.46
363	ASCAT NOAH	CDFM	ND	Constant	API	0.69
364	ASCAT NOAH	CDFM	ND	Constant	NOAH	0.72
365	ASCAT NOAH	CDFM	ND	Constant	WASM	0.72
366	ASCAT NOAH	CDFM	ND	TV	ASCAT	0.53
367	ASCAT NOAH	CDFM	ND	TV	AMSR-E	0.6
368	ASCAT NOAH	CDFM	ND	TV	API	0.56
369	ASCAT NOAH	CDFM	ND	TV	NOAH	0.73
370	ASCAT NOAH	CDFM	ND	TV	WASM	0.82
371	ASCAT NOAH	CDFM	SA	Constant	ASCAT	0.64
372	ASCAT NOAH	CDFM	SA	Constant	AMSR-E	0.51
373	ASCAT NOAH	CDFM	SA	Constant	API	0.65
374	ASCAT NOAH	CDFM	SA	Constant	NOAH	0.71
375	ASCAT NOAH	CDFM	SA	Constant	WASM	0.71
376	ASCAT NOAH	CDFM	SA	TV	ASCAT	0.53
377	ASCAT NOAH	CDFM	SA	TV	AMSR-E	0.61
378	ASCAT NOAH	CDFM	SA	TV	API	0.57
379	ASCAT NOAH	CDFM	SA	TV	NOAH	0.74
380	ASCAT NOAH	CDFM	SA	TV	WASM	0.82
381	ASCAT NOAH	CDFM	SD	Constant	ASCAT	0.66
382	ASCAT NOAH	CDFM	SD	Constant	AMSR-E	0.56
383	ASCAT NOAH	CDFM	SD	Constant	API	0.68
384	ASCAT NOAH	CDFM	SD	Constant	NOAH	0.72
385	ASCAT NOAH	CDFM	SD	Constant	WASM	0.72
386	ASCAT NOAH	CDFM	SD	TV	ASCAT	0.55
387	ASCAT NOAH	CDFM	SD	TV	AMSR-E	0.65

ID	Parent Couples	Rescaling Method	Rescaling Technique	Application Style	Reference	Cor (WASM)
388	ASCAT NOAH	CDFM	SD	TV	API	0.6
389	ASCAT NOAH	CDFM	SD	TV	NOAH	0.74
390	ASCAT NOAH	CDFM	SD	TV	WASM	0.84
391	ASCAT NOAH	MAR	ND	Constant	ASCAT	0.62
392	ASCAT NOAH	MAR	ND	Constant	AMSR-E	0.71
393	ASCAT NOAH	MAR	ND	Constant	API	0.7
394	ASCAT NOAH	MAR	ND	Constant	NOAH	0.74
395	ASCAT NOAH	MAR	ND	Constant	WASM	0.76
396	ASCAT NOAH	MAR	ND	TV	ASCAT	0.57
397	ASCAT NOAH	MAR	ND	TV	AMSR-E	0.65
398	ASCAT NOAH	MAR	ND	TV	API	0.59
399	ASCAT NOAH	MAR	ND	TV	NOAH	0.74
400	ASCAT NOAH	MAR	ND	TV	WASM	0.86
401	ASCAT NOAH	MAR	SA	Constant	ASCAT	0.57
402	ASCAT NOAH	MAR	SA	Constant	AMSR-E	0.7
403	ASCAT NOAH	MAR	SA	Constant	API	0.63
404	ASCAT NOAH	MAR	SA	Constant	NOAH	0.75
405	ASCAT NOAH	MAR	SA	Constant	WASM	0.8
406	ASCAT NOAH	MAR	SA	TV	ASCAT	0.56
407	ASCAT NOAH	MAR	SA	TV	AMSR-E	0.65
408	ASCAT NOAH	MAR	SA	TV	API	0.59
409	ASCAT NOAH	MAR	SA	TV	NOAH	0.75
410	ASCAT NOAH	MAR	SA	TV	WASM	0.87
411	ASCAT NOAH	MAR	SD	Constant	ASCAT	0.62
412	ASCAT NOAH	MAR	SD	Constant	AMSR-E	0.69
413	ASCAT NOAH	MAR	SD	Constant	API	0.71
414	ASCAT NOAH	MAR	SD	Constant	NOAH	0.74
415	ASCAT NOAH	MAR	SD	Constant	WASM	0.78
416	ASCAT NOAH	MAR	SD	TV	ASCAT	0.57
417	ASCAT NOAH	MAR	SD	TV	AMSR-E	0.66
418	ASCAT NOAH	MAR	SD	TV	API	0.61
419	ASCAT NOAH	MAR	SD	TV	NOAH	0.74
420	ASCAT NOAH	MAR	SD	TV	WASM	0.89
421	ASCAT NOAH	SVM	ND	Constant	ASCAT	0.62
422	ASCAT NOAH	SVM	ND	Constant	AMSR-E	0.71
423	ASCAT NOAH	SVM	ND	Constant	API	0.7
424	ASCAT NOAH	SVM	ND	Constant	NOAH	0.74
425	ASCAT NOAH	SVM	ND	Constant	WASM	0.75
426	ASCAT NOAH	SVM	ND	TV	ASCAT	0.55

ID	Parent Couples	Rescaling Method	Rescaling Technique	Application Style	Reference	Cor (WASM)
427	ASCAT NOAH	SVM	ND	TV	AMSR-E	0.66
428	ASCAT NOAH	SVM	ND	TV	API	0.55
429	ASCAT NOAH	SVM	ND	TV	NOAH	0.74
430	ASCAT NOAH	SVM	ND	TV	WASM	0.85
431	ASCAT NOAH	SVM	SA	Constant	ASCAT	0.54
432	ASCAT NOAH	SVM	SA	Constant	AMSR-E	0.68
433	ASCAT NOAH	SVM	SA	Constant	API	0.62
434	ASCAT NOAH	SVM	SA	Constant	NOAH	0.75
435	ASCAT NOAH	SVM	SA	Constant	WASM	0.79
436	ASCAT NOAH	SVM	SA	TV	ASCAT	0.55
437	ASCAT NOAH	SVM	SA	TV	AMSR-E	0.65
438	ASCAT NOAH	SVM	SA	TV	API	0.55
439	ASCAT NOAH	SVM	SA	TV	NOAH	0.74
440	ASCAT NOAH	SVM	SA	TV	WASM	0.86
441	ASCAT NOAH	SVM	SD	Constant	ASCAT	0.61
442	ASCAT NOAH	SVM	SD	Constant	AMSR-E	0.67
443	ASCAT NOAH	SVM	SD	Constant	API	0.7
444	ASCAT NOAH	SVM	SD	Constant	NOAH	0.74
445	ASCAT NOAH	SVM	SD	Constant	WASM	0.77
446	ASCAT NOAH	SVM	SD	TV	ASCAT	0.56
447	ASCAT NOAH	SVM	SD	TV	AMSR-E	0.66
448	ASCAT NOAH	SVM	SD	TV	API	0.58
449	ASCAT NOAH	SVM	SD	TV	NOAH	0.74
450	ASCAT NOAH	SVM	SD	TV	WASM	0.88
451	AMSR-E API	REG	ND	Constant	ASCAT	0.75
452	AMSR-E API	REG	ND	Constant	AMSR-E	0.72
453	AMSR-E API	REG	ND	Constant	API	0.71
454	AMSR-E API	REG	ND	Constant	NOAH	0.79
455	AMSR-E API	REG	ND	Constant	WASM	0.79
456	AMSR-E API	REG	ND	TV	ASCAT	0.6
457	AMSR-E API	REG	ND	TV	AMSR-E	0.67
458	AMSR-E API	REG	ND	TV	API	0.66
459	AMSR-E API	REG	ND	TV	NOAH	0.77
460	AMSR-E API	REG	ND	TV	WASM	0.85
461	AMSR-E API	REG	SA	Constant	ASCAT	0.68
462	AMSR-E API	REG	SA	Constant	AMSR-E	0.7
463	AMSR-E API	REG	SA	Constant	API	0.68
464	AMSR-E API	REG	SA	Constant	NOAH	0.77
465	AMSR-E API	REG	SA	Constant	WASM	0.79

ID	Parent Couples	Rescaling Method	Rescaling Technique	Application Style	Reference	Cor (WASM)
466	AMSR-E API	REG	SA	TV	ASCAT	0.59
467	AMSR-E API	REG	SA	TV	AMSR-E	0.67
468	AMSR-E API	REG	SA	TV	API	0.66
469	AMSR-E API	REG	SA	TV	NOAH	0.77
470	AMSR-E API	REG	SA	TV	WASM	0.86
471	AMSR-E API	REG	SD	Constant	ASCAT	0.71
472	AMSR-E API	REG	SD	Constant	AMSR-E	0.72
473	AMSR-E API	REG	SD	Constant	API	0.7
474	AMSR-E API	REG	SD	Constant	NOAH	0.82
475	AMSR-E API	REG	SD	Constant	WASM	0.82
476	AMSR-E API	REG	SD	TV	ASCAT	0.6
477	AMSR-E API	REG	SD	TV	AMSR-E	0.67
478	AMSR-E API	REG	SD	TV	API	0.66
479	AMSR-E API	REG	SD	TV	NOAH	0.78
480	AMSR-E API	REG	SD	TV	WASM	0.86
481	AMSR-E API	VAR	ND	Constant	ASCAT	0.79
482	AMSR-E API	VAR	ND	Constant	AMSR-E	0.79
483	AMSR-E API	VAR	ND	Constant	API	0.79
484	AMSR-E API	VAR	ND	Constant	NOAH	0.79
485	AMSR-E API	VAR	ND	Constant	WASM	0.79
486	AMSR-E API	VAR	ND	TV	ASCAT	0.65
487	AMSR-E API	VAR	ND	TV	AMSR-E	0.71
488	AMSR-E API	VAR	ND	TV	API	0.67
489	AMSR-E API	VAR	ND	TV	NOAH	0.78
490	AMSR-E API	VAR	ND	TV	WASM	0.84
491	AMSR-E API	VAR	SA	Constant	ASCAT	0.77
492	AMSR-E API	VAR	SA	Constant	AMSR-E	0.77
493	AMSR-E API	VAR	SA	Constant	API	0.74
494	AMSR-E API	VAR	SA	Constant	NOAH	0.77
495	AMSR-E API	VAR	SA	Constant	WASM	0.77
496	AMSR-E API	VAR	SA	TV	ASCAT	0.64
497	AMSR-E API	VAR	SA	TV	AMSR-E	0.7
498	AMSR-E API	VAR	SA	TV	API	0.67
499	AMSR-E API	VAR	SA	TV	NOAH	0.78
500	AMSR-E API	VAR	SA	TV	WASM	0.84
501	AMSR-E API	VAR	SD	Constant	ASCAT	0.77
502	AMSR-E API	VAR	SD	Constant	AMSR-E	0.79
503	AMSR-E API	VAR	SD	Constant	API	0.78
504	AMSR-E API	VAR	SD	Constant	NOAH	0.81

ID	Parent Couples	Rescaling Method	Rescaling Technique	Application Style	Reference	Cor (WASM)
505	AMSR-E API	VAR	SD	Constant	WASM	0.8
506	AMSR-E API	VAR	SD	TV	ASCAT	0.63
507	AMSR-E API	VAR	SD	TV	AMSR-E	0.7
508	AMSR-E API	VAR	SD	TV	API	0.68
509	AMSR-E API	VAR	SD	TV	NOAH	0.79
510	AMSR-E API	VAR	SD	TV	WASM	0.85
511	AMSR-E API	CDFM	ND	Constant	ASCAT	0.67
512	AMSR-E API	CDFM	ND	Constant	AMSR-E	0.68
513	AMSR-E API	CDFM	ND	Constant	API	0.7
514	AMSR-E API	CDFM	ND	Constant	NOAH	0.77
515	AMSR-E API	CDFM	ND	Constant	WASM	0.76
516	AMSR-E API	CDFM	ND	TV	ASCAT	0.55
517	AMSR-E API	CDFM	ND	TV	AMSR-E	0.69
518	AMSR-E API	CDFM	ND	TV	API	0.63
519	AMSR-E API	CDFM	ND	TV	NOAH	0.78
520	AMSR-E API	CDFM	ND	TV	WASM	0.85
521	AMSR-E API	CDFM	SA	Constant	ASCAT	0.67
522	AMSR-E API	CDFM	SA	Constant	AMSR-E	0.67
523	AMSR-E API	CDFM	SA	Constant	API	0.73
524	AMSR-E API	CDFM	SA	Constant	NOAH	0.75
525	AMSR-E API	CDFM	SA	Constant	WASM	0.76
526	AMSR-E API	CDFM	SA	TV	ASCAT	0.56
527	AMSR-E API	CDFM	SA	TV	AMSR-E	0.68
528	AMSR-E API	CDFM	SA	TV	API	0.64
529	AMSR-E API	CDFM	SA	TV	NOAH	0.78
530	AMSR-E API	CDFM	SA	TV	WASM	0.85
531	AMSR-E API	CDFM	SD	Constant	ASCAT	0.74
532	AMSR-E API	CDFM	SD	Constant	AMSR-E	0.75
533	AMSR-E API	CDFM	SD	Constant	API	0.77
534	AMSR-E API	CDFM	SD	Constant	NOAH	0.8
535	AMSR-E API	CDFM	SD	Constant	WASM	0.8
536	AMSR-E API	CDFM	SD	TV	ASCAT	0.58
537	AMSR-E API	CDFM	SD	TV	AMSR-E	0.71
538	AMSR-E API	CDFM	SD	TV	API	0.65
539	AMSR-E API	CDFM	SD	TV	NOAH	0.78
540	AMSR-E API	CDFM	SD	TV	WASM	0.87
541	AMSR-E API	MAR	ND	Constant	ASCAT	0.69
542	AMSR-E API	MAR	ND	Constant	AMSR-E	0.72
543	AMSR-E API	MAR	ND	Constant	API	0.71

ID	Parent Couples	Rescaling Method	Rescaling Technique	Application Style	Reference	Cor (WASM)
544	AMSR-E API	MAR	ND	Constant	NOAH	0.8
545	AMSR-E API	MAR	ND	Constant	WASM	0.82
546	AMSR-E API	MAR	ND	TV	ASCAT	0.6
547	AMSR-E API	MAR	ND	TV	AMSR-E	0.67
548	AMSR-E API	MAR	ND	TV	API	0.63
549	AMSR-E API	MAR	ND	TV	NOAH	0.78
550	AMSR-E API	MAR	ND	TV	WASM	0.88
551	AMSR-E API	MAR	SA	Constant	ASCAT	0.63
552	AMSR-E API	MAR	SA	Constant	AMSR-E	0.67
553	AMSR-E API	MAR	SA	Constant	API	0.68
554	AMSR-E API	MAR	SA	Constant	NOAH	0.77
555	AMSR-E API	MAR	SA	Constant	WASM	0.81
556	AMSR-E API	MAR	SA	TV	ASCAT	0.59
557	AMSR-E API	MAR	SA	TV	AMSR-E	0.67
558	AMSR-E API	MAR	SA	TV	API	0.62
559	AMSR-E API	MAR	SA	TV	NOAH	0.77
560	AMSR-E API	MAR	SA	TV	WASM	0.89
561	AMSR-E API	MAR	SD	Constant	ASCAT	0.69
562	AMSR-E API	MAR	SD	Constant	AMSR-E	0.71
563	AMSR-E API	MAR	SD	Constant	API	0.69
564	AMSR-E API	MAR	SD	Constant	NOAH	0.8
565	AMSR-E API	MAR	SD	Constant	WASM	0.83
566	AMSR-E API	MAR	SD	TV	ASCAT	0.62
567	AMSR-E API	MAR	SD	TV	AMSR-E	0.68
568	AMSR-E API	MAR	SD	TV	API	0.62
569	AMSR-E API	MAR	SD	TV	NOAH	0.77
570	AMSR-E API	MAR	SD	TV	WASM	0.9
571	AMSR-E API	SVM	ND	Constant	ASCAT	0.65
572	AMSR-E API	SVM	ND	Constant	AMSR-E	0.72
573	AMSR-E API	SVM	ND	Constant	API	0.69
574	AMSR-E API	SVM	ND	Constant	NOAH	0.79
575	AMSR-E API	SVM	ND	Constant	WASM	0.82
576	AMSR-E API	SVM	ND	TV	ASCAT	0.57
577	AMSR-E API	SVM	ND	TV	AMSR-E	0.68
578	AMSR-E API	SVM	ND	TV	API	0.65
579	AMSR-E API	SVM	ND	TV	NOAH	0.77
580	AMSR-E API	SVM	ND	TV	WASM	0.88
581	AMSR-E API	SVM	SA	Constant	ASCAT	0.61
582	AMSR-E API	SVM	SA	Constant	AMSR-E	0.66

ID	Parent Couples	Rescaling Method	Rescaling Technique	Application Style	Reference	Cor (WASM)
583	AMSR-E API	SVM	SA	Constant	API	0.67
584	AMSR-E API	SVM	SA	Constant	NOAH	0.77
585	AMSR-E API	SVM	SA	Constant	WASM	0.8
586	AMSR-E API	SVM	SA	TV	ASCAT	0.56
587	AMSR-E API	SVM	SA	TV	AMSR-E	0.68
588	AMSR-E API	SVM	SA	TV	API	0.65
589	AMSR-E API	SVM	SA	TV	NOAH	0.76
590	AMSR-E API	SVM	SA	TV	WASM	0.88
591	AMSR-E API	SVM	SD	Constant	ASCAT	0.65
592	AMSR-E API	SVM	SD	Constant	AMSR-E	0.7
593	AMSR-E API	SVM	SD	Constant	API	0.68
594	AMSR-E API	SVM	SD	Constant	NOAH	0.8
595	AMSR-E API	SVM	SD	Constant	WASM	0.83
596	AMSR-E API	SVM	SD	TV	ASCAT	0.58
597	AMSR-E API	SVM	SD	TV	AMSR-E	0.68
598	AMSR-E API	SVM	SD	TV	API	0.66
599	AMSR-E API	SVM	SD	TV	NOAH	0.77
600	AMSR-E API	SVM	SD	TV	WASM	0.89
601	AMSR-E NOAH	REG	ND	Constant	ASCAT	0.75
602	AMSR-E NOAH	REG	ND	Constant	AMSR-E	0.74
603	AMSR-E NOAH	REG	ND	Constant	API	0.75
604	AMSR-E NOAH	REG	ND	Constant	NOAH	0.76
605	AMSR-E NOAH	REG	ND	Constant	WASM	0.76
606	AMSR-E NOAH	REG	ND	TV	ASCAT	0.58
607	AMSR-E NOAH	REG	ND	TV	AMSR-E	0.68
608	AMSR-E NOAH	REG	ND	TV	API	0.61
609	AMSR-E NOAH	REG	ND	TV	NOAH	0.75
610	AMSR-E NOAH	REG	ND	TV	WASM	0.83
611	AMSR-E NOAH	REG	SA	Constant	ASCAT	0.57
612	AMSR-E NOAH	REG	SA	Constant	AMSR-E	0.72
613	AMSR-E NOAH	REG	SA	Constant	API	0.66
614	AMSR-E NOAH	REG	SA	Constant	NOAH	0.75
615	AMSR-E NOAH	REG	SA	Constant	WASM	0.76
616	AMSR-E NOAH	REG	SA	TV	ASCAT	0.57
617	AMSR-E NOAH	REG	SA	TV	AMSR-E	0.68
618	AMSR-E NOAH	REG	SA	TV	API	0.62
619	AMSR-E NOAH	REG	SA	TV	NOAH	0.75
620	AMSR-E NOAH	REG	SA	TV	WASM	0.84
621	AMSR-E NOAH	REG	SD	Constant	ASCAT	0.65

ID	Parent Couples	Rescaling Method	Rescaling Technique	Application Style	Reference	Cor (WASM)
622	AMSR-E NOAH	REG	SD	Constant	AMSR-E	0.74
623	AMSR-E NOAH	REG	SD	Constant	API	0.75
624	AMSR-E NOAH	REG	SD	Constant	NOAH	0.76
625	AMSR-E NOAH	REG	SD	Constant	WASM	0.77
626	AMSR-E NOAH	REG	SD	TV	ASCAT	0.58
627	AMSR-E NOAH	REG	SD	TV	AMSR-E	0.67
628	AMSR-E NOAH	REG	SD	TV	API	0.62
629	AMSR-E NOAH	REG	SD	TV	NOAH	0.75
630	AMSR-E NOAH	REG	SD	TV	WASM	0.84
631	AMSR-E NOAH	VAR	ND	Constant	ASCAT	0.76
632	AMSR-E NOAH	VAR	ND	Constant	AMSR-E	0.76
633	AMSR-E NOAH	VAR	ND	Constant	API	0.76
634	AMSR-E NOAH	VAR	ND	Constant	NOAH	0.76
635	AMSR-E NOAH	VAR	ND	Constant	WASM	0.76
636	AMSR-E NOAH	VAR	ND	TV	ASCAT	0.63
637	AMSR-E NOAH	VAR	ND	TV	AMSR-E	0.7
638	AMSR-E NOAH	VAR	ND	TV	API	0.64
639	AMSR-E NOAH	VAR	ND	TV	NOAH	0.75
640	AMSR-E NOAH	VAR	ND	TV	WASM	0.82
641	AMSR-E NOAH	VAR	SA	Constant	ASCAT	0.75
642	AMSR-E NOAH	VAR	SA	Constant	AMSR-E	0.74
643	AMSR-E NOAH	VAR	SA	Constant	API	0.7
644	AMSR-E NOAH	VAR	SA	Constant	NOAH	0.75
645	AMSR-E NOAH	VAR	SA	Constant	WASM	0.76
646	AMSR-E NOAH	VAR	SA	TV	ASCAT	0.62
647	AMSR-E NOAH	VAR	SA	TV	AMSR-E	0.69
648	AMSR-E NOAH	VAR	SA	TV	API	0.64
649	AMSR-E NOAH	VAR	SA	TV	NOAH	0.75
650	AMSR-E NOAH	VAR	SA	TV	WASM	0.82
651	AMSR-E NOAH	VAR	SD	Constant	ASCAT	0.74
652	AMSR-E NOAH	VAR	SD	Constant	AMSR-E	0.75
653	AMSR-E NOAH	VAR	SD	Constant	API	0.75
654	AMSR-E NOAH	VAR	SD	Constant	NOAH	0.76
655	AMSR-E NOAH	VAR	SD	Constant	WASM	0.76
656	AMSR-E NOAH	VAR	SD	TV	ASCAT	0.61
657	AMSR-E NOAH	VAR	SD	TV	AMSR-E	0.69
658	AMSR-E NOAH	VAR	SD	TV	API	0.65
659	AMSR-E NOAH	VAR	SD	TV	NOAH	0.76
660	AMSR-E NOAH	VAR	SD	TV	WASM	0.83

ID	Parent Couples	Rescaling Method	Rescaling Technique	Application Style	Reference	Cor (WASM)
661	AMSR-E NOAH	CDFM	ND	Constant	ASCAT	0.66
662	AMSR-E NOAH	CDFM	ND	Constant	AMSR-E	0.65
663	AMSR-E NOAH	CDFM	ND	Constant	API	0.72
664	AMSR-E NOAH	CDFM	ND	Constant	NOAH	0.76
665	AMSR-E NOAH	CDFM	ND	Constant	WASM	0.76
666	AMSR-E NOAH	CDFM	ND	TV	ASCAT	0.52
667	AMSR-E NOAH	CDFM	ND	TV	AMSR-E	0.65
668	AMSR-E NOAH	CDFM	ND	TV	API	0.6
669	AMSR-E NOAH	CDFM	ND	TV	NOAH	0.75
670	AMSR-E NOAH	CDFM	ND	TV	WASM	0.82
671	AMSR-E NOAH	CDFM	SA	Constant	ASCAT	0.69
672	AMSR-E NOAH	CDFM	SA	Constant	AMSR-E	0.66
673	AMSR-E NOAH	CDFM	SA	Constant	API	0.66
674	AMSR-E NOAH	CDFM	SA	Constant	NOAH	0.74
675	AMSR-E NOAH	CDFM	SA	Constant	WASM	0.75
676	AMSR-E NOAH	CDFM	SA	TV	ASCAT	0.54
677	AMSR-E NOAH	CDFM	SA	TV	AMSR-E	0.65
678	AMSR-E NOAH	CDFM	SA	TV	API	0.6
679	AMSR-E NOAH	CDFM	SA	TV	NOAH	0.75
680	AMSR-E NOAH	CDFM	SA	TV	WASM	0.82
681	AMSR-E NOAH	CDFM	SD	Constant	ASCAT	0.72
682	AMSR-E NOAH	CDFM	SD	Constant	AMSR-E	0.72
683	AMSR-E NOAH	CDFM	SD	Constant	API	0.73
684	AMSR-E NOAH	CDFM	SD	Constant	NOAH	0.76
685	AMSR-E NOAH	CDFM	SD	Constant	WASM	0.77
686	AMSR-E NOAH	CDFM	SD	TV	ASCAT	0.58
687	AMSR-E NOAH	CDFM	SD	TV	AMSR-E	0.7
688	AMSR-E NOAH	CDFM	SD	TV	API	0.63
689	AMSR-E NOAH	CDFM	SD	TV	NOAH	0.75
690	AMSR-E NOAH	CDFM	SD	TV	WASM	0.85
691	AMSR-E NOAH	MAR	ND	Constant	ASCAT	0.64
692	AMSR-E NOAH	MAR	ND	Constant	AMSR-E	0.71
693	AMSR-E NOAH	MAR	ND	Constant	API	0.74
694	AMSR-E NOAH	MAR	ND	Constant	NOAH	0.76
695	AMSR-E NOAH	MAR	ND	Constant	WASM	0.78
696	AMSR-E NOAH	MAR	ND	TV	ASCAT	0.58
697	AMSR-E NOAH	MAR	ND	TV	AMSR-E	0.67
698	AMSR-E NOAH	MAR	ND	TV	API	0.62
699	AMSR-E NOAH	MAR	ND	TV	NOAH	0.75

ID	Parent Couples	Rescaling Method	Rescaling Technique	Application Style	Reference	Cor (WASM)
700	AMSR-E NOAH	MAR	ND	TV	WASM	0.87
701	AMSR-E NOAH	MAR	SA	Constant	ASCAT	0.57
702	AMSR-E NOAH	MAR	SA	Constant	AMSR-E	0.7
703	AMSR-E NOAH	MAR	SA	Constant	API	0.65
704	AMSR-E NOAH	MAR	SA	Constant	NOAH	0.75
705	AMSR-E NOAH	MAR	SA	Constant	WASM	0.8
706	AMSR-E NOAH	MAR	SA	TV	ASCAT	0.57
707	AMSR-E NOAH	MAR	SA	TV	AMSR-E	0.67
708	AMSR-E NOAH	MAR	SA	TV	API	0.6
709	AMSR-E NOAH	MAR	SA	TV	NOAH	0.75
710	AMSR-E NOAH	MAR	SA	TV	WASM	0.88
711	AMSR-E NOAH	MAR	SD	Constant	ASCAT	0.62
712	AMSR-E NOAH	MAR	SD	Constant	AMSR-E	0.71
713	AMSR-E NOAH	MAR	SD	Constant	API	0.73
714	AMSR-E NOAH	MAR	SD	Constant	NOAH	0.76
715	AMSR-E NOAH	MAR	SD	Constant	WASM	0.79
716	AMSR-E NOAH	MAR	SD	TV	ASCAT	0.6
717	AMSR-E NOAH	MAR	SD	TV	AMSR-E	0.67
718	AMSR-E NOAH	MAR	SD	TV	API	0.62
719	AMSR-E NOAH	MAR	SD	TV	NOAH	0.74
720	AMSR-E NOAH	MAR	SD	TV	WASM	0.9
721	AMSR-E NOAH	SVM	ND	Constant	ASCAT	0.58
722	AMSR-E NOAH	SVM	ND	Constant	AMSR-E	0.71
723	AMSR-E NOAH	SVM	ND	Constant	API	0.71
724	AMSR-E NOAH	SVM	ND	Constant	NOAH	0.76
725	AMSR-E NOAH	SVM	ND	Constant	WASM	0.78
726	AMSR-E NOAH	SVM	ND	TV	ASCAT	0.56
727	AMSR-E NOAH	SVM	ND	TV	AMSR-E	0.68
728	AMSR-E NOAH	SVM	ND	TV	API	0.61
729	AMSR-E NOAH	SVM	ND	TV	NOAH	0.75
730	AMSR-E NOAH	SVM	ND	TV	WASM	0.86
731	AMSR-E NOAH	SVM	SA	Constant	ASCAT	0.51
732	AMSR-E NOAH	SVM	SA	Constant	AMSR-E	0.7
733	AMSR-E NOAH	SVM	SA	Constant	API	0.63
734	AMSR-E NOAH	SVM	SA	Constant	NOAH	0.76
735	AMSR-E NOAH	SVM	SA	Constant	WASM	0.79
736	AMSR-E NOAH	SVM	SA	TV	ASCAT	0.55
737	AMSR-E NOAH	SVM	SA	TV	AMSR-E	0.68
738	AMSR-E NOAH	SVM	SA	TV	API	0.61

ID	Parent Couples	Rescaling Method	Rescaling Technique	Application Style	Reference	Cor (WASM)
739	AMSR-E NOAH	SVM	SA	TV	NOAH	0.75
740	AMSR-E NOAH	SVM	SA	TV	WASM	0.87
741	AMSR-E NOAH	SVM	SD	Constant	ASCAT	0.56
742	AMSR-E NOAH	SVM	SD	Constant	AMSR-E	0.71
743	AMSR-E NOAH	SVM	SD	Constant	API	0.71
744	AMSR-E NOAH	SVM	SD	Constant	NOAH	0.76
745	AMSR-E NOAH	SVM	SD	Constant	WASM	0.78
746	AMSR-E NOAH	SVM	SD	TV	ASCAT	0.57
747	AMSR-E NOAH	SVM	SD	TV	AMSR-E	0.68
748	AMSR-E NOAH	SVM	SD	TV	API	0.64
749	AMSR-E NOAH	SVM	SD	TV	NOAH	0.75
750	AMSR-E NOAH	SVM	SD	TV	WASM	0.88
751	API NOAH	REG	ND	Constant	ASCAT	0.75
752	API NOAH	REG	ND	Constant	AMSR-E	0.74
753	API NOAH	REG	ND	Constant	API	0.7
754	API NOAH	REG	ND	Constant	NOAH	0.76
755	API NOAH	REG	ND	Constant	WASM	0.77
756	API NOAH	REG	ND	TV	ASCAT	0.57
757	API NOAH	REG	ND	TV	AMSR-E	0.65
758	API NOAH	REG	ND	TV	API	0.61
759	API NOAH	REG	ND	TV	NOAH	0.76
760	API NOAH	REG	ND	TV	WASM	0.85
761	API NOAH	REG	SA	Constant	ASCAT	0.7
762	API NOAH	REG	SA	Constant	AMSR-E	0.73
763	API NOAH	REG	SA	Constant	API	0.67
764	API NOAH	REG	SA	Constant	NOAH	0.76
765	API NOAH	REG	SA	Constant	WASM	0.79
766	API NOAH	REG	SA	TV	ASCAT	0.56
767	API NOAH	REG	SA	TV	AMSR-E	0.65
768	API NOAH	REG	SA	TV	API	0.61
769	API NOAH	REG	SA	TV	NOAH	0.76
770	API NOAH	REG	SA	TV	WASM	0.86
771	API NOAH	REG	SD	Constant	ASCAT	0.74
772	API NOAH	REG	SD	Constant	AMSR-E	0.74
773	API NOAH	REG	SD	Constant	API	0.69
774	API NOAH	REG	SD	Constant	NOAH	0.76
775	API NOAH	REG	SD	Constant	WASM	0.77
776	API NOAH	REG	SD	TV	ASCAT	0.56
777	API NOAH	REG	SD	TV	AMSR-E	0.65

ID	Parent Couples	Rescaling Method	Rescaling Technique	Application Style	Reference	Cor (WASM)
778	API NOAH	REG	SD	TV	API	0.61
779	API NOAH	REG	SD	TV	NOAH	0.76
780	API NOAH	REG	SD	TV	WASM	0.86
781	API NOAH	VAR	ND	Constant	ASCAT	0.75
782	API NOAH	VAR	ND	Constant	AMSR-E	0.75
783	API NOAH	VAR	ND	Constant	API	0.75
784	API NOAH	VAR	ND	Constant	NOAH	0.75
785	API NOAH	VAR	ND	Constant	WASM	0.75
786	API NOAH	VAR	ND	TV	ASCAT	0.63
787	API NOAH	VAR	ND	TV	AMSR-E	0.7
788	API NOAH	VAR	ND	TV	API	0.62
789	API NOAH	VAR	ND	TV	NOAH	0.77
790	API NOAH	VAR	ND	TV	WASM	0.84
791	API NOAH	VAR	SA	Constant	ASCAT	0.75
792	API NOAH	VAR	SA	Constant	AMSR-E	0.73
793	API NOAH	VAR	SA	Constant	API	0.71
794	API NOAH	VAR	SA	Constant	NOAH	0.76
795	API NOAH	VAR	SA	Constant	WASM	0.75
796	API NOAH	VAR	SA	TV	ASCAT	0.62
797	API NOAH	VAR	SA	TV	AMSR-E	0.7
798	API NOAH	VAR	SA	TV	API	0.62
799	API NOAH	VAR	SA	TV	NOAH	0.77
800	API NOAH	VAR	SA	TV	WASM	0.84
801	API NOAH	VAR	SD	Constant	ASCAT	0.73
802	API NOAH	VAR	SD	Constant	AMSR-E	0.74
803	API NOAH	VAR	SD	Constant	API	0.74
804	API NOAH	VAR	SD	Constant	NOAH	0.75
805	API NOAH	VAR	SD	Constant	WASM	0.75
806	API NOAH	VAR	SD	TV	ASCAT	0.61
807	API NOAH	VAR	SD	TV	AMSR-E	0.7
808	API NOAH	VAR	SD	TV	API	0.62
809	API NOAH	VAR	SD	TV	NOAH	0.77
810	API NOAH	VAR	SD	TV	WASM	0.85
811	API NOAH	CDFM	ND	Constant	ASCAT	0.6
812	API NOAH	CDFM	ND	Constant	AMSR-E	0.57
813	API NOAH	CDFM	ND	Constant	API	0.71
814	API NOAH	CDFM	ND	Constant	NOAH	0.75
815	API NOAH	CDFM	ND	Constant	WASM	0.73
816	API NOAH	CDFM	ND	TV	ASCAT	0.53

ID	Parent Couples	Rescaling Method	Rescaling Technique	Application Style	Reference	Cor (WASM)
817	API NOAH	CDFM	ND	TV	AMSR-E	0.65
818	API NOAH	CDFM	ND	TV	API	0.6
819	API NOAH	CDFM	ND	TV	NOAH	0.78
820	API NOAH	CDFM	ND	TV	WASM	0.85
821	API NOAH	CDFM	SA	Constant	ASCAT	0.62
822	API NOAH	CDFM	SA	Constant	AMSR-E	0.55
823	API NOAH	CDFM	SA	Constant	API	0.68
824	API NOAH	CDFM	SA	Constant	NOAH	0.75
825	API NOAH	CDFM	SA	Constant	WASM	0.74
826	API NOAH	CDFM	SA	TV	ASCAT	0.54
827	API NOAH	CDFM	SA	TV	AMSR-E	0.63
828	API NOAH	CDFM	SA	TV	API	0.6
829	API NOAH	CDFM	SA	TV	NOAH	0.77
830	API NOAH	CDFM	SA	TV	WASM	0.85
831	API NOAH	CDFM	SD	Constant	ASCAT	0.67
832	API NOAH	CDFM	SD	Constant	AMSR-E	0.65
833	API NOAH	CDFM	SD	Constant	API	0.71
834	API NOAH	CDFM	SD	Constant	NOAH	0.75
835	API NOAH	CDFM	SD	Constant	WASM	0.74
836	API NOAH	CDFM	SD	TV	ASCAT	0.55
837	API NOAH	CDFM	SD	TV	AMSR-E	0.69
838	API NOAH	CDFM	SD	TV	API	0.61
839	API NOAH	CDFM	SD	TV	NOAH	0.77
840	API NOAH	CDFM	SD	TV	WASM	0.86
841	API NOAH	MAR	ND	Constant	ASCAT	0.71
842	API NOAH	MAR	ND	Constant	AMSR-E	0.71
843	API NOAH	MAR	ND	Constant	API	0.68
844	API NOAH	MAR	ND	Constant	NOAH	0.76
845	API NOAH	MAR	ND	Constant	WASM	0.79
846	API NOAH	MAR	ND	TV	ASCAT	0.57
847	API NOAH	MAR	ND	TV	AMSR-E	0.66
848	API NOAH	MAR	ND	TV	API	0.6
849	API NOAH	MAR	ND	TV	NOAH	0.76
850	API NOAH	MAR	ND	TV	WASM	0.89
851	API NOAH	MAR	SA	Constant	ASCAT	0.61
852	API NOAH	MAR	SA	Constant	AMSR-E	0.67
853	API NOAH	MAR	SA	Constant	API	0.63
854	API NOAH	MAR	SA	Constant	NOAH	0.77
855	API NOAH	MAR	SA	Constant	WASM	0.82

ID	Parent Couples	Rescaling Method	Rescaling Technique	Application Style	Reference	Cor (WASM)
856	API NOAH	MAR	SA	TV	ASCAT	0.56
857	API NOAH	MAR	SA	TV	AMSR-E	0.65
858	API NOAH	MAR	SA	TV	API	0.6
859	API NOAH	MAR	SA	TV	NOAH	0.75
860	API NOAH	MAR	SA	TV	WASM	0.89
861	API NOAH	MAR	SD	Constant	ASCAT	0.7
862	API NOAH	MAR	SD	Constant	AMSR-E	0.71
863	API NOAH	MAR	SD	Constant	API	0.68
864	API NOAH	MAR	SD	Constant	NOAH	0.76
865	API NOAH	MAR	SD	Constant	WASM	0.79
866	API NOAH	MAR	SD	TV	ASCAT	0.58
867	API NOAH	MAR	SD	TV	AMSR-E	0.66
868	API NOAH	MAR	SD	TV	API	0.6
869	API NOAH	MAR	SD	TV	NOAH	0.75
870	API NOAH	MAR	SD	TV	WASM	0.9
871	API NOAH	SVM	ND	Constant	ASCAT	0.68
872	API NOAH	SVM	ND	Constant	AMSR-E	0.71
873	API NOAH	SVM	ND	Constant	API	0.67
874	API NOAH	SVM	ND	Constant	NOAH	0.76
875	API NOAH	SVM	ND	Constant	WASM	0.78
876	API NOAH	SVM	ND	TV	ASCAT	0.53
877	API NOAH	SVM	ND	TV	AMSR-E	0.66
878	API NOAH	SVM	ND	TV	API	0.59
879	API NOAH	SVM	ND	TV	NOAH	0.75
880	API NOAH	SVM	ND	TV	WASM	0.88
881	API NOAH	SVM	SA	Constant	ASCAT	0.56
882	API NOAH	SVM	SA	Constant	AMSR-E	0.66
883	API NOAH	SVM	SA	Constant	API	0.63
884	API NOAH	SVM	SA	Constant	NOAH	0.78
885	API NOAH	SVM	SA	Constant	WASM	0.81
886	API NOAH	SVM	SA	TV	ASCAT	0.53
887	API NOAH	SVM	SA	TV	AMSR-E	0.66
888	API NOAH	SVM	SA	TV	API	0.59
889	API NOAH	SVM	SA	TV	NOAH	0.75
890	API NOAH	SVM	SA	TV	WASM	0.88
891	API NOAH	SVM	SD	Constant	ASCAT	0.68
892	API NOAH	SVM	SD	Constant	AMSR-E	0.69
893	API NOAH	SVM	SD	Constant	API	0.68
894	API NOAH	SVM	SD	Constant	NOAH	0.75

ID	Parent Couples	Rescaling Method	Rescaling Technique	Application Style	Reference	Cor (WASM)
895	API NOAH	SVM	SD	Constant	WASM	0.79
896	API NOAH	SVM	SD	TV	ASCAT	0.54
897	API NOAH	SVM	SD	TV	AMSR-E	0.66
898	API NOAH	SVM	SD	TV	API	0.6
899	API NOAH	SVM	SD	TV	NOAH	0.75
900	API NOAH	SVM	SD	TV	WASM	0.89

CURRICULUM VITAE

PERSONAL INFORMATION

Surname, Name	: Hesami Afshar, Mahdi
Nationality	: Iranian (IR)
Date and Place of Birth	: 10 March 1990, Urmia
Phone	: +90 312 210 24 85
E-mail	: Afshar.mahdi@metu.edu.tr

EDUCATION

Degree	**Institution**	**Year of Graduation**
MS	Urmia Uni. Water Resources Engineering	2014
BS	Urmia Uni. Water Engineering	2012
High School	İran 22 Behmen Okulu, Ankara	2008

WORK EXPERIENCE

Year	**Place**	**Enrollment**
2015-Present	METU	Project Assistant
2012 August	Sadrab Nirou	Intern Engineering Student

FOREIGN LANGUAGES

Fluent English, Fluent Turkish, Fluent Persian

PUBLICATIONS

1. Hesami Afshar M., Yilmaz MT. "The added utility of nonlinear methods compared to linear methods in rescaling soil moisture products", Remote sensing of environment, 196, 224-237 (2017)

2. Mahmoudzadeh M., Mahmoudzadeh H., Hesami Afshar and M., Yousefi S. "Applying First-Order Markov Chains and SPI Drought Index to Monitor and Forecast Drought in West Azerbaijan Province of Iran", International Journal of Geo Science and Environmental Planning, 1(2), 44-53 (2016)

3. Hesami Afshar M., Sorman AU., and Yilmaz MT. "Copula based drought characteristics analysis - case study over Ankara metropolitan city of Turkey", Water, 8(10), 246 (2016)

4. Montaseri M., Hesami Afshar M., and Bozorg-Haddad O. "Optimization of Stormwater Treatment Measure Using MUSIC-GA (Case Study: Canberra City, Australia)", Water Resources Management, 29(13), 4649-4665 (2015)

HOBBIES

Sport, Movies, Computer Technologies